CHANNEL PLANFORM DYNAMICS OF AN ALLUVIAL TROPICAL RIVER

A Dissertation

by

ALDO ALVAREZ

Submitted to the Office of Graduate Studies of
Texas A&M University
in partial fulfillment of the requirements for the degree of

DOCTOR OF PHILOSOPHY

May 2005

Major Subject: Geography

CHANNEL PLANFORM DYNAMICS OF AN

ALLUVIAL TROPICAL RIVER

A Dissertation

by

ALDO ALVAREZ

Submitted to Texas A&M University
in partial fulfillment of the requirements
for the degree of

DOCTOR OF PHILOSOPHY

Approved as to style and content by:

_____	_____
Anne Chin (Chair of Committee)	Bradford Wilcox (Member)
_____	_____
Daniel Z. Sui (Member)	Hongxing Liu (Member)

_____
Douglas J. Sherman
(Head of Department)

May 2005

Major Subject: Geography

ABSTRACT

Channel Planform Dynamics of an Alluvial Tropical River. (May 2005)

Aldo Alvarez, B.S., University of Puerto Rico;

M.S., Massachusetts Institute of Technology

Chair of Advisory Committee: Dr. Anne Chin

The meandering stream has been well studied in temperate environments but the same level of research has not been achieved for meandering streams in tropical areas. The overall objective of this research was to gain an increased understanding of meandering planform dynamics in humid tropical rivers. The objective was pursued by examining the rate of change of channel pattern and results indicate that migration rate and the range of radius of curvature to width ratio where maximum migration occurs is similar to those reported for humid temperate rivers. In summary, as regards to these aspects, the results suggest that the representative humid tropical river is no more dynamic than its temperate counterparts.

A second objective was to document the response and recovery of a humid tropical river system to an extreme flood event. As a result, the trend of shorter recovery times following a major perturbation was demonstrated, and suggests that in the long term, a large flood such as a 100-year event apparently plays a relatively minor role as a formative event in shaping the overall humid tropical landscape.

A third objective was to develop an empirical model for predicting bend migration rates in humid tropical rivers, resulting in empirical relationships that indicate that meander migration has a high degree of correlation with the number of bankfull discharge events under all scenarios, and that model correlation can be enhanced when the silt-clay composition of the banks, and the radius of curvature to width ratio are included as independent variables. The resulting equations were tested to predict maximum meander migration distance, and predictions produced very satisfactory results.

In addition to increasing basic understanding of meander processes in tropical areas and for developing fluvial geomorphological theory, the results of this research have potentially important benefits to society. Because property and structures are often threatened by channel movement, there is a need for improved predictive capability of deformation of stream channels, and the results can therefore be useful to engineers and other professionals in delineating channel hazard zones.

DEDICATION

This work is dedicated with love and appreciation to my parents, and especially my father who recently passed away. In addition to many positive qualities, he taught me to be a free thinker and explorer of ideas at a young age. Furthermore, I dedicate this work to my loving wife Carmen Teresa for her continued support, enthusiasm, inspiration and friendship, and for sharing this difficult but wonderful experience. Without her my studies and research would not have been possible.

It is also dedicated to my children and especially my grandchildren, future explorers of ideas. My special message to them is that they should not limit their dreams, imagination, perseverance, and hard work in their quest of new frontiers, either sub-atomic or galactic. Do not restrict your imagination or creativity by life's quotidian obstacles. **You can, if you think you can**. The future of mankind and life on the planet depend on it.

"Every obstacle no matter how great yields to effort."

Leonardo da Vinci

ACKNOWLEDGEMENTS

The author wishes to thank his advisor Dr. Anne Chin for providing guidance, valuable feedback, and kindling my interest in the field of fluvial geomorphology, an area vibrant and yearning discovery. I thank her for the many stimulating intellectual discussions, long hours, support and insight during the course of my graduate experience. I am grateful to my committee members, Dr. Daniel Z. Sui and Dr. Bradford Wilcox, for their observations, encouragement and enlightenment during this process. Special thanks go to Dr. Hongxing Liu who introduced me to the fascinating and rapidly developing fields of GIS and remote sensing. His guidance, cooperation, and unselfish open office atmosphere was very helpful. Thanks also go to Cesar Arias who developed the TCTM method and taught me its use, Dr. Sherman for stimulating my research topic, and Dr. Klein and the other faculty members who gave guidance and encouragement. The author is grateful for the cooperation and assistance provided. I would like to also thank my colleagues and friends of the department who assisted in my endeavors, most notably, José Gavinha, Jean Ellis, Paul Rindfleisch, and Barry Priest.

Special thanks go to Prof. Ismael Pagán Trinidad, Prof. Linda Vélez, and Dr. Bernal of the Department of Civil Engineering and Surveying of the University of Puerto Rico for their support and making available resources such as the Surveying Laboratory, and the Geotechnical Engineering Laboratory that were instrumental in the fieldwork of this research. Finally, I wish to thank the people of the town of Añasco for providing

information on the history of the Rio Grande de Añasco, and especially Licenciado Eiton Arroyo for serving as an experienced field guide and providing his valuable knowledge and observations of the historic Rio Grande de Añasco.

TABLE OF CONTENTS

CHAPTER Page

CHAPTER Page

LIST OF FIGURES

FIGURE Page

FIGURE Page

LIST OF TABLES

TABLE Page

CHAPTER I

INTRODUCTION

Alluvial rivers, whose bed and banks are composed of sediment being transported by the river (Schumm 1977), are generally divided into three major types based on planform. These are straight, meandering, and braided, with other subsets continuously evolving. Of these the meandering pattern is the most common. Because these dynamic streams migrate laterally across their floodplains, features such as avulsions, cutoffs, and oxbow lakes frequently develop. River meandering has been studied both for its geomorphological and engineering importance using empirical and theoretical approaches. Channel migration can occur gradually, as a river erodes one bank and deposits sediment along the other, or it may occur during a single flood event as an abrupt shift of the channel to a new location.

The meandering stream has been well studied in temperate environments (e.g. Leopold and Wolman 1957; Wolman and Miller 1960; Hooke 1980), but the same level of research has not been achieved for meandering streams in tropical areas. Although notable tropical river studies include those of Salo *et al.* (1986) on the Peruvian Amazon and Ucayili Rivers and Speight (1965) on the Angabunga River in central Papua, there remains a dearth of studies examining the nature of tropical rivers in general. This is surprising given that the tropics cover half of the earth's surface and support 75 percent of the world's population (Mark 2002). This paucity of studies has led Gupta

---

This dissertation follows the style of the *Professional Geographer.*

(1995) to call for more research into the channel form of tropical rivers. Gupta and Dutt (1989) have further suggested that humid tropical rivers may not fit well with existing geomorphic models due to strong seasonality of discharge. Theory developed for humid temperate rivers may also not apply because the tropical climate frequently produces precipitation rates that are more than double their temperate counterparts. Unlike temperate streams, tropical rivers are additionally not exposed to the physical extremes created by freeze-thaw cycles. The incommensurate amount of research on tropical rivers therefore limits opportunities for meaningful contrasts with their temperate counterparts, which hinders theory development. Because tropical areas represent a large proportion of the surface of the earth (Mark 2002), enhanced understanding of the operation of tropical rivers is critical to fluvial geomorphologic theory in general.

Research Objectives

The overall objective of this research is to gain an increased understanding of meandering planform dynamics in humid tropical rivers. The central hypothesis is that, due to a climate regime that produces approximately double the amount of precipitation than humid temperate environments, tropical rivers may develop different morphological characteristics than those of temperate regions. Higher discharge may produce higher sediment loads, for example, and also result in higher frequencies of bankfull discharge. This is expected to increase energy inputs into the system, possibly resulting in rapid planform change and higher meander migration rates. At the same time, higher resistance is also expected in the tropics given greater vegetation resilience. High

temperatures are also expected to encourage faster chemical weathering rates than those in temperate regions (Ritter *et al.* 2002), leading to finer soils producing more resistant channel banks (Schumm 1967). In short, the higher precipitation, sediment loads, and frequencies of bankfull discharge combined with greater vegetation resilience and faster chemical weathering rates of the humid tropical climate regime may produce different force-resistance relationships that may result in channel morphologies distinct from those in temperate regions.

The overall objective will be accomplished by pursuing the following three specific objectives. The first objective is to examine the pattern and channel planform dynamics of a representative alluvial humid tropical river in order to characterize planform change. This objective seeks to answer the following questions: (1) how static or dynamic is the channel pattern; (2) what are its meander migration rates and how do they compare with rivers from temperate climates; and (3) how does the ratio of meander-bend curvature to channel width (r/w) relate to the maximum meander migration rate? The working hypotheses are that (a) change in channel pattern of a representative humid tropical river is highly dynamic, experiencing rapid changes in relatively short time periods, and that the primary mechanism for planform change is through cutoffs and avulsions, rather than braiding. Both the mean meander migration rate (b) and the ratio of meander-bend curvature to channel width (r/w) for maximum migration (c) in a humid tropical river, will be similar to those demonstrated in humid temperate rivers.

These hypotheses were derived because, although a higher frequency of bankfull discharge events is expected in the humid tropical regime, higher silt-clay content in the channel banks and a resilient vegetation cover would also provide greater resistance to deformation, leading to similar overall migration rates and r/w ratios as those in temperate environments. Rapid planform changes are also hypothesized because of large precipitation amounts and high variability.

The second objective is to document the response and recovery of a humid tropical river system to an extreme flood event. The working hypothesis is that, when disturbed by an extreme flood event, both channel width changes and the recovery period will be significantly less in a humid tropical river than in humid temperate streams. This is because a humid tropical river is expected to have highly cohesive banks that limit channel width changes. Instead, the depth of the less cohesive channel bed is expected to change more rapidly in response to a high discharge. Tropical river channels are also expected to recuperate more quickly because of rapid vegetation growth, higher precipitation rates, and abundant sediment flow than rivers in humid temperate regions (Wolman and Gerson 1978).

The third objective is to develop an empirical model for predicting bend migration in humid tropical rivers based on spatial and temporal relationships of morphometric and hydrologic parameters. The working hypothesis for this objective is that meander migration in tropical rivers will be controlled by a set of independent variables that best represent force and resistance components in these systems. Variables that characterize the tropical precipitation regime (large quantity and

variability) and high bank resistance include, bankfull discharge frequency, the r/w ratio, the silt-clay content of the meander banks, bank strength, and valley slope. The approach used to develop this empirical model will be to combine these five parameters as independent variables in a multiple regression analysis that should therefore account for a large portion of the variability in channel migration.

Significance

Planimetric movement of rivers is difficult to explain or predict because of the numerous variables involved and the complexity of their interactions. Channel planform is one of the most rapidly changing features of a river channel and is therefore highly sensitive (Hooke 1997). Analysis of planform changes provides opportunity to quantify sensitivity and estimate time scale of adjustments to various disturbances to the fluvial system. Additional knowledge from field investigations is therefore needed for theoretical and model development.

A review of the literature reveals an inordinate amount of studies based on meandering rivers in temperate climate regions (e.g. Hudson and Kesel 2000; Milton *et al.* 1995; Simon *et al.* 2004). However, because of hydro-climatic differences, existing geomorphic models may not fit well with humid tropical systems. As suggested by Gupta (1995), more research into the channel planform dynamics of tropical rivers is sorely needed. This proposed study promises to expand the theoretical base in this area by examining the temporal and spatial relationships of channel migration and planform geometry in an alluvial humid tropical river. Knowledge of migration rates is

fundamental to the understanding of river landscape, especially in the development of floodplains (Nanson and Hickin 1983; Thorne 1992). This knowledge is also valuable to understanding the effects of human activities on channel processes (Hudson and Kesel 2000) and short term prediction of erosion (Hickin and Nanson 1984). This study therefore seeks to enhance basic theory and also enlarge the limited data set available for tropical river regimes, an area that covers half of the earth's surface and supports 75 percent of the world's population.

Benefits to Society

In addition to increasing basic understanding of meander processes in tropical areas and for developing fluvial geomorphological theory, such knowledge has potentially important benefits to society. Because property and structures are often threatened by channel movement, there is a need for improved predictive capability with respect to the deformation of stream channels (Li and Eddleman 2002; Simon and Downs 1995). Channel migration may influence the site selection, design, and maintenance of structures such as highways, railways, bridges, pipelines, transmission lines, flood control works, buildings, dams, navigation channels, and river intakes and outlets built on the floodplain. Knowledge of rates and patterns of planform change may also be important in understanding habitat diversity in floodplain environments, of archaeological studies, and even oil and gas exploration (Sun *et al* 1996; Swanson 1993). Migrating river systems may be the least recognized of the destructive effects caused by

flooding (Perkins 1996). Results of this study would therefore be useful to planners, engineers, and other professionals in delineating channel hazard zones.

Organization of Study

This document is organized into nine chapters. Following an introductory chapter, Chapter II synthesizes the literature concerning channel planform dynamics of meandering rivers. The background to the topics of meandering planform, rates of meander migration, radius of curvature, and the response and recovery of channel planform to an extreme event is discussed, providing insight for theory building. Chapter III is an overview of the study area including the selection of study channel reaches. In Chapter IV, the methodology for the study is detailed with a theoretical discussion explaining each analytical assignment. This is followed by an explanation of field and laboratory procedures to perform each task.

The remainder of this report focuses on the results and significance of the findings. Chapter V presents the results of the analysis of the study river while Chapter VI addresses the response and recovery of the representative tropical river to an extreme flood event. Chapters VII and VIII discuss the development and verification of an empirical meander migration model. A summary of the major findings, an evaluation of methods, and suggestions for future work appear in the final chapter.

CHAPTER II

BACKGROUND

Compared to temperate environments where channel planform dynamics have been studied extensively (e.g. Leopold and Wolman 1957; Ackers and Charlton 1970; Schumm 1963), a limited number of studies has examined the nature of tropical rivers. Ahmad *et al*. (1993) focused on steep hillslopes and related mass movement that supplies a large amount of coarse sediment to mountain streams in eastern Jamaica and eastern Puerto Rico. Salo *et al.* (1986) studied the Peruvian Amazon and Ucayili Rivers to determine large-scale natural forest disturbance in lowland rainforests caused by lateral erosion and channel changes of meandering rivers. In Central Papua, Speight (1965) determined that the dominant wavelength of the meandering portion of the Angabunga River is proportional to the square root of the bankfull discharge. In the Zaire Basin in equatorial Africa, Savat (1975) found that river stability depends on its flow regime and the stability of its banks, with clayey forested banks being the most stable. Also, studies of three rivers in this basin revealed that the bed-sediments were all the same grain size with almost identical sorting. Pickup and Warner (1984) studied the Fly and Purari Rivers in Papua New Guinea, where annual rainfall varies from 8,000 to 11,000 mm. Examining the relationship of channel adjustment to sediment load and discharge, they found that a moderate correlation exists between slope and bed-material size. In addition, channel size was revealed to depend on discharge and that bankfull frequencies are highly variable and increase downstream. Blake and Ollier (1971) also studied the Fly River in Papua New Guinea and described the floodplain of this 1,100

km long river. Gupta and Dutt (1989) described the complex bar formations of the Auranga River in India, a tropical monsoon environment. They found that in the dry season, the lowland portion of the river is braided, but it acts as a meandering river during part of the wet monsoon.

Although these studies provide important background to the understanding of tropical rivers, they did not address the subject of meandering planform, rates of meander migration, or response and recovery of channel planform to an extreme event. Furthermore, none of these studies have investigated the meander-bend curvature that produces maximum meander migration rates, even though this relationship is well understood for temperate rivers (e.g. Leopold *et al.* 1964; Hickin and Nanson 1984; Hooke 1987). This study therefore seeks to examine characteristics of meandering rivers in a humid tropical setting, thereby filling some of the gaps found in the literature. The following paragraphs summarize the background literature to river meandering. They focus on issues directly relevant to this proposal: channel pattern and planform changes, meander migration processes, models and rates, radius of curvature, silt-clay content of banks, and response to flood events.

Channel Pattern

Channel pattern is the planimetric geometry, or the form of the channel when viewed from above. This pattern represents a form of adjustment in the horizontal plane that influences resistance to flow. For example, the effect of a meander is to increase resistance and reduce channel slope when compared to a straight reach occupying the

same channel length. Leopold and Wolman (1957) introduced the conventional classification of straight, meandering, and braided to distinguish between channel pattern types. Although additional patterns are now recognized (e.g. Brice 1984; Rosgen 1996), this original classification can be used to discuss the development and controlling processes of channel pattern.

The ability of a river to modify its form depends on the balance between the erosional force exerted by the river flow and the strength or resistance to erosion of the material forming its bed and banks. This balance is influenced by independent variables that control the physical processes in the river. The principal controls are stream discharge and valley slope (representing force) and the sediment load, bed material size, bank material composition and strength (representing resistance; Richards 1982; Robert 2003). The size of the bedload, the capacity of the stream to transport it, and the relative stability of the channel banks, are therefore key variables in determining channel patterns.

Various empirical equations have been developed to differentiate between straight, meandering or braiding patterns using these variables. Leopold and Wolman (1957) first distinguished channel patterns based on channel slope and bankfull discharge.

$$S_b = 0.013\ Q_b^{-0.44}$$

Here S_b is channel slope and Q_b is bankfull discharge. In this seminal work, this equation differentiated fields corresponding to straight, braided or meandering reaches on a graph of discharge versus slope. Thus a threshold slope exists above which the channel would

experience braiding. Numerous equations subsequently have differentiated between straight, meandering or braiding patterns using other parameters. Ferguson (1987) distinguished channel patterns based on channel slope, discharge and the silt-clay contents of the banks.

$$S = 0.0013\ Q^{-0.24}\ B^{1.00}$$

Here S is the channel slope, Q is discharge and B is the silt-clay content of the banks. Slopes that are steeper than those predicted by this equation will induce braiding. Analogous equations exist using other parameters such as slope, discharge and median-bed material diameter (Ferguson 1987).

Sinuosity, or the ratio of stream length measured along the center of the channel to valley length, is commonly used to describe channel pattern (e.g. Brice 1984; Hooke 1977). Leopold and Wolman (1957) originally proposed a sinuosity of 1.5 as the boundary between straight and meandering, but others have suggested that this traditional classification is insufficient in describing the range of patterns that exist in nature. Schumm (1963) recommended five classifications depending on sinuosity value: straight (1.1), transitional (1.3), regular (1.7), irregular (1.8), and tortuous (2.3). Brice (1984) similarly suggested that if sinuosity is less than 1.05, the channel is straight; if sinuosity is within the 1.05 to 1.50 range, the pattern as sinuous, and if it is greater than 1.5, the river is meandering. Brice (1984) further added additional classifications such as sinuous canaliform, sinuous point bar, sinuous braided and nonsinuous braided. An even more elaborate classification scheme developed by Rosgen (1996) defined 41 types of

channel types. Regardless of the system being used, however, it is clear that the boundaries between types are arbitrary.

Sinuosity values have been determined for many rivers in temperate climate regions. For example, the Powder River, the Solomon River, and the Republican and Sappa Rivers showed sinuosities of 1.2, 2.4, 1.3, and 1.9, respectively (Schumm 1963). The Beaver River in Alberta, Canada, and the Mississippi River, from Cairo to Memphis, also exhibited sinuosities of 1.25, and 1.55 respectively (Chitale 1970) whereas the Murrumbidgee River in New South Wales, Australia, had a sinuosity of 2.0 (Schumm 1977). A study of 47 rivers in the Great Plains, U.S.A., further showed a mean sinuosity of 1.57 (Schumm 1963). The sinuosity of rivers has also been demonstrated to change over time. For example, Catherine Creek in northeastern Oregon experienced a sinuosity change of six percent from 1979 to 1998 (Laliberte 2001). In England, sinuosity changes of 18% were measured in the River Culm, 16% in the River Creedy, 20% in the River Otter, and 28% in the River Yarty from 1903 to 1953 (Hooke 1977). The change in the River Culm is attributed to human interference with the channel. For the other rivers, the extent of human interference, and how much the change is an adjustment of agricultural practices, filed drainage, and urban activity, is difficult to assess (Hickin 1977; Hooke 1977). This study will examine the sinuosity of a humid tropical river and assess the extent to which it is comparable to values reported in the literature for temperate rivers.

Channel Planform Changes

Channel planform changes by erosion of the banks (growth of meanders), by deposition within the channel (braiding), or by cutoffs and avulsions that involve switching of channel position (Brook and Luft 1987; Hooke 1987). Several types of meander cutoffs can occur. Neck cutoffs are produced by the breaching of narrow gaps between adjacent channel bends, whereas chute cutoffs involve more extensive scouring of new channels across floodplains. High sinuosity and low floodplain slope favor the neck cutoff; erodible, non-cohesive, and poorly vegetated surfaces encourage chute cutoffs (Lewin 1977). In a study of 1000 km of lowland rivers in England over a 100 year period, Lewis and Lewin (1983) reported 145 cutoffs: 55% were chute, and 16% were neck. Avulsions form as a result of water super-elevation on the outside of banks during flood conditions, and tend to exploit old channels of the river. Large-scale avulsions have been observed on large meandering rivers such as the Mississippi (Hooke 1995), where overbank flow can be diverted for many kilometers. At a smaller scale, chute cutoffs and avulsions tend to take place where the meander bend curvature is such that at high flow the flood waters spill over to take a straighter course.

In summary, cutoffs and avulsions are significant for the termination of meander sequences (Werrity 1997; Lewin 1996). The most active rivers rarely exhibit a stability of form but show progressive development (e.g. Hickin 1983; Hooke 1984). Hooke (1995) suggested that the spatial and temporal occurrences of cutoffs and avulsions have received little analysis in temperate rivers. This study therefore seeks to examine the

nature of these planform changes to enhance the limited theory available not only for a humid tropical river, but for all rivers in general.

Meander Migration and Radius of Curvature

Meanders migrate across the floodplain because alluvial rivers erode and deposit sediment along their banks. Migration rates for temperate rivers have been documented from less than 0.1 m per year (Hooke 1980) to more than 7.26 m per year (Nanson and Hickin 1983). Two opposing factors control the rate of erosion of riverbanks and the resulting migration of the river channel. These are the fluid shear stresses acting on the channel boundaries, which are controlled by the channel planform and cross sectional shape governing the velocity distribution near channel boundaries, and the resistance to erosion of the sediment comprising these boundaries, determined by the cohesive strength of the bank materials (Williams 1986; Chang 1988). Studies in temperate rivers show that migration rates are higher in rivers with non-cohesive banks, inversely proportional to the silt-clay content of the banks (Daniel 1971), and proportional to discharge (Hooke 1980).

Migration rates depend upon channel geometry. Leopold and Wolman (1957) first suggested that the radius of curvature affects channel migration. The radius of curvature (r) is the radius of a circle drawn around a meander bend. It expresses the degree of tightness of a specific bend, with large r values indicating wide-open meander bends. The radius of curvature is usually scaled according to channel size (width (w)) so

that it is expressed as a dimensionless ratio of *r to w* (r/w). Also called bend curvature ratio, a smaller r/w ratio indicates a tighter bend.

Migration rate varies according to how tight a bend is (r/w) because tightness of bend determines total resistance. Using the analogy of flow in a closed pipe, Bagnold (1960) suggested that total resistance of the boundary reaches a local minimum when r/w is approximately two. At values below two, Bagnold (1960) suggested that the flow along the inner boundary becomes unstable and breaks away from the boundary. Energy dissipation occurs and the flow loses force. At values above two, the bend opens and there is higher resistance of the boundary. The angle at which the flow meets the boundary changes with varying r/w values.

Empirical evidence to support Bagnold's theory was provided by Hickin and Nanson (1984), who showed that migration rates for the Beatton River, British Columbia were greatest when the bend curvature was between 2.0 and 3.0. Erosion rates decreased markedly beyond this critical range of values. The relationship of a critical r/w in the range of 2.0 to 3.0 to maximize migration rates in temperate rivers is now well accepted (Biedenharn *et al.*1989; Begin 1986; Thorne 1992; Nanson and Hickin 1983). Despite its importance to meander dynamics, however, this relationship has not been investigated in humid tropical environments. This study seeks to compile a data set for a humid tropical river, which will provide a broader base of values for determining the global coverage of this spatial relationship.

Extreme Flood Events

The work done by catastrophic events, floods that occur once every 50 years or more (Wolman and Miller 1960), can be related to the mean annual erosion of a channel (Wolman and Gerson 1978). The effectiveness of such events in forming the landscape can also be related to the recovery time of the channel to its equilibrium form following perturbations (Wolman and Gerson 1978). Landform change produced by an extreme event need not be the same in two different regions, and will depend on the characteristics of the climate, position within the drainage basin, and the processes occurring in the interval between such rare events. Although great erosion can occur in some channels during exceptionally large flows (Dury 1977; Costa and Conner 1995, Hickin and Sichingabula 1988), in other channels even a 1000 year flood may not produce significant effects (Baker 1977, 1988; Komar 1988). Wolman and Miller (1960) found that most of the sediment transported by a river in temperate environments is carried by relatively frequent events. Catastrophic events, which individually transport large sediment loads, occur too infrequently to be effective in forming the channel. Although the potential for large floods to disrupt the regime condition and cause major channel changes exists, large floods are not usually channel- forming provided that the return period of these extreme events is longer than the period required for subsequent, lesser events to restore the long term average condition (Wolman and Gerson 1978).

Literature indicates that the amount of change caused by floods and the recovery period differs according to climate and flow regimes. For example, in a wet climate whereby vegetation growth is rapid, then, regardless of the channel erosion caused by

the flood, and assuming ample sediment supply, one should expect the vegetation to recover rapidly and the channel to return to its original condition prior to the flood (Baker 1988; Kilpatrick and Barnes 1964). Following destructive floods, re-vegetation and deposition of sediment would cause the channel to narrow and eventually return to pre-event conditions. This restoration of channel width after an extreme event can be relatively rapid in humid regions (Gupta and Fox 1995).

In their seminal 1978 paper, *Relative scales of time and effectiveness of climate in watershed geomorphology*, Wolman and Gerson presented quantitative data to illustrate this point, with a sequence of channel width changes and recovery periods for selected rivers in different climate regions following large storm events. Using the Patuxent River in Maryland and the Baisman Run in north central Baltimore County, to represent humid temperate regions (precipitation of approximately 1000 mm per year), Wolman and Gerson (1978) showed that the impacts of an extreme event resulted in a 40 percent increase in stream width with a recovery period of 15 years for the Patuxent river, and a 20 percent increase in width and a recovery period of 10 years for the Baisman Run. The semi-arid climate region, width increase on the other hand, represented by the Cimarron River in southern Kansas, showed an effectiveness of over 200 percent with a recovery period of over 28 years. Further observations by Wolman and Gerson (1978) in the Sinai desert showed a widening of as much as 1000 percent during individual storms, with a recovery period in the 100 year interval. Thus, with dryer climatic regions, rivers widen more and recover less quickly to extreme events.

Although the trend of shorter recovery time following a major perturbation has been demonstrated for areas ranging from humid temperate regions compared to desert environments, this issue has not been examined for humid tropical regimes. In this climate regime, annual mean precipitation may be higher than 2000 mm per year, double their temperate counterparts (Larsen 2000). Therefore, recovery rates may be even more rapid than those in temperate regions. This study seeks to document the response and recovery period of a humid tropical river to a catastrophic event in order to contribute to this gap in the literature.

Models of Meander Migration

Although the cause of meandering has attracted interest for many years, a completely satisfactory explanation of this phenomenon has not been achieved (Rhoads and Welford 1991). Numerous arguments have been advanced to explain why rivers meander, including dissipation of excess energy (Jefferson 1902), minimization of energy expenditure (Chang 1988), and minimization of the variance in bed shear stress and boundary friction (Langbein and Leopold 1966), although minimization of energy or shear stress could easily be the result of meandering as it could be the cause (Richards 1982).

Meandering begins when a certain threshold discharge is reached in a straight channel, and the thalweg (the lowest point across a river channel), begins to migrate back and forth across the channel. As flow increases, oscillations of the thalweg increase until one of the banks is impacted by the core velocity and erosion begins (Davies and

Tinker 1984). Secondary circulation is an important characteristic of flow in a meandering system. Centrifugal force acting on the water as it moves around the evolving bend causes a slight elevation in the water surface along the outside segment of the bend. The difference in water elevation produces a variation in pressure across the section that gives the flow a circulating motion, called helicoidal flow (Dietrich 1987). The midsection of the channel contains the majority of the discharge that moves downstream in a corkscrew motion, but near the outer bank, at the boundary layer between the water and the bank sediments, differences in pressure cause the water to move upward along the bank and then outward toward the center (Markham and Thorne 1992). The flow direction of this cell is opposite to that observed in the middle areas of the channel. The two rotating flows meet at the surface in a zone of convergence that promotes erosion at the outside bend. At the inside bank of the bend there is a net outward component of flow that favors deposition of sediments at this area creating a point bar (Dietrich 1987). With time, the meander bend evolves.

Several theoretical and empirical approaches have been used to develop predictive models of meander bend migration. Theoretical approaches include mathematical models founded upon simplified physical principles. These fall into two main categories: models based on equations that describe dominant processes, (e.g. Ikeda and Parker 1981), and models that postulate a condition regarding the behavior of stable channels, such as minimum stream power (Chang 1988). Ikeda and Parker's (1981) model estimates bank velocities and erosion rates for a channel reach comprised of one or more bends of specified dimension, plan geometry, and flow conditions.

Meander migration rates are calculated by taking the product of a coefficient of bank erosion (estimated in a laboratory channel), and the incremental bank velocity in excess of the average velocity of the cross section. The model has been used to show how bank material characteristics can theoretically influence cross sectional form. Using this model (Ikeda and Parker 1981), Beck (1988) predicted the migration of three bends over five years on the Genesee River in Mount Morris, New York within ± 30 percent.

Because theoretical mathematical models require vast quantities of data often difficult and costly to obtain, meander migration has also been investigated with empirical approaches. In a study of meanders on the Squamish River, British Columbia, Hickin (1974) found that variation in friction, shear stress, velocity and strength of transverse secondary flow related to the degree of channel curvature. Based on these data, Hickin and Nanson (1975) derived empirical relationships to predict migration rate (M) for the Beatton River, Canada, using the radius of curvature (r) to channel width (w) ratio, and spacing of meander scrolls (d) as independent variables. Scrolls were defined as the distance between levees left by meander migration on the flood plain. Streamflow data was not available and the authors saw a correlation of migration with the scrolls. The migration rates of 0.2 m to 0.7 m per year were determined. Their regression analysis generated the following equations:

$$M = 0.05\ (r/w)^{2.05} + 0.00035d^{\,2.63} \quad (1.3 < r/w < 2.9)$$

$$M = 2.75\ (r/w)^{-1.73} + 0.00035d^{\,2.63} \quad (2.9 < r/w < 7.0)$$

The two equations represent the r/w values from 1.3 to the maximum of 2.9, and from r/w of 2.9 to 7.0. This model contains a standard error of 0.091 m per year or ± 19.07 percent variability and was not tested (Hickin and Nanson 1975).

Another empirical meander migration model developed by Hooke (1980) emphasized watershed area as a surrogate for discharge. Using data from Southeast Devon, England, Hooke (1980) derived the following regression relation for meander migration rate (M):

$$M = 2.45\ A^{0.45}$$

This relationship was derived from a sample size of 50 temperate rivers with the regression yielding a coefficient of determination (r^2) of 0.40 (Hooke 1980). This model therefore explained 40 percent of the variability in mean meander migration rates for these study streams. The predicted rate was tested over a three year period for the River Otter in Southeast Devon and Hooke (1980) concludes that the results were "*...close enough that the relationship may at least illustrate a regional trend and indicate an order of magnitude for estimating rates of erosion for such streams*."

The models described above were developed using data from temperate climate regions. However, relationships between process control variables may not be the same as for humid tropical climates. For example, these empirical models assume constant movement of the meander bend each year. This implies the assumption of uniform frequency of channel forming discharge, which is unlikely given the highly variable precipitation regime of a humid tropical river. Additionally, these empirical models do not include other potentially important process control variables such as bank

composition or bank strength which may be significant in controlling meander migration in humid tropical rivers. This study therefore seeks to develop an empirical meander migration model applicable to humid tropical rivers. This model will emphasize independent variables that better represent both the force and resistance components controlling meander migration in humid tropical rivers, as well as channel geometry. These include frequency of bankfull discharge and valley slope (to represent forces), silt-clay composition of banks and bank strength (to represent resistance), and r/w ratio (to characterize channel geometry.

In summary, the body of work reviewed in this section indicates a clear need for a better understanding of meandering processes in tropical areas. A model for estimating meander migration rates in such regions is especially needed, not only to increase basic understanding of meander processes in tropical areas and for developing theory, but also to potentially produce important benefits to society by helping planners, engineers, and other professionals in delineating channel hazard zones.

CHAPTER III

STUDY AREA

Location

Western Puerto Rico was selected as the study area (Fig. 1) because it has a humid tropical rain forest climate characterized by high annual precipitation and temperatures always above 18° C, making this climate winterless (Christopherson 2003). This study will focus on the Rio Grande de Añasco (Fig. 1). Located between latitudes 18º 05' and 18º'20' N, and longitudes 67º 15' and 66º 45' W, the Rio Grande de Añasco is the largest river in the western region of Puerto Rico, with a drainage area of 515 km^2 and a length of 46 km. The river is non-regulated and the lowland alluvial valley portion is free to migrate laterally, and experiences minimal human impact. The river originates near the *Cordillera Central*, flows west, and discharges into the *Bahia de Añasco* (Fig. 1). It is bounded by hills to the north, east, and south, and by the *Bahia de Añasco* to the west (Diaz and Jordan 1987). Elevations within the drainage basin vary from mean sea level to 1,205 meters. The two principal population centers in the Rio Grande de Añasco basin are the cities of Añasco and Mayagüez, with populations in the year 2000 of 28,000 and 102,000 respectively (U.S. Department of Commerce 2000).

Climate

The Rio Grande de Añasco watershed receives a mean annual rainfall of 2283 mm (89.9 inches; Slack 1993). The area is influenced by local orographic effects, cold fronts from the north, and tropical storms. Annual rainfall varies from 4500 mm (177

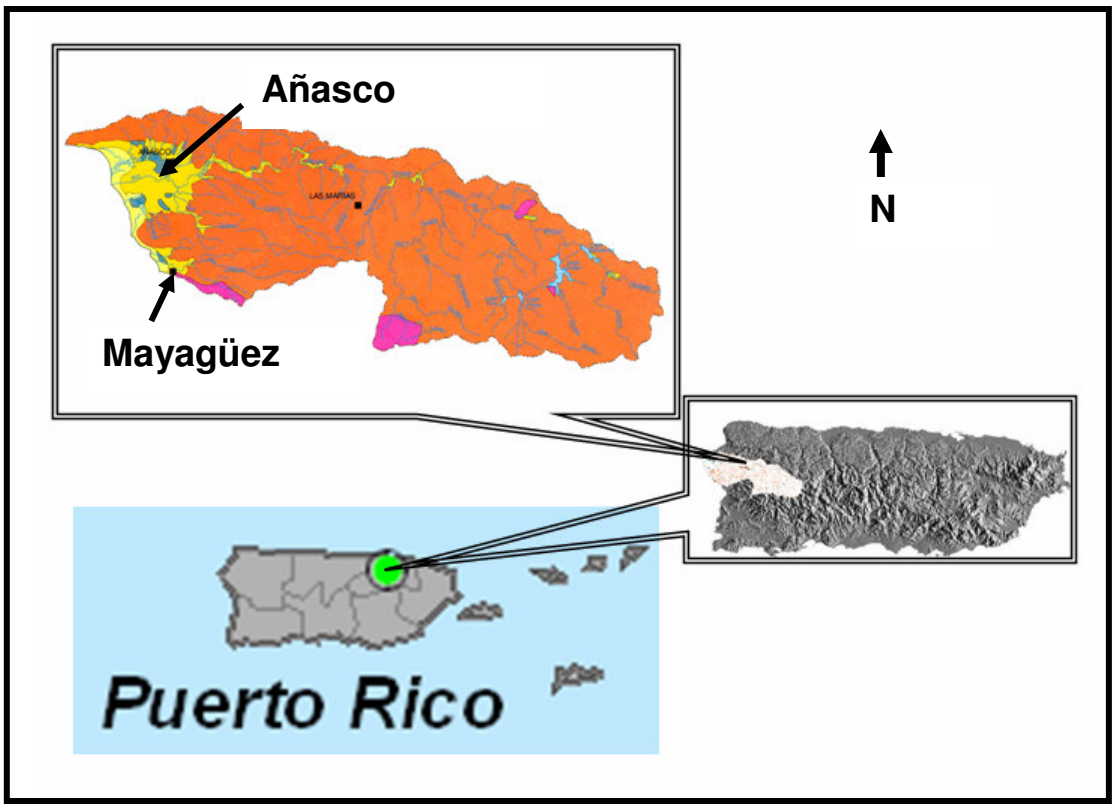

Figure 1 *Location map of the Rio Grande de Añasco Drainage Basin in Puerto Rico.*

inches) in the mountainous headwaters to 1500 mm (60 inches) along the coastal plain (Clark and Wilcock 2000; Larsen 2000). Rainfall is weakly seasonal, with tropical disturbances and hurricanes occurring between July to November, although slow moving cold fronts can deliver considerable amounts of rain from December to May (Veve and Taggert 1994). Average daily temperatures in the valley range from 23 to 28 degrees Celsius (73 to 82° F).

Geology

Volcanic and volcaniclastic rocks of Cretaceous age, most of which were formed or deposited in a marine environment, are present throughout the Añasco region. In the Río Grande de Añasco valley, these rocks are overlain by alluvial deposits of Quaternary age. The alluvial fill in the valley is composed of clay, silt, and sand with localized gravel deposits (Veve and Taggart 1994). Thin corridors of alluvium have been deposited along the course of the Río Grande de Añasco. Swamp deposits are present over relatively large areas of the valley. Beach deposits are extensive along the coast, extending inland as far as six miles. Seismic surveys were used to locate and describe the subsurface materials in the lower Río Grande de Añasco valley (Díaz and Jordan, 1987).

The surface of the volcanic rocks underlying the valley is deeply incised to depths of about 350 feet below present mean sea level, indicating that the Río Grande de Añasco cut deeply into the valley floor during these lower sea levels. A zone of clay, interbedded with limestone, is present in the central part of the valley along the ancient

incision. The interbedded clay and limestone layer is about 250 feet thick. Alluvial deposits of Quaternary age, which have a thickness of as much as 100 feet, overlie the clay and limestone zone and the volcanic and volcaniclastic bedrock (Mattson 1960).

Vegetation

Riparian vegetation along the valley reaches is dense, and it consists mostly of herbaceous bambusoid grasses (Ayala-Silva and Twumasi 2004), many of which can reach over seven meters in length, have tough culms with cutting leaves, and branch abundantly. Some of these are *Anomochloa Brongniart*, *Crytochloa Swallen*, *Ekmanochloa Hitchcock*, and *Maclurolyra Soderstrom* (Soderstrom and Calderon 1979).

Study Areas

The proposed analysis will specifically focus on two study areas within the Rio Grande de Añasco (Fig. 2). The Rio Grande de Añasco flows from its confined segment in the mountains into the unconfined alluvial valley approximately 9 km from the ocean. The first study area is the broad meander belt that develops within a 4 km stretch defined between two bridges on highway 430 and ending close to highway 2 (Study Area One, Fig. 2). The second study area is a 1.5 km reach that is immediately east of the bridge at highway 430 (north is toward the left). This segment of the river is directly above the meander belt portion of the river as it leaves the confined mountainous region and enters the valley. The remaining segment of the river has low slope, is virtually straight and flows towards its outlet to the Mona Channel.

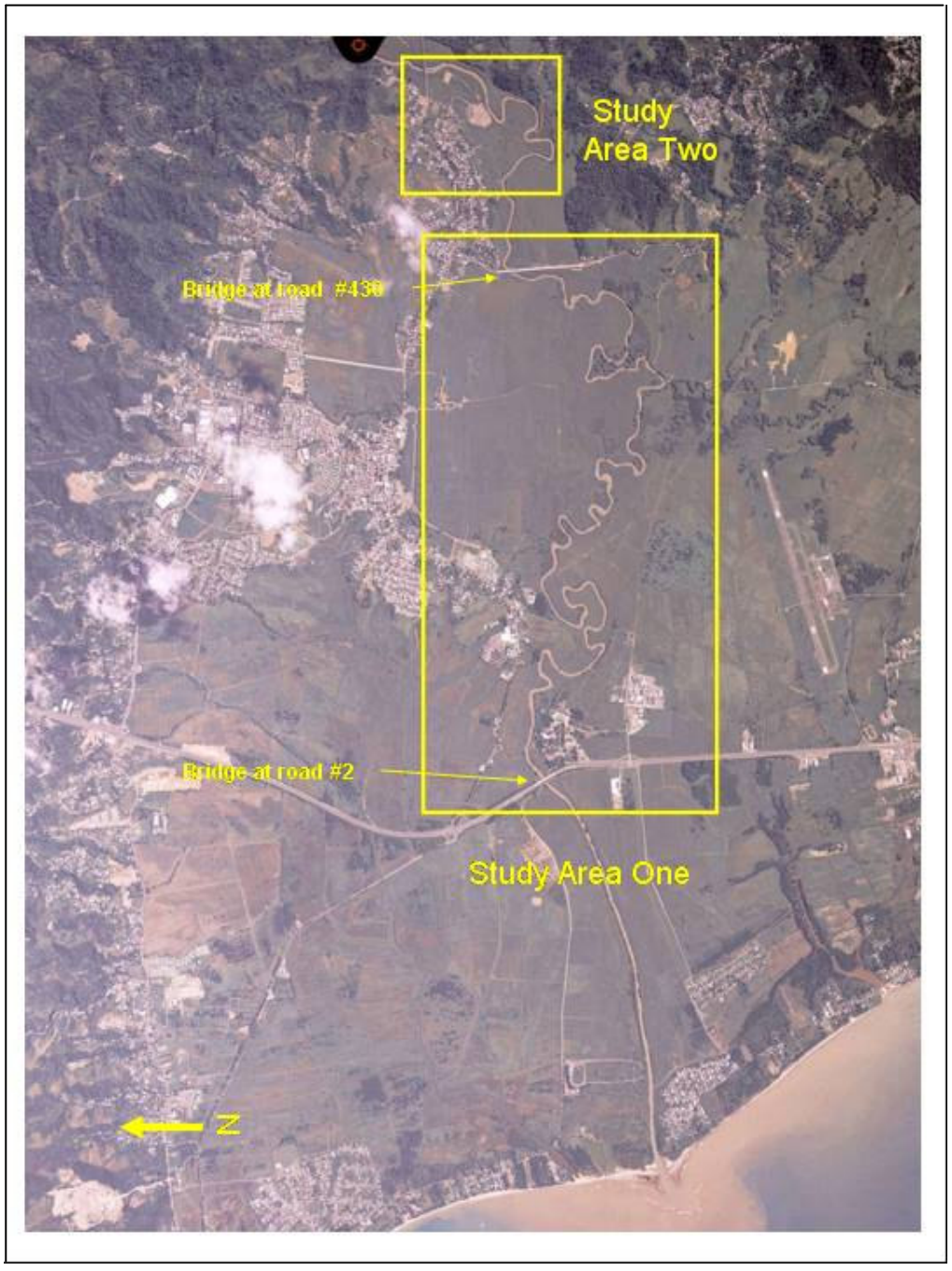

Figure 2 *Location of Study Area One and Study Area Two.*

Hurricane Georges

A catastrophic hurricane passing over the Rio Grande de Añasco in 1998 offers an opportunity to assess the response of such a system to extreme events. From September 21 to 30, 1998, Hurricane Georges left a trail of destruction in the Caribbean region and across the southern U.S. Gulf coast. Estimated deaths in the Caribbean exceeded 600 people (Westrup 1998). In Puerto Rico, the U.S. Federal Emergency Management Agency (FEMA) estimated that 33,113 homes were destroyed, with nearly 50,000 more suffering major or minor damage (U.S. Federal Emergency Management Agency 1999). With winds from 115 mph to gusts of 150 mph (U.S. Geological Survey 1999), the hurricane's eye bisected the island from east to west on September 21 (Fig. 3.), and entered the Rio Grande de Añasco basin through the mountains in its eastern portion, and left through its southwest boundary near Mayagüez (Fig. 1).

In addition to wind devastation, Hurricane Georges also brought large volumes of precipitation. In the Rio Grande de Añasco drainage basin, rainfall was 356 mm (14 inches) on the coastal plain, and 560 mm (22 inches) in the higher altitudes of the watershed. The central forests of the island received 787 mm (31 inches) around the town of Jayuya, 10 km due east of the highest portion of the watershed (Garza and Atwell 1999; Fig. 3), all in less than 24 hours. The precipitation rate reached 75 mm/hr (Cangialosis and Chen 2002). Heavy rainfall fell upon nearly saturated soils since the tropics were already wet in the weeks leading up to the hurricane. Flow records for the U.S.G.S. gauge station (50144000; U.S. Geological Survey 2004) showed a peak discharge of 4,615 cms (163,000 cfs), estimated to be a 100 year peak discharge for the

river (Ramos-Ginés 1999). Annual peak discharge, and mean annual hydrograph of the river are presented in Appendix A. Nonetheless, the resilience of the humid environment was suggested, as Ostertag *et al.* (2003) reported rapid refoliation of the forest canopy and floor vegetation within 3 to 4 weeks of passage of the hurricane. Changes in channel geometry will be measured to assess the recovery of the river system to this catastrophic event.

Summary

The two study areas are segments of the study river that are within the lowland alluvial valley portion where the river is free to migrate laterally and where it experiences minimal human impact. Thus, they are ideal for investigating channel planform dynamics. In addition to channel characteristics, the Rio Grande de Añasco is representative of other humid tropical rivers with similar geology, climate and vegetation. Therefore, generalizations resulting from this river research could apply to other streams in Puerto Rico in particular, and to other similar humid tropical watersheds in general. The next chapter describes the methods used to measure and analyze the two study reaches.

CHAPTER IV

METHODOLOGY

Approach

The general approach to this study is to use aerial photography and geographic information systems (GIS) to quantify planform changes and to obtain the primary data for model building.

Although satellite based sensors, such as the Landsat Thematic Mapper, have also been used successfully to study large rivers together with GIS to document the impact of floods on vegetation diversity in the Amazon River and elsewhere (e.g. Mertes *et al.* 1995; Magilligan *et al.* 1998; Khan and Islam 2003), for smaller rivers such as the Rio Grande de Añasco, airborne remote sensing (such as aerial photography) is a more suitable approach (Bryant and Gilvear 1999). Aerial photography can provide high resolution, frequently less than one meter, and improved temporal and spatial flexibility for mapping and monitoring change (Hooke and Redmond 1989; Milton *et al.* 1995).

This approach has been used successfully by previous investigators to assess changes in river systems (e.g. Laliberte *et al.* 2001; Bryant and Gilvear 1999). Gurnell (1997), for example, used aerial photography with GIS to study channel width changes of meanders of the regulated River Dee in England. Gillespie and Giardino (1996) also used aerial photographs with GIS to assess changes in meander migration rates resulting from the construction of several dams on the Brazos River, Texas, over four decades. Laliberte *et al.* (2001) used aerial photography over a 20 year period with GIS to determine bankfull width and sinuosity of Catherine Creek in northeastern Oregon to

determine changes in riparian rangeland area. Marston *et al.* (1995) similarly used aerial photography and GIS to document channel change of the Ain River in east-central France to assess their effects on floodplain disturbance and vegetation development from 1945 to 1991. Urban and Rhoads (2003) have also used aerial photography and GIS to assess human induced changes to the Embarrass River in Illinois from 1936 to 1993.

These successful applications of GIS to analyze aerial photographs suggest that this approach should be useful for the Rio Grande de Añasco as well. Thus, the valley and river lengths of the meander belt of the study area were measured along with meander migration distance, radius of curvature, and channel widths from the time sequential series of aerial photography in order to characterize channel planform change and determine channel responses.

These data were augmented by field measurements of the silt-clay content and bank strength to develop the empirical model which combine, the information obtained for the above parameters with streamflow gauge data to relate the migration distance as a function of the potential control variables in a multiple regression analysis. The following sections describe the preparation of the aerial photography, the GIS methods used in the quantification of planform change, the measurement of radius of curvature, silt-clay composition and bank strength of the banks.

Aerial Photographs

In this study, planform characteristics of the Rio Grande de Añasco were examined using a time sequential series of aerial photographs. The following aerial

photography data sources were used. Photographs of the study area for July-1966, March-1977, February-1983, January-1990, October-1993, and September-1995 are available from the U.S. Geological Survey (Appendix B). Additional aerial photographs for August-1997, October-1998, and June-1999, are also available from *Aerofoto Internacional,* a private company based in San Juan, Puerto Rico. *West Wings,* a private company based in Lajas (Puerto Rico), and the National Oceanic and Atmospheric Administration (NOAA) provide additional images (August-2004, and November-1999, respectively). There are therefore eight photographs ranging from 1966 to 1999 to calculate meander migration rates over a 33 year period. The series of photographs from 1998 to 1999 were used to investigate the recovery of the Rio Grande de Añasco to Hurricane Georges. All images were georeferenced to the Universal Tranverse Mercator Zone 19 map coordinate system using the North American Datum of 1983 (NAD83; Longley *et al.* 2001). The photographs were registered to a 1 meter digital orthorectified quadrangle image (DOQ) from the U.S. Geological Survey. The aerial photographs are listed in Appendix B. Digital copies of the aerial photographs were made using a scanner and computer and saved at resolutions from 600 to 900 dpi depending on the photograph (Tiegs and Pohl 2005). This technique yielded imagery with cell sizes from 0.5 m to 1.0 m, and root mean square errors (RMSE) of less than 1.0 m (Appendix B).

Georeferencing Aerial Photography

Georeferencing (geocoding, co-registration) is the process of transforming an uncorrected raw image from an arbitrary coordinate system into a geographic or map

projection coordinate system. Once the image has been transformed to a map projection system, it becomes a map from which accurate planimetric measurements can be taken. To ensure accurate co-registration between multi-temporal images various factors are taken into consideration. First, all images must be georeferenced to the same map coordinate system. Map coordinate systems are better than latitudes and longitudes that may cause serious distortions in distance and other properties (Longley *et al.* 2001). A common and preferred map coordinate system is the Universal Transverse Mercator projection whose coordinates are in meters, making it easy to make accurate calculations of short distances between points (Longley *et al.* 2001). Second, all maps coordinate systems should use the same datum ellipsoid. The ellipsoid known as WGS84 (World Geodetic system of 1984) and NAD83 (North American Datum of 1983) are now widely accepted. A GIS program is helpful in transforming old data from NAD27 to NAD83.

The mathematical relationships used in geocoding require ground control points (GCPs) to fit the mathematical functions. A GCP is a point on the earth's surface where both image coordinates (rows and columns) and map coordinates can be identified. When using multi-temporal images it is better if the GCPs stay constant through time. This means that, if possible, the georeferencing process should try to use exactly the same locations throughout all images. These points should be clearly identified and precisely located. Small permanent well defined features such as corners of buildings, airport runways, road intersections, and bridges are good choices. The GCPs should be selected in a regular pattern covering as much image space as possible, all the way to the corners and edges. As terrain variations and geometric distortions increase, the more

GCPs should be used. Another method to improve accuracy is by georeferencing all images to GCP points from an existing orthorectified image such as a DOQ. Although the polynomial method of transformation requires a minimum of 4 GCPs, it is best to use as many as possible in order to reduce the Root Mean Square Error (RMSE; Jensen 2005).

The polynomial will not transform every GCP with 100 percent accuracy and it is important before the full rectification proceeds that errors are within acceptable limits. The RMSE is a statistical measure of the error between the calculated coordinates of a GCP from the fitted polynomial equation and the measured coordinates of the GCP from the fitted polynomial equation and the measured coordinates of the GCP from the orthorectified (or previously georeferenced) image.

$$RMSE= [((\Sigma (x^{measured} - x^{calculated})^2 + (y^{measured} - y^{calculated})^2 / N)]^{½}$$

N is the number of GCPs. The more GCPs that are used the larger the *N* and smaller the RMSE. Also, the error value for each GCP effects and is affected by other GCPs. By using many GCPs, the ones with the highest errors can be eliminated increasing the overall RMSE (Chang 2002; Hutchinson 2004). The RMSE for the aerial photographs used in this study were all less than 1 m, and are listed in Appendix B.

GIS and the Topologically Constrained Transect Method

A geographic information system (GIS) is a computerized spatial support system that can be used for performing operations such as planimetric measurements on geographic data (Longley *et al.* 2001). Within the GIS, georeferenced aerial photographs projected to a map coordinate system can be used to measure distances, such as river and

valley lengths, channel widths and meander migration. To simplify the tedious nature of repeated measurements of meander migration distances, this study applies the Topologically Constrained Transect Method (TCTM) developed by Arias-Moran (2003). This method uses dynamic segmentation to proportionally divide a shapefile into any number of equally spaced transects. The method is useful for measuring meander migration because this extension allows the flexibility to define and measure the length of large amount of transects, while also determining azimuth of the cross section. By using more cross sections, the procedure facilitates more detailed analysis, and the meander apex can be accurately determined. Rotational characteristics of the meander can also potentially be quantified.

The process is the following. By manually tracing the bankfull boundary lines of the river and creating shapefiles using ArcGis 8.3 software, the geometry of the planform of meanders could be extracted into shapefiles for each of the years of study. Bankfull width was consistently measured as the major break separating the well defined channel from the floodplain (Chin *et al*. 2002; Riley 1972). After creating the bankfull boundary lines shapefiles, the centroid or centerline of the meander was determined also using the TCTM method. Then, by placing the shapefiles one on top of another within the GIS, in a process referred to as overlaying, the distance from one meander centerline to the next could be measured by the TCTM algorithm. By repeating these measurements between the elapsed times between aerial photographs, the changes could be quantified.

Radius of Curvature

The radius of curvature is the radius of a circle drawn around a meander bend (Fig. 3). It expresses the degree of tightness of a specific bend, with large values indicating wide-open meander bends. The radius of curvature is usually scaled according to channel width (w) so that it is expressed as a dimensionless ratio of *r to w* (r/w). Also called bend curvature ratio, a smaller r/w ratio indicates a tighter bend.

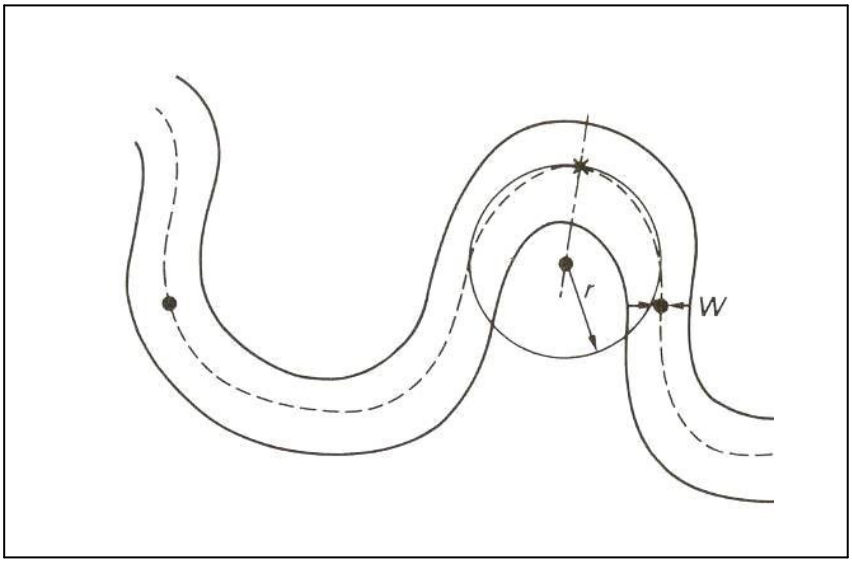

Figure 3 *Radius of curvature of a meander bend.*

The methods commonly used for determining the radius of curvature of a meander bend incorporate visually fitting an approximate circle that best approximates the circular shape of the centerline of the bend or approximating a sine curve (e.g., Leopold and Wolman 1960; Nanson and Hickin 1983; Goudie 1990). These methods

work well if the bend is symmetrical or close to it. When the bend is asymmetrical, these methods may produce inaccurate approximations. A more precise methodology for determining the radius of curvature was therefore developed in this research by combining mathematics with GIS to determine radius of curvature, as follows.

At a given point on a curve, *R* is defined as the radius of the circle of curvature, called the osculating circle (Fig. 4), or the circle which shares the same tangent as the curve at a given point (Kreyszig 1991).

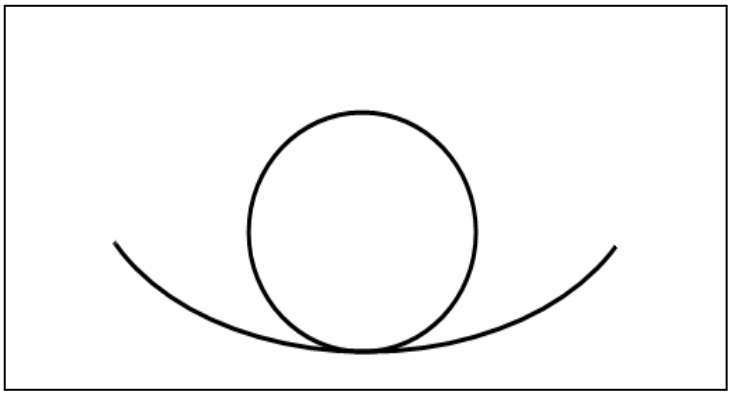

Figure 4 *Osculating circle.*

The radius of curvature of this osculating circle at a given point is given by the equation

$$R = \frac{\left[1+\left(\frac{dy}{dx}\right)^2\right]^{3/2}}{\left(\frac{d^2y}{dx^2}\right)}$$

where dy/dx is the first derivative of the polynomial equation that describes the curve and d^2y/dx^2 is the second derivative of the polynomial equation (Kreyszig 1991). By determining the polynomial equation that describes the circular shape of the meander bend, the radius of curvature of points on this curve can be computed and the mean of the radii of curvature determined.

First, a shapefile of the meander bend curve is created in ArcGis software. This shapefile is then converted to a coverage in ArcInfo. In ArcInfo, the command UNGENERATE is then used to create a text file of the coordinates of the vertices that comprise the curve. These coordinates are then opened in Microsoft Excel, and a scatterplot graph is created. On the "Chart Menu" the "Add Trendline" in the "Options" menu is used to "Display equation on chart." The polynomial equation that describes the curve of the meander bend will be displayed. Once the equation of the curve is known, the radii of curvature are computed by the radius of curvature of the osculating curve equation for each vertex. The radius of curvature of the meander curve is then taken as the mean of these radii.

Silt-Clay Composition of Banks

An important controlling variable in the ability of a stream to shift laterally is the resistance of its banks (Hickin and Nanson 1984). Although bank strength is not simply the function of one material property, it does depend on the degree of cohesion, which can be expressed by its silt-clay content (Ferguson 1987). Silt-clay is defined as sediment smaller than a grain size of 0.074 mm (Schumm 1960), with clay being finer

than 0.0020 mm (Boggs 1987). Most river banks contain significant amounts of silt and clay, and possess some degree of cohesion and resistance to erosion through inter-particle, and electromagnetic bonding (Robert 2003). When erosion does take place, it is often aggregates of grains that are detached (Thorne 1992). Packing and cohesion of bank materials and the likely presence of vegetation and root systems may increase the strength of the bank material and its resistance to erosion (Hickin 1984). The strength of such soil is also dependent on antecedent conditions of wetting and drying (Robert 2003). For all these reasons, the critical conditions for erosion of cohesive banks are complex and difficult to define accurately, and are usually higher than for non-cohesive banks (Thorne 1992).

Several relationships relating to channel planform parameters have been developed using the silt-clay percentage of the channel boundary. For example, Schumm (1963) determined a relationship between sinuosity and channel boundary composition, and showed that sinuosity (S) increases with the percentage of silt-clay content of the channel boundary (M):

$$S = 0.94\ M^{0.25}$$

Schumm (1960, 1969) also developed a relationship between the width (w) and depth (d) ratio to the silt-clay content of the channel boundary (M):

$$w/d = 255\ M^{-1.08}$$

Further, Ferguson (1987) developed a relationship for width (w), but with mean annual flood ($Q_{2..33}$), and the silt-clay content of the banks (B):

$$w = 33.1\ Q_{2..33}\ B^{-0.66}$$

Both of these relationships imply a strong dependence of channel shape on the silt-clay percentage of the channel boundary.

The silt-clay content of channel banks in temperate rivers varies enormously. The soil profile of a particular location varies enormously with intensity of weathering processes and the character of the original and paleoenvironmental conditions (Ritter 2002). For example, Medano Creek in Colorado was found to have silt-clay content in its banks of 0.5%, while the Sage Creek in South Dakota was found to have 96% (Schumm 1960). In a study that included 90 alluvial channels across the United States, the silt-clay percentages of the banks were found to have a mean value of 59% (Schumm 1960). In a study that included 11 streams in Devon, England, the silt-clay percentages of the banks were found to have a mean value 60.6% (Hooke 1980). The silt-clay content of the Rio Grande de Añasco was investigated to evaluate the extent to which it affects meandering dynamics and channel morphology.

To determine the silt-clay content of the study concave banks, eight composite samples were collected and analyzed. The sampling sites were bends B1 through B8 of Study Area One (Fig. 10). Four samples of bank soil were collected from different points of the concave portion, or the outer bank, and combined to form one composite sample that represents that particular bend. This was repeated for the eight bends.

Sieve Analysis

Standard mechanical sediment analysis was used to determine the silt-clay content of the concave banks of the Rio Grande de Añasco. Mechanical analysis is the

determination of the size distribution of sediments in a sample. Sieve analysis consists of shaking the sediment sample through a set of sieves that have progressively smaller openings. U.S. standard sieve sizes range from sieve number 4 (4.75 mm opening) to sieve number 275 (0.053 mm opening; Boggs 1987). Silt-clay, sediment smaller than a grain size of 0.074 mm (Schumm 1960; 1963; 1977), corresponds to material that passes the 200 mesh sieve (U.S. Standard, Braja 2000) in a standard sediment size analysis. The percentage of silt-clay by weight is then computed by weighing all the material that passes the 200 mesh sieve and dividing this amount by the total weight of the sample (Boggs 1987).

The specific procedures are as follows. First, the sediment sample is oven dried for approximately 24 hours at 100°C. Second, all lumps are separated into small particles. Third, they are passed through sieves and shaken with sieve shaker for at least 10 minutes. Fourth, after the shaking period is over, the weight of sediment sample retained in each sieve is determined (Braja 2000). However, when cohesive soils are analyzed, such as might be expected in the study samples, it may be difficult to break lumps into individual particles. In that case, the soil is mixed with water to make a slurry and then washed through the sieves (wet sieving; Gordon *et al.* 2004). Fifth, the remaining lumped particles are placed into the 200 mesh sieve with the pan below and washed under running water, gently rubbing the mud balls to break them apart and wash out of the sample. Lastly, the samples are let dry and the silt-clay portion of the sediment sample was then determined. The silt-clay percentage of the sediment sample can then be computed.

Bank Strength

In this study, a primary potential control variable to be used in the development of the empirical model for estimating meander migration distance is the bank strength of the outer or concave portion of the meander. Previous studies provide guidance on how to measure *in situ* streambank soil shear strength. Micheli and Kirchner (2002) measured bank strength by using a vane shear tester and found that herbaceous riparian vegetation increases the cohesion of the streambank up to eight times in comparison with non-vegetated soils through root reinforcement. The vane shear tester measures the shear strength of a soil (Braja 2000). In another study of flow structure and development of meander pools, Andrle (1994) used a pocket penetrometer to measure bank strength. The pocket penetrometer is an instrument that estimates the compressive strength of a soil, usually to assist in classification (Parsons *et al.* 2001).

For this study, the vane shear test was used as it is considered a more complete measurement of bank strength (Braja 2000). Also, it has an American Standard for Testing and Materials (ASTM) standard (D4648-00), whereas the pocket penetrometer does not. More reliable results for the *in situ* shear strength of very cohesive soils can be obtained directly from the vane shear test (Braja 2000). The shear vane consists of four thin, equal-sized steel plates welded to a steel torque rod. The vane is pushed into the soil, and then torque is applied to rotate the vane at a uniform speed until the soil fails. The shear strength magnitude is then read off the calibrated tester and appropriate conversion factors applied if necessary (Braja 2000). In this study, four measurements of

the bank shear strength were taken at different locations within the wetted area of the meander concave bank for each of the eight study bends B1 to B8.

Summary

In summary, the general approach to this study is to use aerial photography and geographic information systems (GIS) to quantify planform changes and obtain the necessary data to determine relationships and develop the model for meander migration. This approach has been used successfully by previous investigators to assess changes in river systems. Analysis of a time sequential series of aerial photographs provided data for sinuosity, meander migration, radius of curvature, and channel width changes. Augmented by field measurements of the silt-clay content and bank strength these data provided the information necessary to accomplish the research objectives of this study.

CHAPTER V

CHANNEL PLANFORM

This chapter examines the pattern and channel planform dynamics of the Rio Grande de Añasco in order to characterize planform change. This objective seeks to answer the following questions: how static or dynamic is the channel pattern; what are its meander migration rates and how do they compare with rivers from temperate climates; and how does the ratio of meander-bend curvature to channel width (r/w) relate to the maximum meander migration rate? The working hypotheses are that change in the Rio Grande de Añasco is highly dynamic, exhibiting rapid changes in short time periods, that the primary mechanism of planform change is through cutoffs and avulsions, rather than braiding, and that the mean meander migration rate and the ratio of meander-bend curvature to channel width (r/w) for maximum migration in a humid tropical river, are similar to those reported in humid temperate rivers.

This study focuses on the alluvial channel at a spatial scale of an entire meander belt several kilometers in length and at a temporal scale of 33 years, a period over which changes in planform and individual meander location can be observed. The approach is to measure sinuosity changes, meander migration, radius of curvature of bends and channel width using aerial photography then analyzed in a GIS. The variation and trends in characteristics and mobility will be analyzed throughout the meander belt to assess changes in form and process.

Sinuosity

Sinuosity was measured for the meander belt of the Rio Grande de Añasco from the georeferenced aerial photos for the years 1966, 1977, 1983, 1990, 1993, 1995, 1997, and 1999 (Study Area One, Fig. 2). The sinuosity ratios were obtained for the study river and are shown in Table 1. Leopold and Wolman (1957) originally proposed a sinuosity of 1.5 as the boundary between straight and meandering. From the results of the measurements, which are all greater than 2.22 with a mean of 2.40, the portion of the Rio Grande de Añasco studied can be classified as meandering according to this criteria. Schumm (1963) further recommended five classifications depending on sinuosity value: straight (1.1), transitional (1.3), regular (1.7), irregular (1.8), and tortuous (2.3). The Rio Grande de Añasco is a tortuous river according to the Schumm (1963) classification. Brice (1984) similarly added additional classifications for meandering rivers such as sinuous canaliform, sinuous point bar, sinuous braided. The canaliform tend to have the narrowest widths and the highest sinuosities (Brice 1984). The Rio Grande de Añasco would classify under this scheme as a sinuous canaliform river. These sinuosity indices indicate that the Rio Grande de Añasco is a highly meandering stream, at least in the reaches studied.

Sinuosity values have been determined for many rivers in temperate climate regions. For example, the Powder River, the Solomon River, and the Republican and Sappa Rivers showed sinuosities of 1.2, 2.4, 1.3, and 1.9, respectively (Schumm 1963). The Beaver River in Alberta, Canada, and the Mississippi River, from Cairo to Memphis, also exhibited sinuosities of 1.25, and 1.55 respectively (Chitale 1970)

whereas the Murrumbidgee River in New South Wales, Australia, had a sinuosity of 2.0 (Schumm 1977). Also, a study of 47 rivers in the Great Plains, U.S.A., showed a mean sinuosity of 1.57, with a range of values from 1.2 to 2.6 (Schumm 1963). The mean sinuosity of the Rio Grande de Añasco was found to be 2.40 over the study period. In contrast, another example of a humid tropical river, the Angabunga, in Central Congo, Africa , showed a sinuosity of 1.60 in 1970 (Chitale 1970).

The sinuosity found for the study river of the humid tropical climate is similar to those found in temperate environments. Furthermore, not only does it compare with the above temperate rivers but also with an example from the semi-arid. The semi-arid White River in Crawford, Nebraska had a sinuosity of 2.40 in 1963, a mean silt-clay composition of its banks of 79%, and a basin area of 801 km^2 (Schumm 1963). The mean annual precipitation of this river is 406mm (16 in.; Ferrick *et al.* 1995). The humid tropical Rio Grande de Añasco and the semi-arid White River have similar sinuosity, silt-clay composition of banks, and watershed area, yet different precipitation regimes.

A controlling variable in the ability of a stream to shift laterally is the resistance of its banks (Hickin and Nanson 1984). Although this resistance is not simply the function of one material property, it does depend on the degree of cohesion, which can be expressed by its silt-clay content (Ferguson 1987). Most river banks contain significant amounts of silt and clay, and possess some degree of cohesion and resistance to erosion (Robert 2003).

Using data from temperate rivers, Schumm (1963) determined a relationship between sinuosity and channel boundary composition, and showed that sinuosity (S) increases with the percentage of silt-clay content of the channel boundary (M):

$$S = 0.94\ M^{0.25}$$

This relationship implies a strong dependence of channel shape on the silt-clay percentage of the channel boundary.

In a study that included 90 alluvial channels across the United States, the silt-clay compositions of the banks were found to have a mean value of 59% (Schumm 1960). A sample of 47 rivers in the Great Plains, U.S.A., showed a mean sinuosity of 1.57 (Schumm 1963). For the Rio Grande de Añasco the mean sinuosity was found to be 2.40. A subsequent chapter that develops the empirical model shows that the mean silt-clay composition of the Rio Grande de Añasco is 83%. The higher sinuosity of the Rio Grande de Añasco (2.40) versus that of the mean of the temperate rivers (1.57) reported by Schumm (1960) is due mainly to the higher silt-clay composition of the channel that produces higher resistance to erosion.

Sinuous streams are characterized by a low width-depth ratio, a high percentage of silt-clay, and a lower gradient than straight channels. Schumm (1960) concluded in his study of sinuosity of alluvial rivers in the Great Plains that, *"Discharge itself does not affect the sinuosity of streams."* However, changes in discharge may cause a modification of sinuosity through its effect on the type of sediment load transported through the channel.

Table 1 *Sinuosities of the Rio Grande de Añasco from 1966 to 1999*

Year	Valley Length (m)	River Length (m)	Sinuosity	Percent Change
1966	3731	8290	2.22	-
1977	3731	9277	2.49	12%
1983	3731	8768	2.35	-5%
1990	3731	8561	2.29	-2%
1993	3731	9059	2.43	6%
1995	3731	9180	2.46	1%
1997	3731	9176	2.46	-
1999	3731	9359	2.51	2%
1966 to 1999	3731	9359	2.51	13%

The sinuosity of the Rio Grande de Añasco shows an overall increase of 13% for the 33 year study period (Table 1). The sinuosity of temperate rivers has also been demonstrated to change over time. For example, Catherine Creek in northeastern Oregon experienced a sinuosity change of six percent from 1979 to 1998 (Laliberte 2001). In England, sinuosity changes of 18% were measured in the River Culm, 16% in the River Creedy, 20% in the River Otter, and 28% in the River Yarty from 1903 to 1953 (Hooke 1977). The Rio Grande de Añasco shows an increase in sinuosity of 12% in the 11 year period from 1966 to 1977, and then a 5% reduction during the 1977 to 1983 period. Sinuosity decreases again during 1983 to 1990 by 2%, for an overall reduction in river length of 8% during the 13 year period from 1977 to 1990 (Fig. 5). For the nine year period from 1990 to 1999 the river increased its length by 798 m or 9%.

Sinuosity of a river increases or decreases to adjust channel gradient which may then increase or decrease flow velocity. This is used as a mechanism to dissipate excess energy. Also, sinuosity increases frictional resistance to flow as a function of the sediment load characteristics (Richards 1982). Changes in the River Culm were attributed not to precipitation variability but to human interference with the channel (Hooke 1977). For the other rivers the cause of change, whether because of human interference, change is an adjustment of agricultural practices, filed drainage, and urban activity, was difficult to assess (Hooke 1977).

The working hypothesis of this study was that change in channel pattern of the representative humid tropical river would be highly dynamic, experiencing rapid changes in relatively short time periods. Overall, the rate of change in sinuosity of the

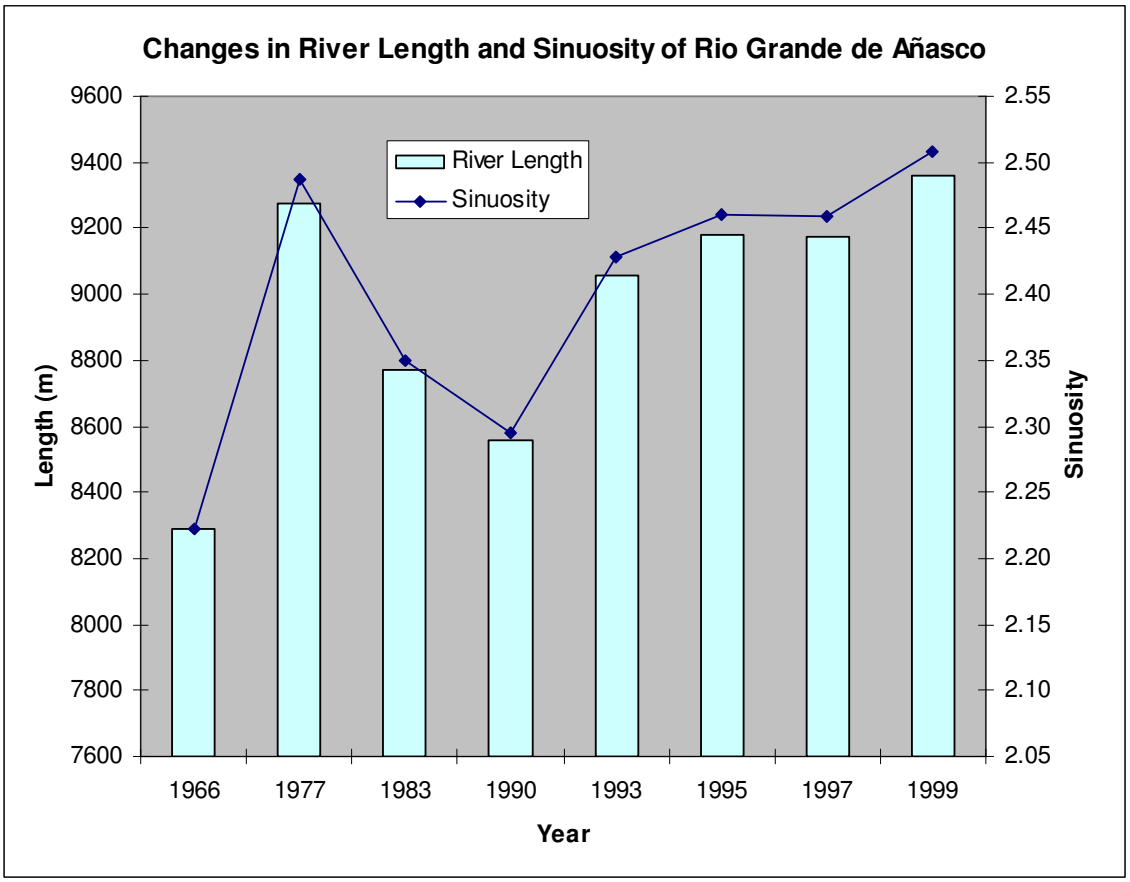

Figure 5 *Changes in river length and sinuosity of the Rio Grande de Añasco.*

Rio Grande de Añasco shows an overall increase of 13% (from 2.22 to 2.51) for the 33 year study period. This is comparable to the rate of change found in the Rivers Culm, Otter and Yarty of temperate climate England (Hooke 1977). In this regard, the humid tropical river represented by the Rio Grande de Añasco can be considered similar in rate of change in sinuosity to those documented for the temperate climate rivers cited. Changes in sinuosity are principally controlled by silt-clay composition of the channel boundary, the type of riparian vegetation and the characteristics of the sediment load, and not by a particular precipitation regime.

Cutoffs and Avulsions

Previous literature suggests that changes in sinuosities are caused by changes in channel planform such as meander cutoffs, avulsions, or braiding. As sinuosity increases, the probability of a chute or neck cutoff increases (Bridge 2003). Cutoff and avulsions are significant for the termination of meandering sequences and the restriction of high sinuosity in meandering channels (Petts and Calow 1996). Several types of meander cutoffs can occur. Neck cutoffs are produced by the breaching of narrow gaps between adjacent channel bends. Chute cutoffs involve more extensive scouring of new channels across floodplains, generally occurring across recently deposited point bar and low floodplain deposits. The probability of their occurrence presumably increases the greater the decrease in bend length provided by the cutoff and the lower the elevation across the cutoff site (Howard 1992). The probability also depends upon main channel flow velocity and depth near the chute and the angle with which the upstream end of the

chute intersects the main stream at its upstream end, decreasing in likelihood as the angle approaches 90° and proportionately less flow is diverted. Cutoffs are initiated primarily during high flows, although complete diversion is generally a slow process (Bridge 2003).

Avulsions occur when the river channel abandons sections of a river in favor of a more direct route at a lower elevation on its floodplain as a result of floodplain aggradation (Howard 1992). It causes a meander or entire segments of rivers to become abandoned and new ones to form (Thomas 2000). Also, avulsions are important in the development of floodplains and may be accompanied by a transformation in channel pattern and are difficult to predict (Petts and Calow 1996). They form as a result of water super-elevation on the outside of banks during flood conditions, and tend to exploit old channels of the river. Large-scale avulsions have been observed on large meandering rivers such as the Mississippi (Hooke 1995) where overbank flow can be diverted for many kilometers. At a smaller scale, chute cutoffs and avulsions tend to take place where the meander bend curvature is such that at high flow the flood waters spill over to take a straighter course.

The braided pattern is one where reaches of the river are divided into various channels separated by bars or islands. The characteristic feature of the braided pattern is the repeated division and joining of channels (Robert 2003). Environments of typically braided rivers include alluvial fan and deltaic regions and glacial outwash. Many streams which meander at high flow may be braided at low stages, and may be as common as meanders in all climatic regions (Morisawa 1985). Braiding has been attributed to many

causes including erodible banks, steep river gradients, an abundant and coarse bedload, and a lack of river competence. Braided rivers have a high width to depth ratio, i.e. their cross sections are wide and shallow (Bridge 2003).

To determine the occurrence of pattern changes, such as cutoffs, avulsions or braiding, the centerlines of the meander belt in Study Area One were overlayed using ArcGis for the years 1966, 1977, 1983, 1990, 1993, 1995, 1997, and 1999. By gradually putting each of these layers one on top of the other starting in 1966, planform change can be more easily identified (Fig. 6). With this process, three cutoffs were shown to have occurred during the period of study. Cutoff 1 (Fig. 7) occurred sometime between 1977 and 1983. Cutoff 2 and 3 (Fig. 8 and Fig. 9 respectively) happened sometime between 1983 and 1990. There were no avulsions during the period from 1966 to 1999, and there is no evidence of braiding.

From 1966 to 1977 the sinuosity of the meander belt changed from 2.22 to 2.49 an increase of 12%. During the period from 1977 to 1983 sinuosity dropped to 2.35. A neck cutoff occurred during this period in the central portion of the meander belt (Fig. 7) that reduced the length of the river by 879 m (Table 2). This explains the lowering of sinuosity for the period. An additional two cutoffs, both chutes, occurred during the period from 1983 to 1990 (Fig. 8 and Fig. 9). These further reduced the length of the river by 308 m. Overall, for the period from 1966 to1977 the river length within Study Area One increased by 1013 m. From 1977 to 1990 it reduced by 716 m (Table 1). Totals for these two periods include reductions by cutoffs and increases by meander

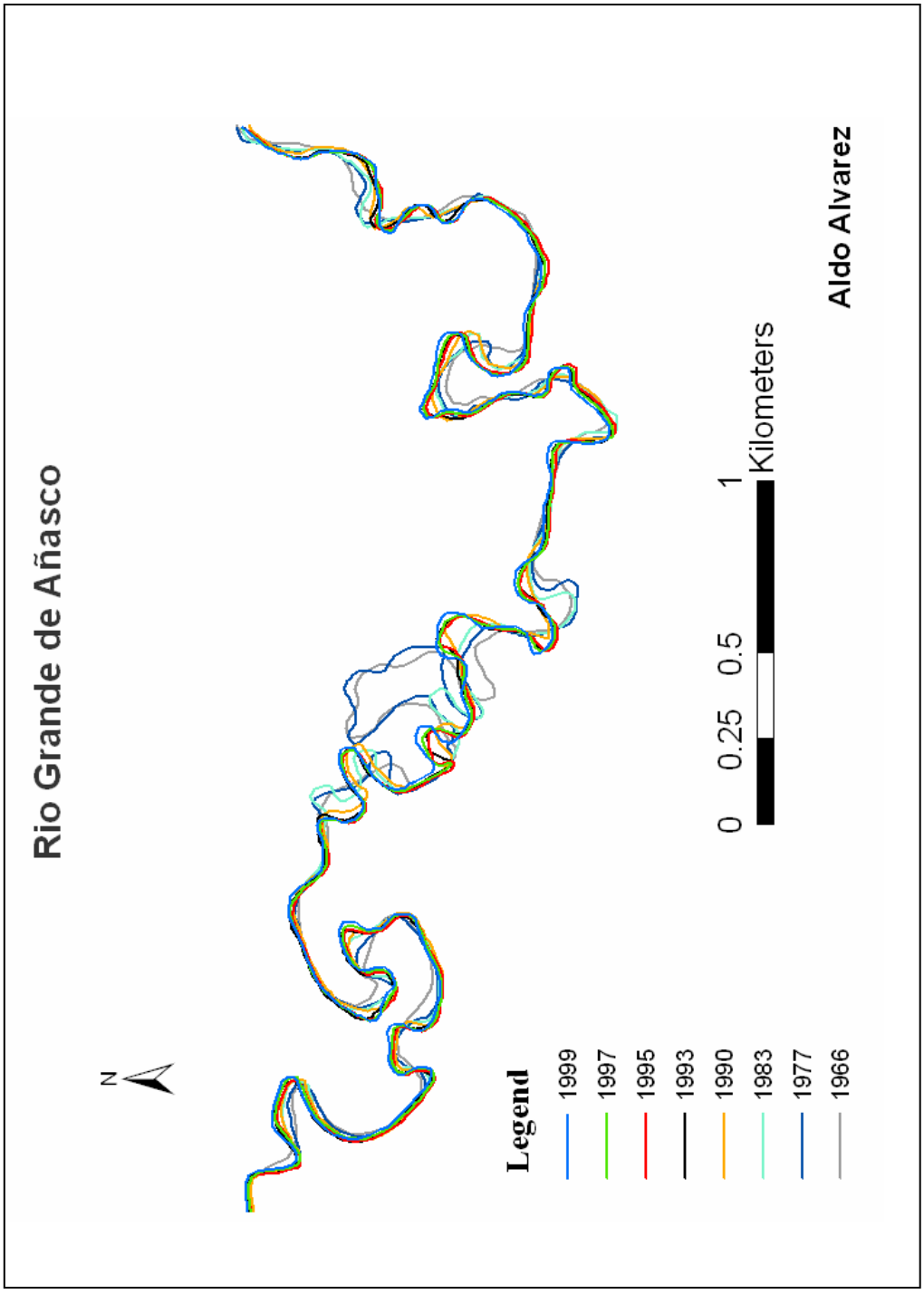

Figure 6 *Planform of the Rio Grande de Añasco for the years 1966 to 1999.*

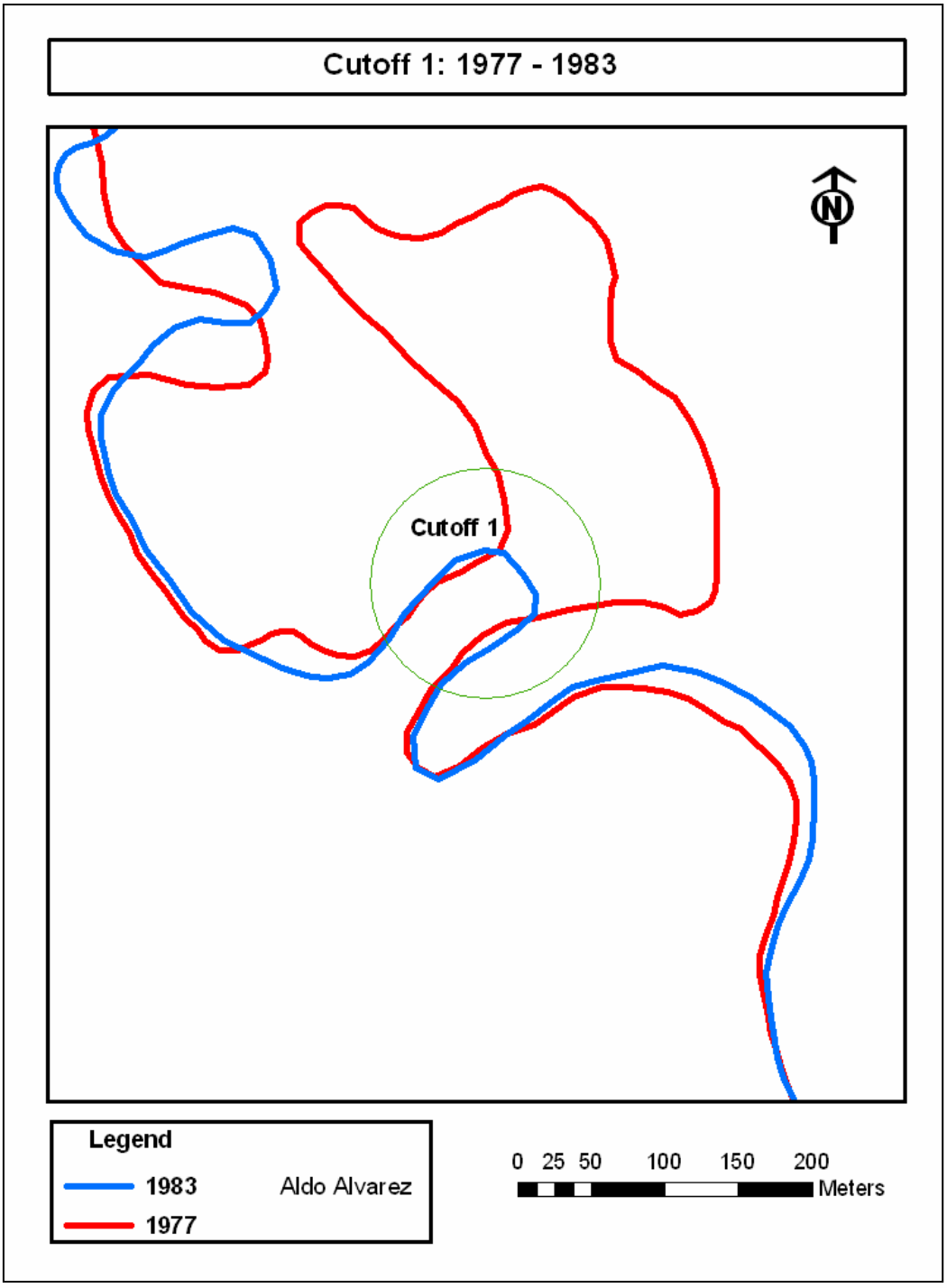

Figure 7 *Meander Cutoff 1 occurring sometime between 1977- 1983.*

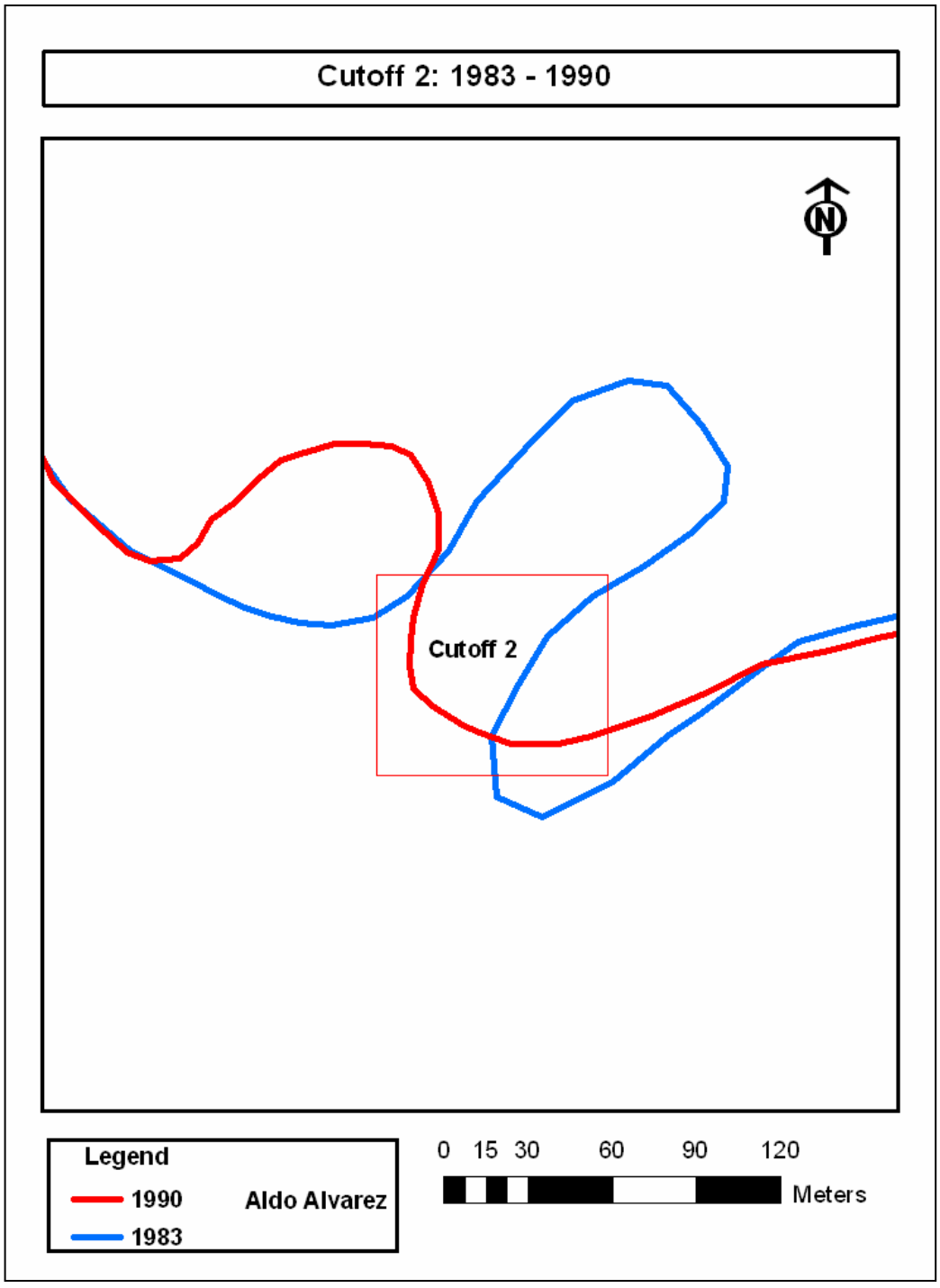

Figure 8 *Meander Cutoff 2 occurring sometime between 1983 - 1990.*

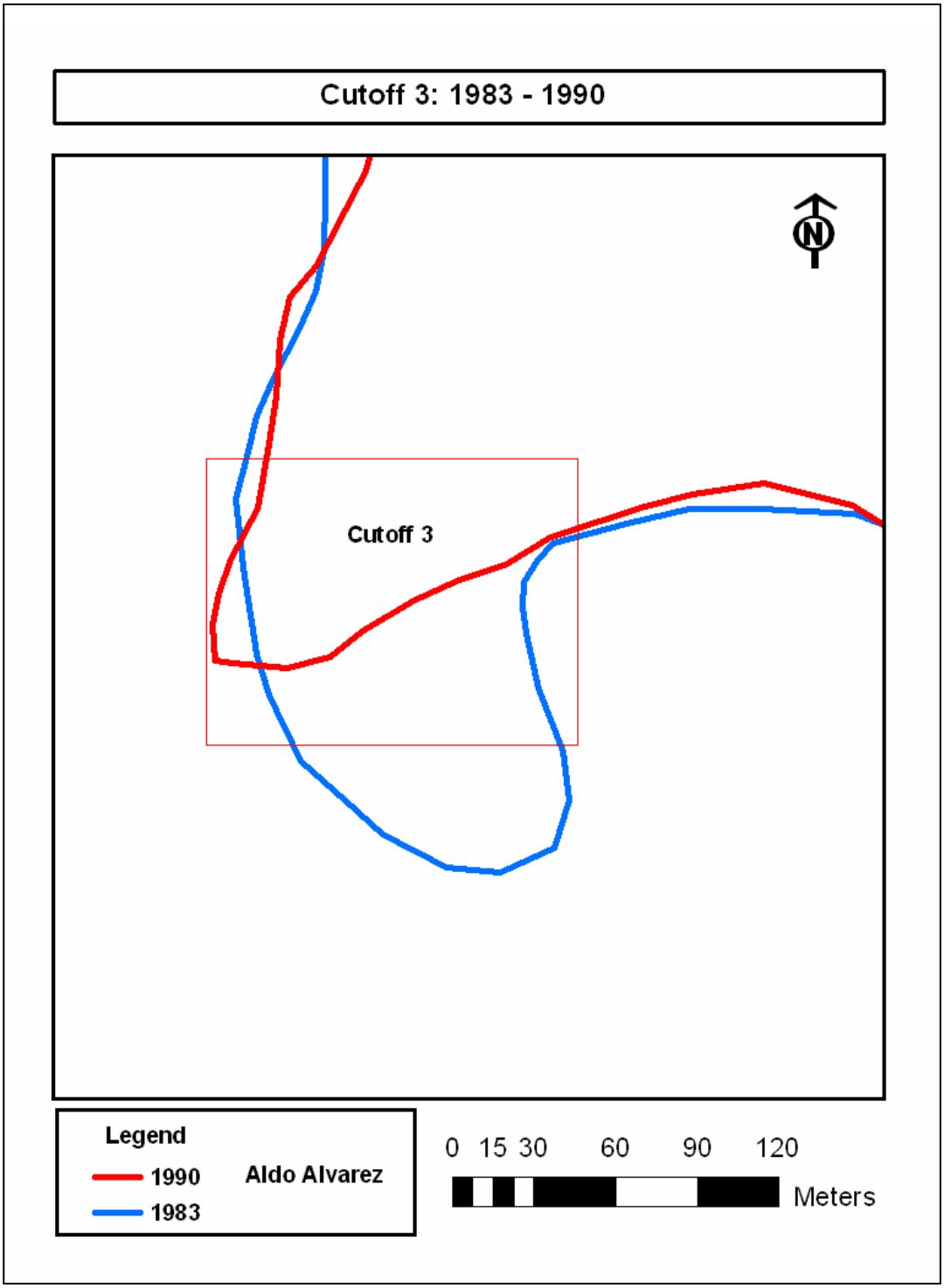

Figure 9 *Meander Cutoff 3 occurring sometime between 1983 - 1990.*

Table 2 *Channel lengths and sinuosity of the three cutoff sites*

	Pre-cutoff	Post-cutoff
Cutoff 1 (Neck)		
Channel length (reach/bend)	1190 m	311 m
Channel length (cutoff)	-	54 m
Valley length (cutoff)	84 m	84 m
Sinuosity	14.2	3.7
Cutoff 2 (Chute)		
Channel length (reach/bend)	394 m	228 m
Channel length (cutoff)	-	74 m
Valley length (cutoff)	138 m	138 m
Sinuosity	2.9	1.7
Cutoff 3 (Chute)		
Channel length (reach/bend)	294 m	152 m
Channel length (cutoff)	-	119 m
Valley length (cutoff)	134 m	134 m
Sinuosity	2.2	1.1

migration. From 1990 to 1999 the river experienced growth in length of 798 m. This represents an increase of 10% in sinuosity from 2.29 to 2.51. For the period of study from 1966 to 1999, the river has grown until reaching a sinuosity of approximately 2.50 when an adjustment such as a cutoff has occurred. The sinuosity of 2.51 in 1999 would hint at the possibility of an adjustment occurring in the near future. The observation of the aerial photography indicates that a neck cutoff between B3 and B4 (Fig. 10) of this study is a possibility in the near future. As sinuosity increases, channel slope decreases, and stream power decreases concomitantly. In order to be able to carry its sediment load, the meandering river is expected to increase its channel slope cyclically in order to increase its sediment transport capability, and this is accomplished by meander cutoffs or avulsions with the consequence of channel straightening.

The working hypothesis for this objective was that the primary mechanism for planform change in the representative humid tropical river was through cutoffs and avulsions, rather than braiding. Although braiding occurs in temperate rivers, this process is less likely to occur in tropical rivers because conditions usually associated with braiding (erodible non-cohesive banks, steep river gradients, abundant coarse bedload, and wide channels; Morisawa 1985) are not common in tropical rivers. The Rio Grande de Añasco has resistive cohesive banks with narrow channels that inhibit braiding. The results of this study reflect that three cutoffs and no avulsions or braiding were observed during the study period and partially supports the stated hypothesis. For this river, the principal mechanism of planform change was through cutoffs during the 33 year period of study. Hooke (1995) suggested that the spatial and temporal

occurrences of cutoffs and avulsions have received little analysis in temperate rivers, and data for comparison with temperate rivers is limited. This study enhances the limited theory available not only for a humid tropical river, but for all rivers in general.

Meander Migration

Meanders migrate across the floodplain because alluvial rivers erode and deposit sediment along their banks. This lateral migration or movement is confined within a certain area of the floodplain known as the meander belt. This section documents the movement of eight meanders in the Rio Grande de Añasco within the meander belt of the floodplain for periods from 1966 to 1999. They have been selected from Study Area One of the Rio Grande de Añasco and are shown in Figure 10. The bends have been selected to represent not only the entire length of the meander belt but also to represent the range of all possible radii of curvatures. This is an important parameter that will be discussed in more detail in the next section.

Using the set of rectified aerial photographs, the centerlines of the stream channel for the eight meander bends were digitized using ArcGis. The movement from the centerline for one period for a particular bend, for example, could then be determined in relation to another period for the same bend. Using the Topologically Constrained Transect Method (TCTM; Arias-Moran 2003) the meander migration for the eight bends for the study period was determined and is shown in Figures 11 through 17. The maximum migration distance and rates for each of the bends are summarized in Table 3.

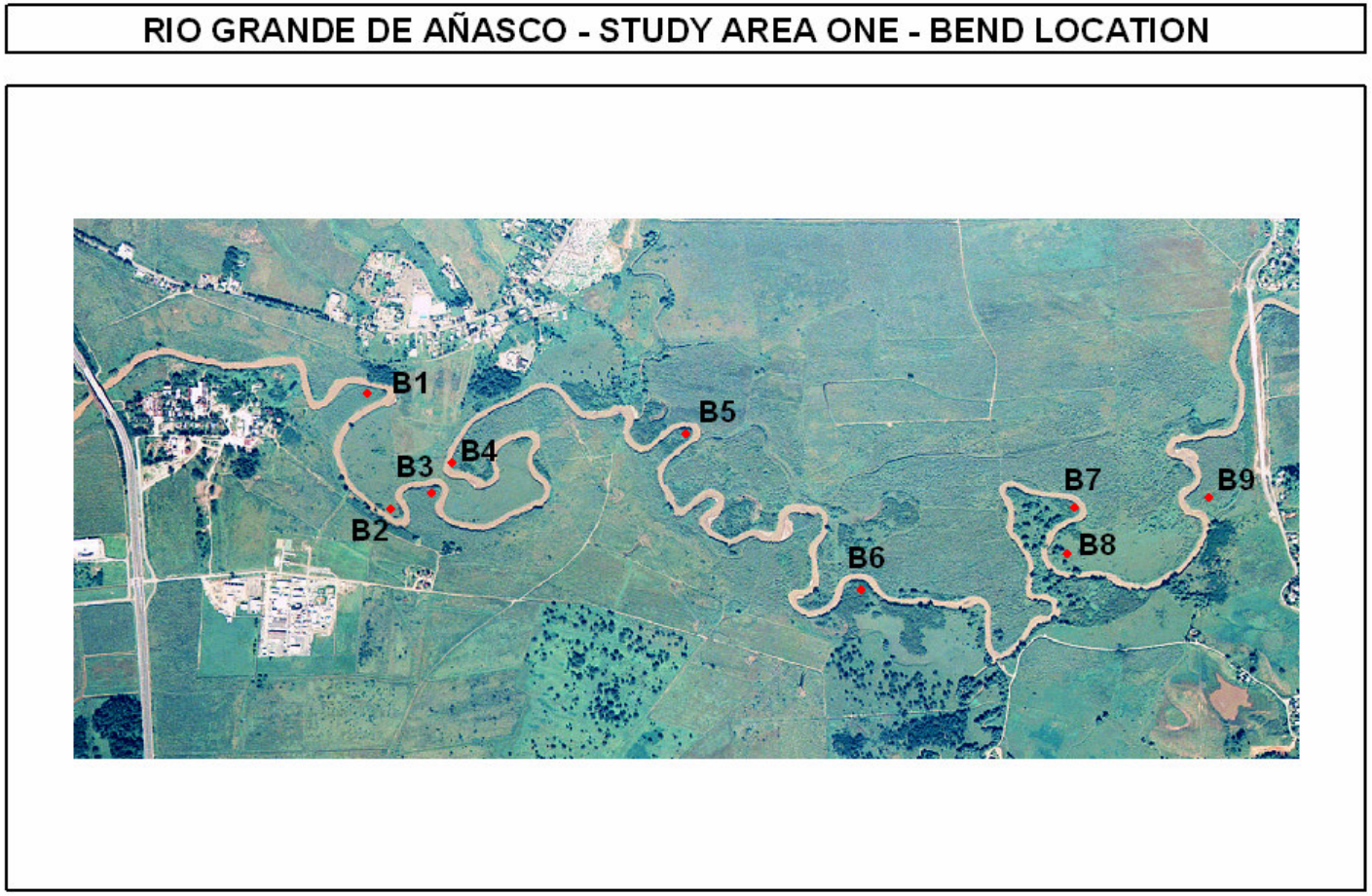

Figure 10 *Location of study bends within Study Area One - Rio Grande de Añasco.*

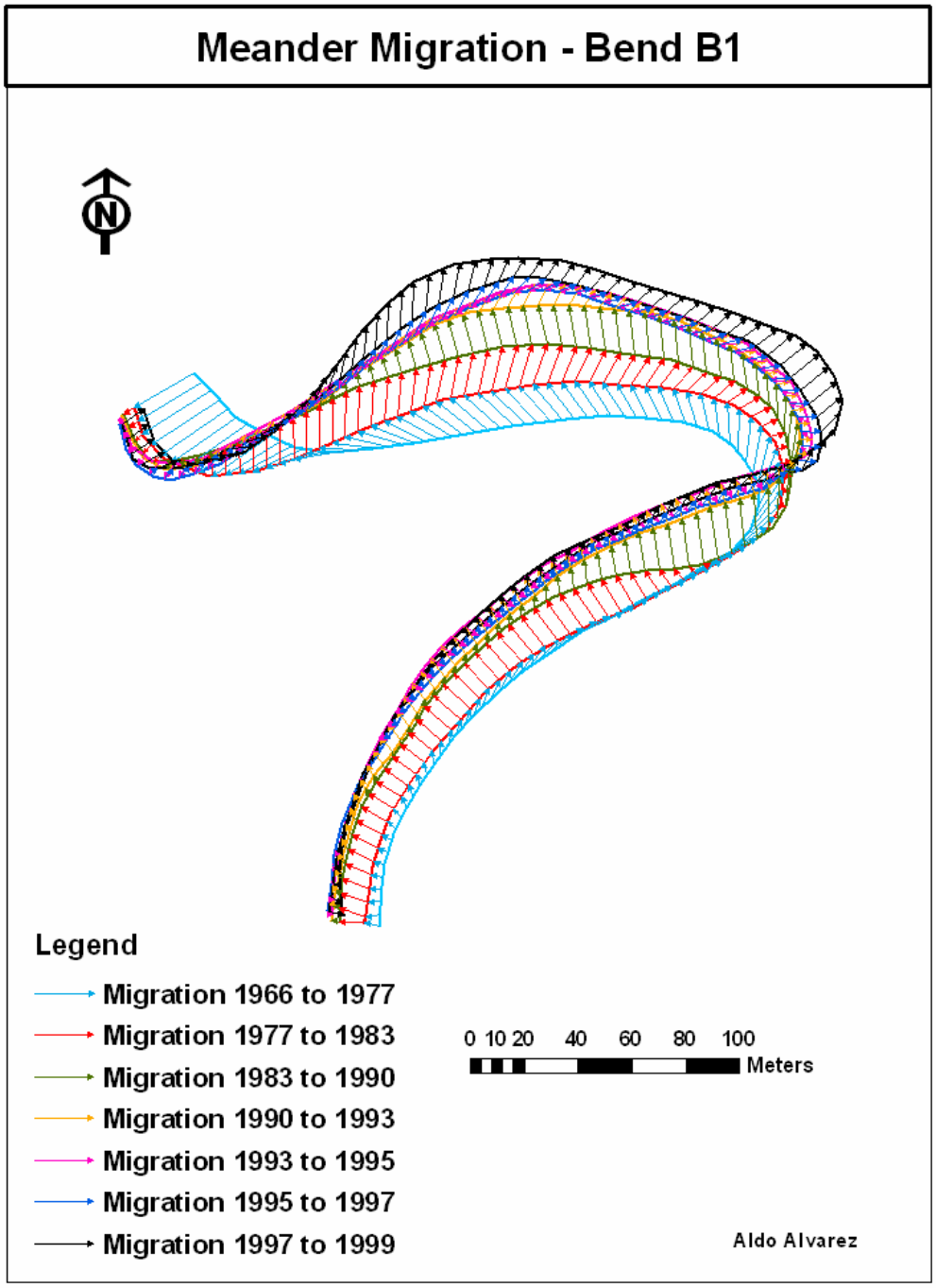

Figure 11 *Meander migration of bend B1 from 1966 to 1999.*

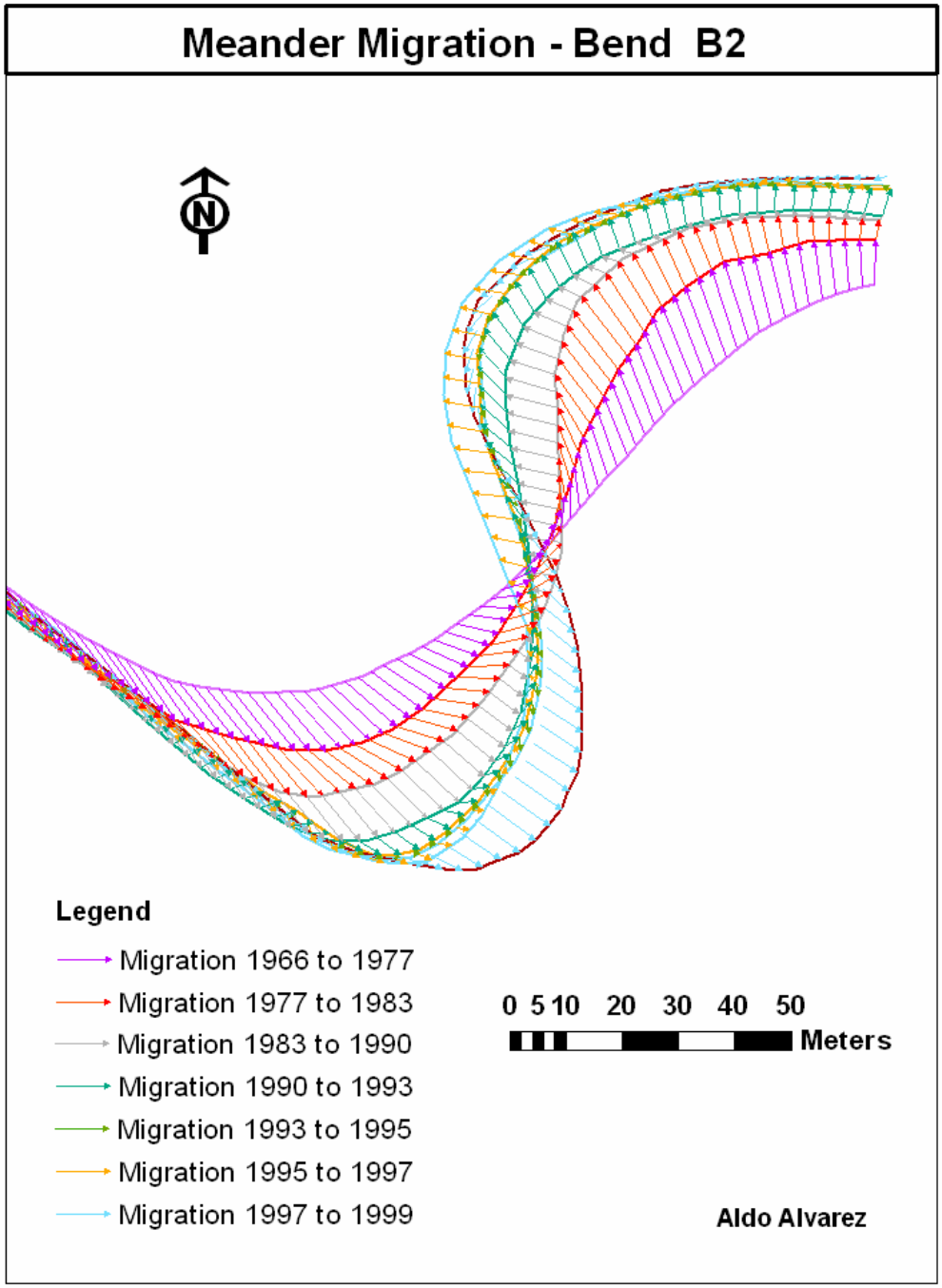

Figure 12 *Meander migration of bend B2 from 1966 to 1999.*

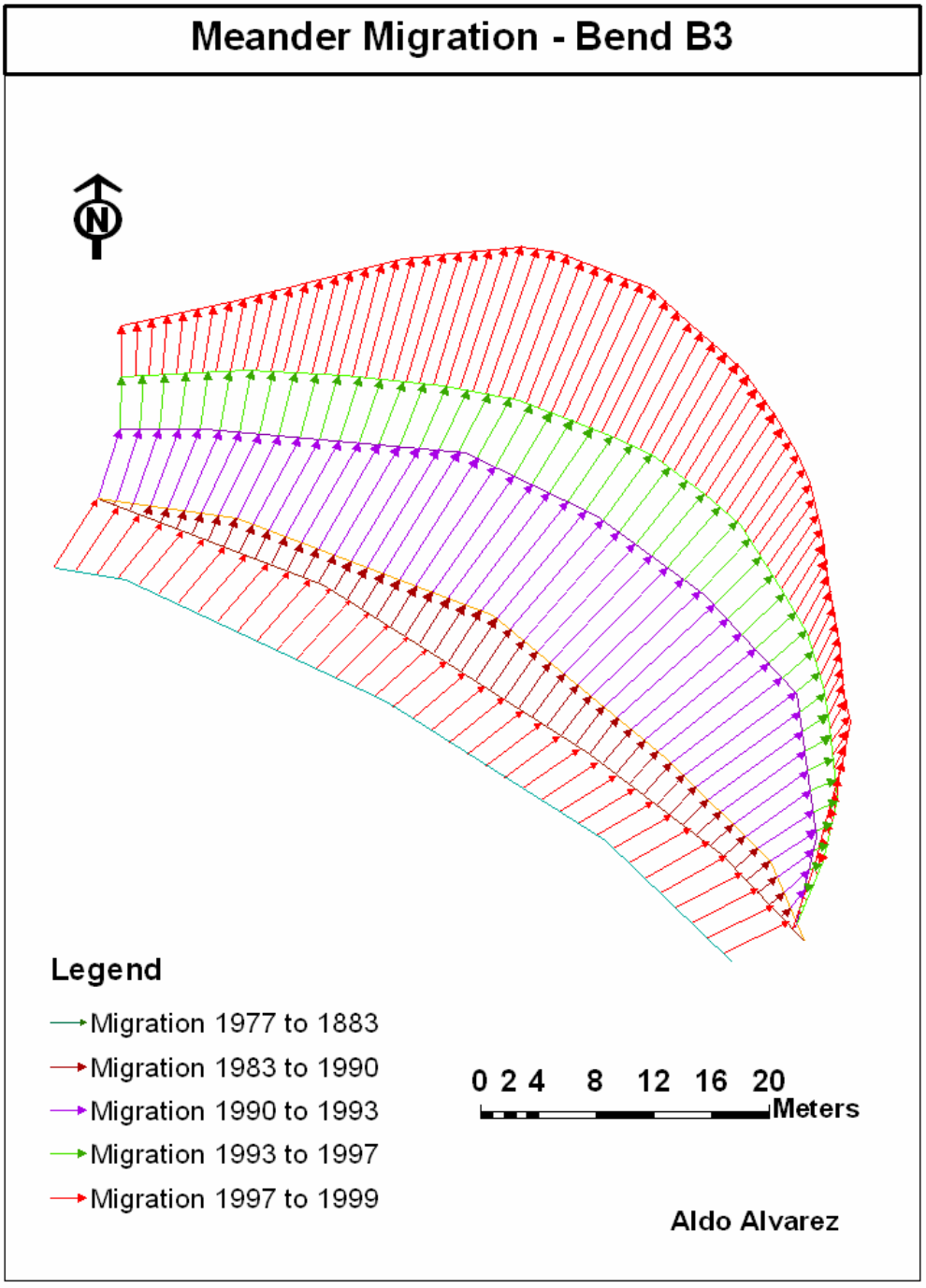

Figure 13 *Meander migration of bend B3 from 1977 to 1999.*

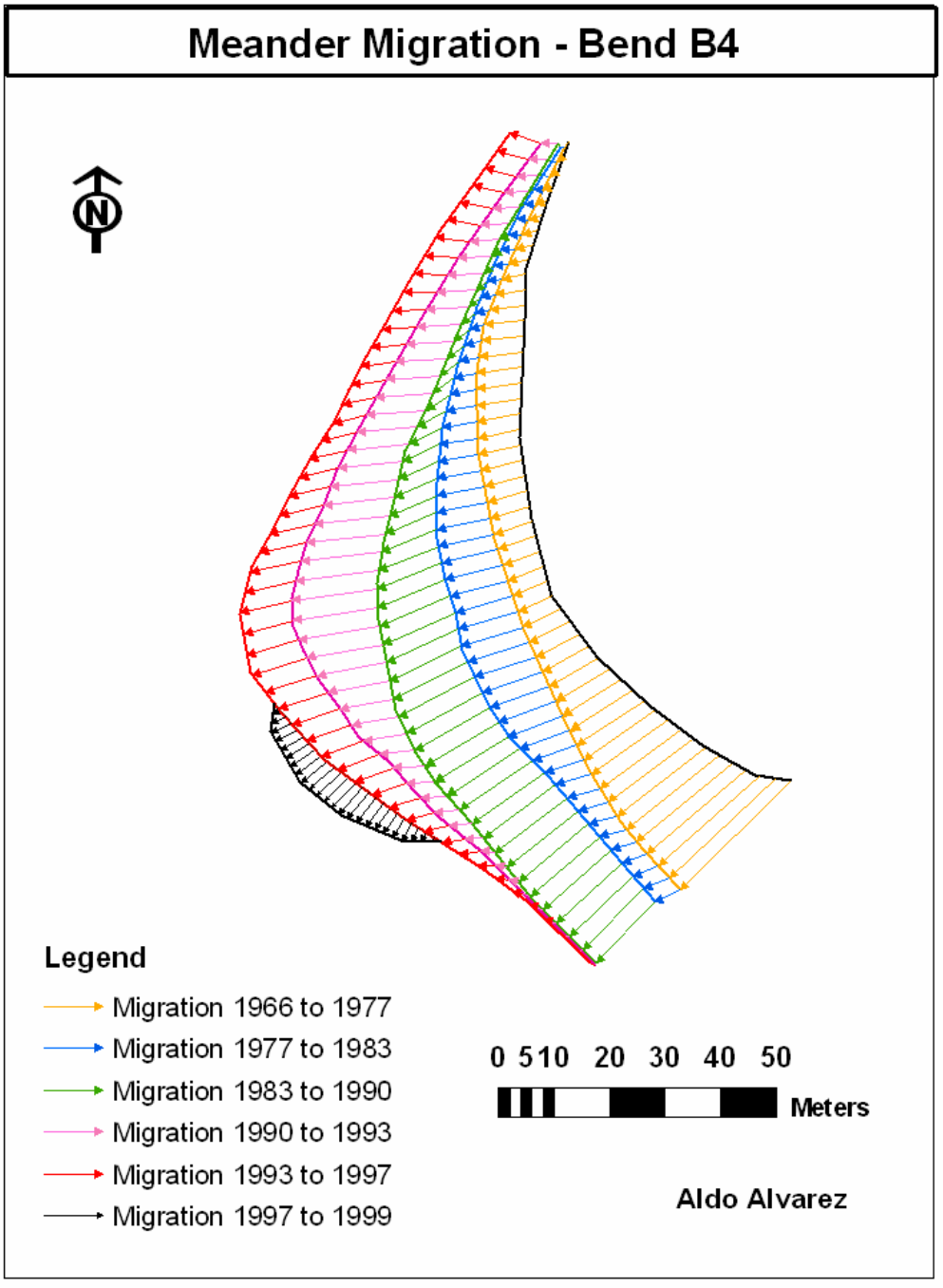

Figure 14 *Meander migration of bend B4 from 1966 to 1999.*

Figure 15 *Meander migration of bend B5 from 1990 to 1999.*

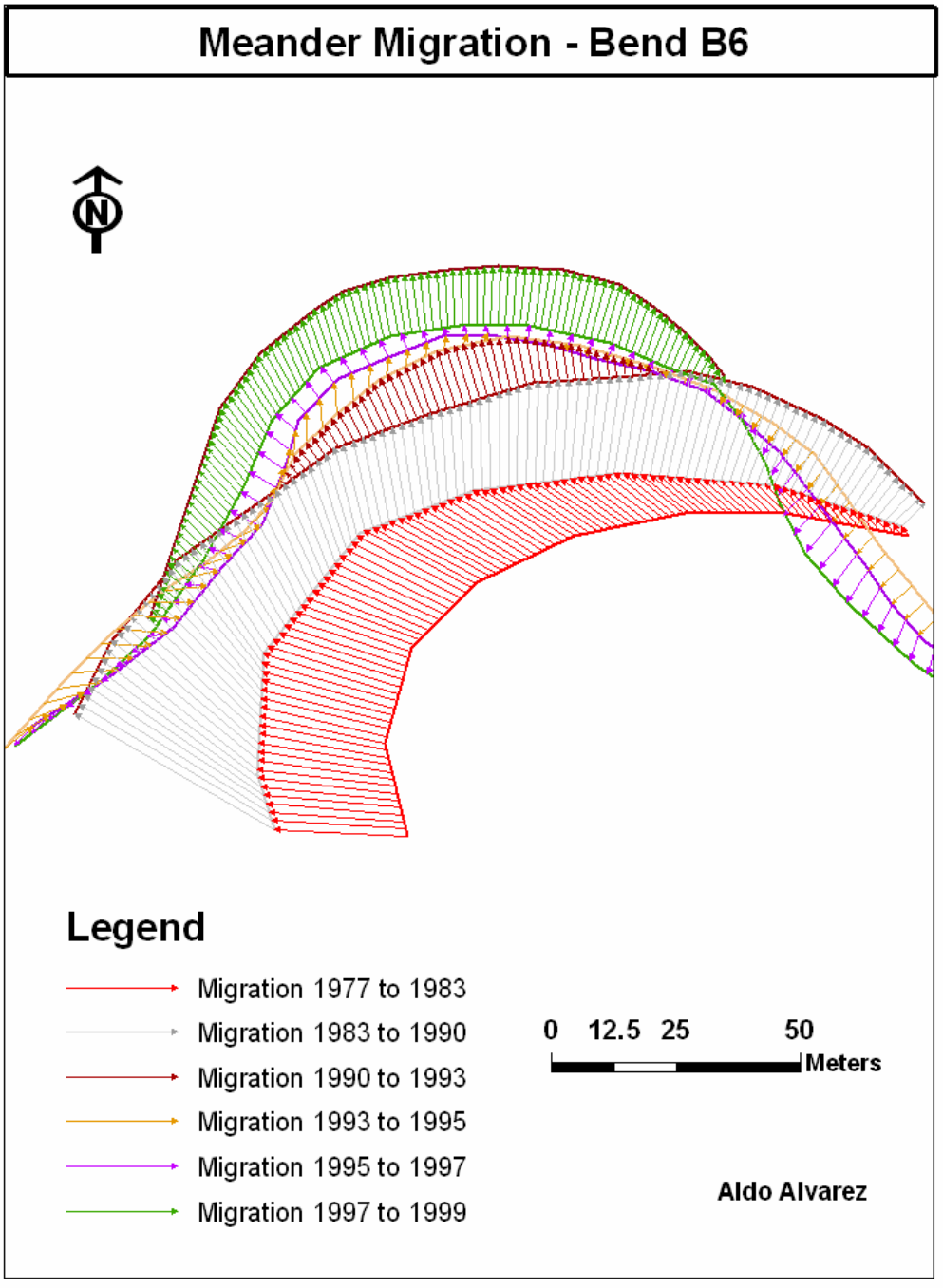

Figure 16 *Meander migration of bend B6 from 1977 to 1999.*

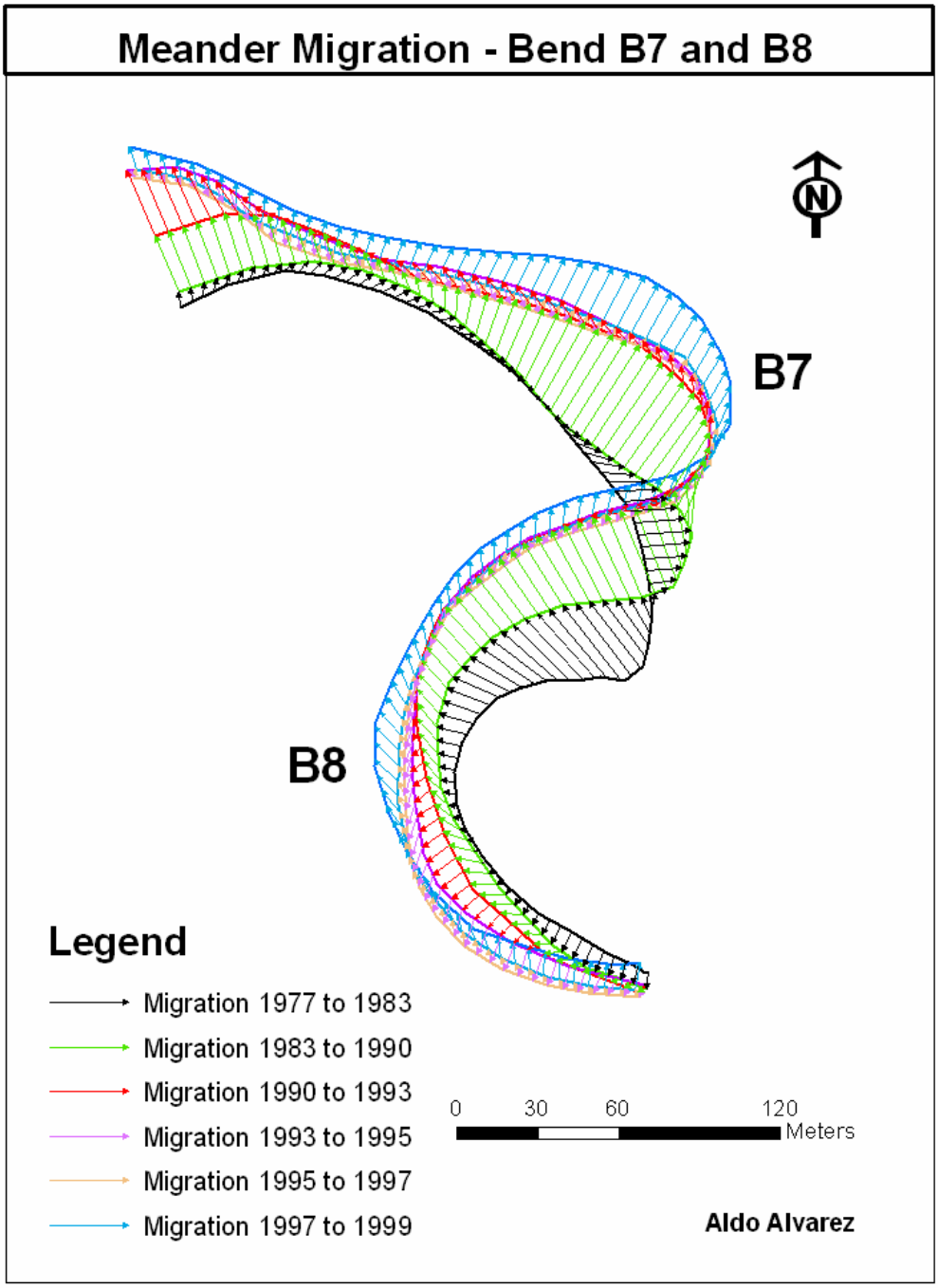

Figure 17 *Meander migration of bends B7 and B8 from 1977 to 1999.*

Table 3 *Maximum migration rates for bends B1 to B8*

Bend	Year	M(m)	Elap.Time (yrs.)	width (m)	M / yr (m)	M/w/yr
1	1966-1977	12.8	10.73	20.5	1.19	0.058
1	1977-1983	8.1	5.89	20.5	1.38	0.067
1	1983-1990	13	6.96	20.5	1.87	0.091
1	1990-1993	3.4	3.77	20.5	0.90	0.044
1	1993-1995	1	1.9	20.5	0.53	0.026
1	1995-1997	3	1.89	20.5	1.59	0.077
1	1997-1999	14.4	2.3	20.5	6.26	0.305
2	1966-1977	22	10.73	16	2.05	0.128
2	1977-1983	16	5.89	16	2.72	0.170
2	1983-1990	10.6	6.96	16	1.52	0.095
2	1990-1993	4.6	3.77	16	1.22	0.076
2	1993-1995	1	1.9	16	0.53	0.033
2	1995-1997	1.9	1.89	16	1.01	0.063
2	1997-1999	10.2	2.3	16	4.43	0.277
3	1977-1983	12	5.89	17	2.04	0.120
3	1983-1990	20	6.96	17	2.87	0.169
3	1990-1993	9.9	3.77	17	2.63	0.154
3	1993-1997	5.7	3.79	17	1.50	0.088
3	1997-1999	10.7	2.3	17	4.65	0.274
4	1966-1977	7.1	10.73	19	0.66	0.035
4	1977-1983	10.9	5.89	19	1.85	0.097
4	1983-1990	13.6	6.96	19	1.95	0.103
4	1990-1993	26.1	3.77	19	6.92	0.364
4	1993-1997	10.4	3.79	19	2.74	0.144
4	1997-1999	6.3	2.3	19	2.74	0.144
5	1983-1990	23.2	6.96	14	3.33	0.238
5	1990-1993	10.6	3.77	14	2.81	0.201
5	1993-1995	1	1.9	14	0.53	0.038
5	1995-1999	12.8	4.19	14	3.05	0.218
6	1977-1983	14.5	5.89	17	2.46	0.145
6	1983-1990	17.6	6.96	17	2.53	0.149
6	1990-1993	11.2	3.77	17	2.97	0.175
6	1993-1995	1.8	1.9	17	0.95	0.056
6	1995-1997	4	1.89	17	2.12	0.124
6	1997-1999	12.5	2.3	17	5.43	0.320
7	1966-1977	25	10.73	15	2.33	0.155
7	1977-1983	19.4	5.89	15	3.29	0.220
7	1983-1990	31.9	6.96	15	4.58	0.306
7	1990-1993	5	3.77	15	1.33	0.088
7	1993-1995	1	1.9	15	0.53	0.035
7	1995-1997	4.7	1.89	15	2.49	0.166
7	1997-1999	6.4	2.3	15	2.78	0.186
8	1977-1983	12	5.89	14	2.04	0.146
8	1983-1990	11.7	6.96	14	1.68	0.120
8	1990-1993	9.7	3.77	14	2.57	0.184
8	1993-1995	1	1.9	14	0.53	0.038
8	1995-1997	2.5	1.89	14	1.32	0.094
8	1997-1999	9	2.3	14	3.91	0.280

The overall mean meander migration rate for the eight bends studied from 1966 to 1999 for the Rio Grande de Añasco was 2.64 meters per year (Table 4), and also presents meander migration rates per year and normalized by width, which will be discussed this section. Migration rates for temperate rivers range from less than 0.1 m per year (Hooke 1980) to more than 7.26 m per year (Nanson and Hickin 1983). Therefore, high variability and distribution of meander migration rates have been documented for temperate rivers. Bank erosion rates can have considerable variation for the several reasons. Some of these are the variability of the magnitude-frequency of discharge events, increase in urbanization, and changes in agricultural practices and drainage (Hooke 1980). Also, variations to migration rates are influenced by local factors, particularly the nature of the bank material (Hudson and Kesel 2000).

For this study, the working hypothesis was that the mean meander migration rate of the study river would be similar to rates experienced in humid temperate rivers. Due to the high range of migration rates that have been documented in temperate rivers, the mean rate of 2.39 meters per year for the Rio Grande de Añasco is found to be within the range of values found in temperate rivers. Therefore, the results of this study indicate that for the period of study the stipulated hypothesis is supported, in that meander migration rate for the representative humid tropical river is similar to those documented for temperate rivers. This indicates that although there is higher precipitation rate in the humid tropical regime, the high silt-clay content in the channel banks coupled with a resilient vegetation cover also provide a higher resistance to deformation, leading to similar overall migration rates as those in temperate environments.

Table 4 *Average meander migration rates per year and normalized by width for bends B1 to B8*

Bend	Avg. M/yr (m)	Std. dev
1	1.96	1.95
2	1.93	1.32
3	2.74	1.19
4	2.81	2.15
5	2.43	1.29
6	2.73	1.49
7	2.48	1.31
8	2.01	1.16
Overall	2.39	1.48

Bend	Avg. M/width/yr (m)	Std. dev
1	0.096	0.095
2	0.122	0.083
3	0.161	0.070
4	0.148	0.113
5	0.174	0.092
6	0.161	0.087
7	0.165	0.088
8	0.143	0.083
Overall	0.146	0.089

Radius of Curvature and Channel Width

Meander bend migration rates have been assessed in relation to meander bend curvature, which is expressed by the ratio of the radius of curvature (r) to channel width (w). The literature suggests that the maximum migration rate is associated with meander bends having a curvature between 2.0 and 3.0 (e.g. Hickin and Nanson; Hooke 1997). This relationship has been interpreted as a natural mechanism in meandering and can be seen as adjustment of the planform geometry toward a stable equilibrium profile that allows the river to control its expenditure of energy (Hooke 1975; Richards 1982). This relationship is significant because it suggests a specific range of channel dimension that influences process. In these cases, bends having r/w ratios between 2.0 and 3.0 are the most effective at eroding their channel.

Because of its influence on the flow dynamics in curved channels, the radius of curvature for the study river needs to be defined. The eight selected meander bends provide data for calculating the ratio of meander bend curvature to channel width (r/w). For each bend, the radius of curvature, width, and migration distance was measured for each of the elapsed time periods. The meanders selected have different bend curvatures and provide 48 data points that cover a broad range of r/w values from 1.32 to 6.79. The potential 56 measurements (8 x 7) were reduced to 48 as some were discarded when the feature measured was smaller than half the image pixel size, according to the Whittaker-Shannon sampling theorem (Seul *et al.* 2000). A summary of these measurements is presented in Table 5 together with meander migration rate data that are discussed in the next paragraphs.

Leopold and Wolman (1957) first suggested that migration rate at a bend was at a maximum between a r/w a range between 2 and 3. Hickin and Nanson (1975) documented that migration rates for the Beatton River, British Columbia were greatest when the bend curvature approximated 2.9. Previous workers have plotted the meander migration rate per year as the dependent variable and the r/w value as the independent variable (e.g. Hickin and Nanson 1975; Biedenharn *et al.* 1989). From this scatterplot the range of r/w values at which maximum migration occurs was determined for the Rio Grande de Añasco, and this relationship is shown in Figure 18.

Plotting the yearly migration average relative to r/w, Figure 18 indicates that, for the Rio Grande de Añasco, maximum migration occurs at an r/w of 2.42 (Table 5). The scatter of data is probably due to a combination of factors such as site variability in local bank strength, material size distribution, cohesiveness, stratigraphic relations, vegetative roots and binding, and disturbance by animals (Hickin and Nanson 1984). Similar scatter has been reported by others (Biedenharn *et al.* 1989; Hickin and Nanson 1984; Hooke 1987; Hudson and Kesel 2000). Other studies have also shown meander migration rates scaled by channel width units (e.g., Nanson and Hickin 1983), and this form of plot is presented in Fig. 19, resulting again in a r/w ratio of 2.42 where maximum migration occurs. Considering the scatter, the approximate range of maximum migration occurs in the range of r/w = 2.0 to 2.5.

Using the rate of average migration distance per year, the Rio Grande de Añasco shows r/w values of maximum meander migration similar to those generally found for

Table 5 *Widths, curvatures, bend curvature ratios and migration rates for bends B1 to B8*

Bend	Year	width (m)	Radius of curv.	r/w	M / yr	M/w/yr
1	1966-1977	20.5	35	1.71	1.2	0.06
1	1977-1983	20.5	38	1.83	1.4	0.07
1	1983-1990	20.5	30	1.46	1.9	0.09
1	1990-1993	20.5	27	1.32	0.9	0.04
1	1993-1995	20.5	30	1.46	0.5	0.03
1	1995-1997	20.5	28	1.34	1.6	0.08
1	1997-1999	20.5	30	1.46	6.3	0.31
2	1966-1977	16	41	2.61	2.1	0.13
2	1977-1983	16	40	2.53	2.7	0.17
2	1983-1990	16	30	1.90	1.5	0.10
2	1990-1993	16	27	1.71	1.2	0.08
2	1993-1995	16	27	1.71	0.5	0.03
2	1995-1997	16	29	1.84	1.0	0.06
2	1997-1999	16	32	2.03	4.4	0.28
3	1977-1983	17	65	3.82	2.0	0.12
3	1983-1990	17	49	2.88	2.9	0.17
3	1990-1993	17	29	1.71	2.6	0.15
3	1993-1997	17	26	1.53	1.5	0.09
3	1997-1999	17	26	1.53	4.7	0.27
4	1966-1977	19	95	5.00	0.7	0.03
4	1977-1983	19	85	4.47	1.9	0.10
4	1983-1990	19	65	3.42	2.0	0.10
4	1990-1993	19	46	2.42	6.9	0.36
4	1993-1997	19	35	1.84	2.7	0.14
4	1997-1999	19	31	1.63	2.7	0.14
5	1983-1990	14	26	1.86	3.3	0.24
5	1990-1993	14	27	1.93	2.8	0.20
5	1993-1995	14	27	1.93	0.5	0.04
5	1995-1999	14	28	2.00	3.1	0.22
6	1977-1983	17	65	3.82	2.5	0.14
6	1983-1990	17	90	5.29	2.5	0.15
6	1990-1993	17	60	3.53	3.0	0.17
6	1993-1995	17	58	3.41	0.9	0.06
6	1995-1997	17	56	3.29	2.1	0.12
6	1997-1999	17	52	3.06	5.4	0.32
7	1966-1977	15	40	2.67	2.3	0.16
7	1977-1983	15	28	1.87	3.3	0.22
7	1983-1990	15	33	2.20	4.6	0.31
7	1990-1993	15	29	1.93	1.3	0.09
7	1993-1995	15	29	1.93	0.5	0.04
7	1995-1997	15	31	2.07	2.5	0.17
7	1997-1999	15	42	2.80	2.8	0.19
8	1977-1983	14	54	3.86	2.0	0.15
8	1983-1990	14	79	5.64	1.7	0.12
8	1990-1993	14	82	5.86	2.6	0.18
8	1993-1995	14	84	6.00	0.5	0.04
8	1995-1997	14	85	6.07	1.3	0.09
8	1997-1999	14	95	6.79	3.9	0.28

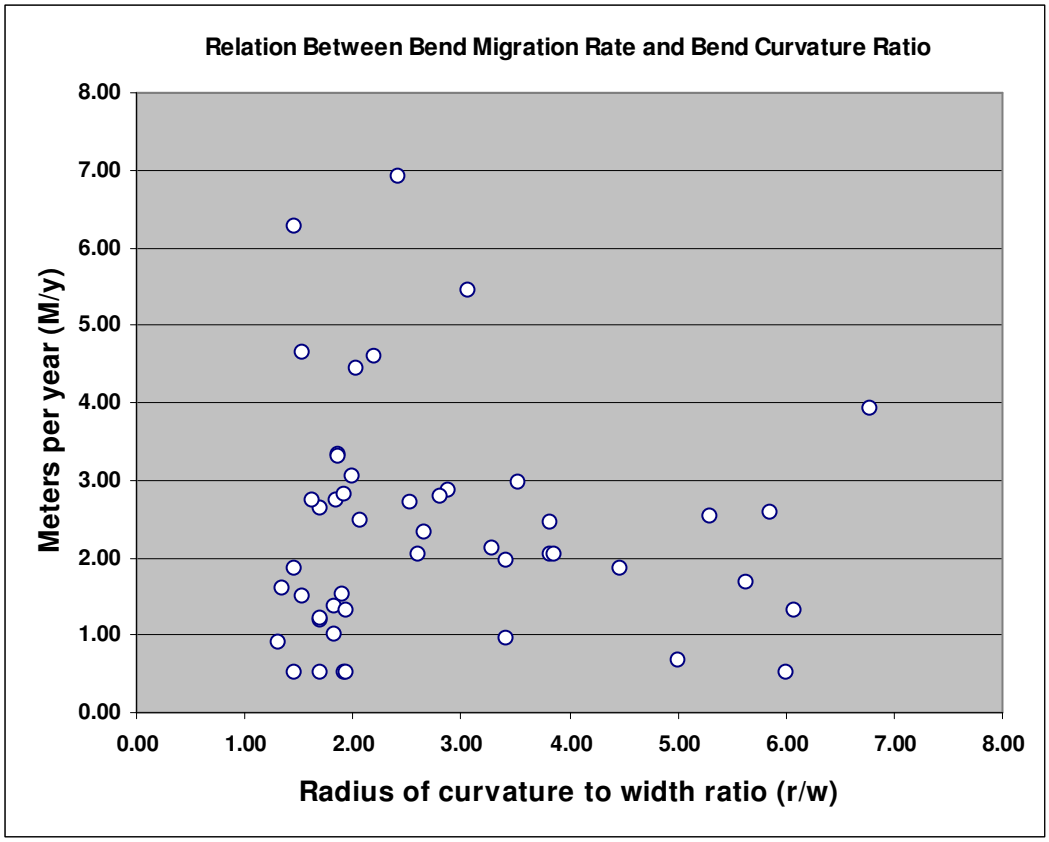

Figure 18 *Relation between bend migration per year and bend curvature ratio for the Rio Grande de Añasco.*

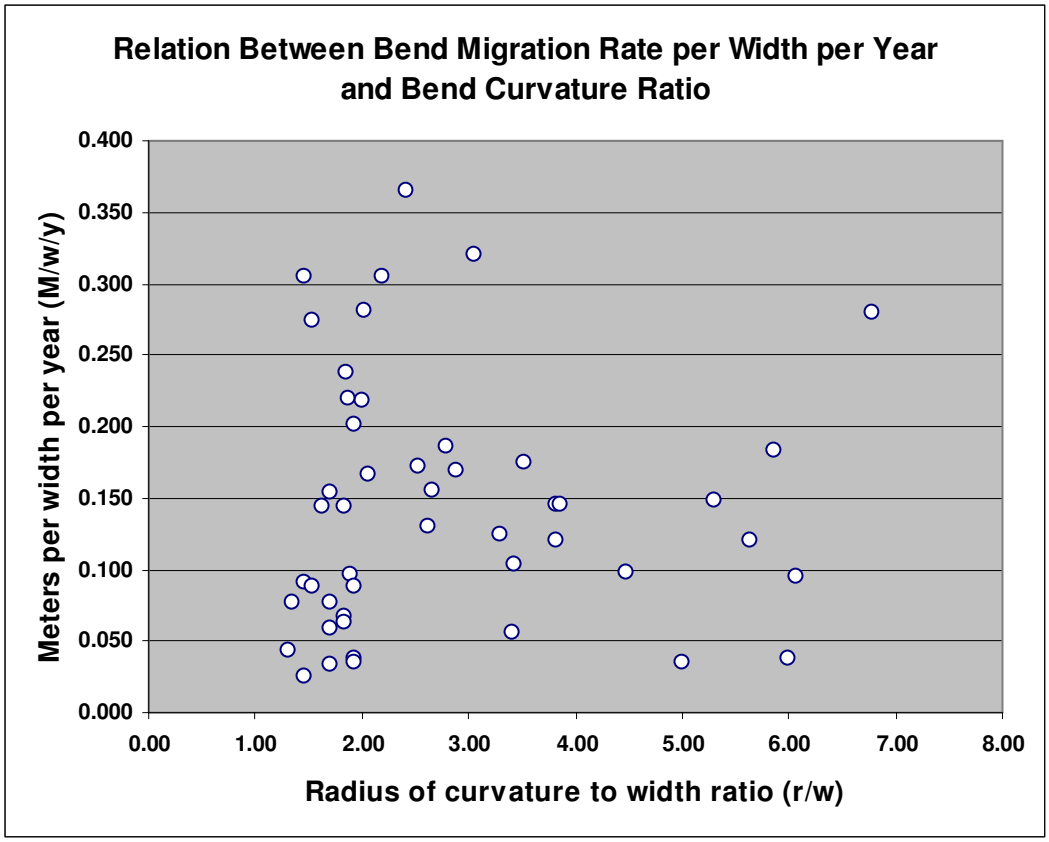

Figure 19 *Relation between bend migration per channel width and bend curvature ratio for the Rio Grande de Añasco.*

rivers located in temperate climate regimes (e.g., Hickin and Nanson 1975; Biedenharn *et al.* 1989; Hudson and Kesel 2000). This relationship expresses the influence of bend planform geometry and its influence of the local flow hydraulics at the concave bank. Shear stresses increase as a meander bend tightens, so that at tight bends (r/w = 2.0 - 3.0), rapid erosion of the concave bank occurs. However, as erosion occurs the channel widens and velocity is reduced and erosion of the bend eventually ceases (Hickin 1974). This geometric relationship is independent of climate region.

The objective of this section was to examine the ratio of meander-bend curvature to channel width (r/w) relate to the meander migration rate in the Rio Grande de Añasco. The working hypothesis was that the r/w ratio for maximum migration would be similar to those of humid temperate regions. The results of this study show that the maximum mean meander migration rate on a yearly basis and when scaled by width occurs at approximately a radius of curvature to width ratio of to 2.42. This value is within the range of 2.0 to 3.0 reported in the literature for humid temperate rivers. Therefore, results for the study period support the stipulated hypothesis.

Summary

The overall objective of this chapter was to examine the pattern and channel planform dynamics of the Rio Grande de Añasco in order to characterize planform change. Several hypotheses were stipulated. The first working hypothesis was that change in channel pattern of the representative humid tropical river would be highly

dynamic, experiencing rapid changes in relatively short time periods. Overall, the rate of change in sinuosity of the Rio Grande de Añasco showed an overall increase of 13% for the 33 year study period. This rate is comparable to the rate of change found of several temperate rivers. In this regard, the representative humid tropical river of this study can be considered similar in rate of change in sinuosity to those documented from these temperate climate rivers. The mean sinuosity was found to be 2.40 over the period of study. Although higher than values reported for temperate rivers in general, the results of this study indicate that the humid tropical river is also similar in the rate of change and sinuosity to temperate rivers.

The second working hypothesis was that the primary mechanism for planform change in the representative humid tropical river was through cutoffs and avulsions, rather than braiding. Results of this study reflect that three cutoffs and no avulsions or braiding were observed during the study period and partially supports the expressed hypothesis. For this river, the principal mechanism of planform change was through cutoffs during the 33 year period of study.

The third working hypothesis was that the mean meander migration rate of the study river would be similar to rates experienced in humid temperate rivers. Due to the high range of migration rates that have been documented in temperate rivers, the mean rate of 2.39 meters per year for the Rio Grande de Añasco was found to be within the range of values found in temperate rivers. Therefore, the hypothesis is supported, in that mean meander migration rate of the representative humid tropical river is similar to those documented in the literature for temperate rivers.

The fourth working hypothesis was that the r/w ratio for maximum migration would be similar to those of humid temperate regions. The results of this study show that the maximum mean meander migration rate on a yearly basis and when scaled by width occurs at approximately a radius of curvature to width ratio of 2.42. This value is within the range of 2.0 to 3.0 reported in the literature for humid temperate rivers. Therefore, the results of this study support the stipulated hypothesis for the Rio Grande de Añasco.

In summary, the processes that govern planform operating in humid tropical rivers are similar to those operating in temperate rivers. Changes in sinuosity are principally controlled by silt-clay composition of the channel boundary, the type of riparian vegetation and the characteristics of the sediment load, and not by a particular precipitation regime. Furthermore, results of this study indicate that for the period of study meander migration rate for the representative humid tropical river was similar to those found in temperate rivers. This indicates that although there may be a higher precipitation rate in the humid tropical regime, the high silt-clay content in the channel banks coupled with a resilient vegetation also provide higher resistance to deformation, leading to similar overall migration rates. The Rio Grande de Añasco also shows r/w values of maximum meander migration similar to those generally found for rivers located in temperate climate regimes. What this suggests is that the resulting balance between form and control variables that dictate channel planform is adjusted not only by the prevailing levels of the control variables such as precipitation and discharge but also presents the question of whether a general physical principle is governing channel form

adjustment. The search for the answer to that question is still an ongoing concern (Knighton 1998).

CHAPTER VI

RESPONSE AND RECOVERY OF PLANFORM OF A HUMID TROPICAL RIVER TO AN EXTREME FLOOD EVENT

The goal of this chapter is to document the impact on channel planform of a 100-year flood event induced on September 21-22, 1998 by Hurricane Georges on the Rio Grande de Añasco (Ramos-Ginés 1999). The working hypothesis is that, when disturbed by an extreme flood event, both channel width enlargement and the recovery period will be significantly less in the study river than those in humid temperate environments. This is because a humid tropical river is expected to have highly cohesive banks that limit channel width increases. Instead, the depth of the less cohesive channel bed is expected to change more rapidly in response to a high discharge. Tropical river channels are also expected to recuperate more quickly because of rapid vegetation growth, higher precipitation rates, and abundant sediment flow than rivers in humid temperate regions (Wolman and Gerson 1978).

The objective of this section was accomplished by measuring channel width changes using high-resolution aerial photographs (Appendix B), and by evaluating the recovery time necessary for its return to pre-hurricane conditions. Channel width changes were measured for three reaches of the Rio Grande de Añasco (Study Area Two, Fig. 20). The aerial photographs for these areas, although taken for other purposes, coincided with the passage of Hurricane Georges. They capture a 1.5 km length section of the Rio Grande de Añasco that enters the flat alluvial valley and provide a history of

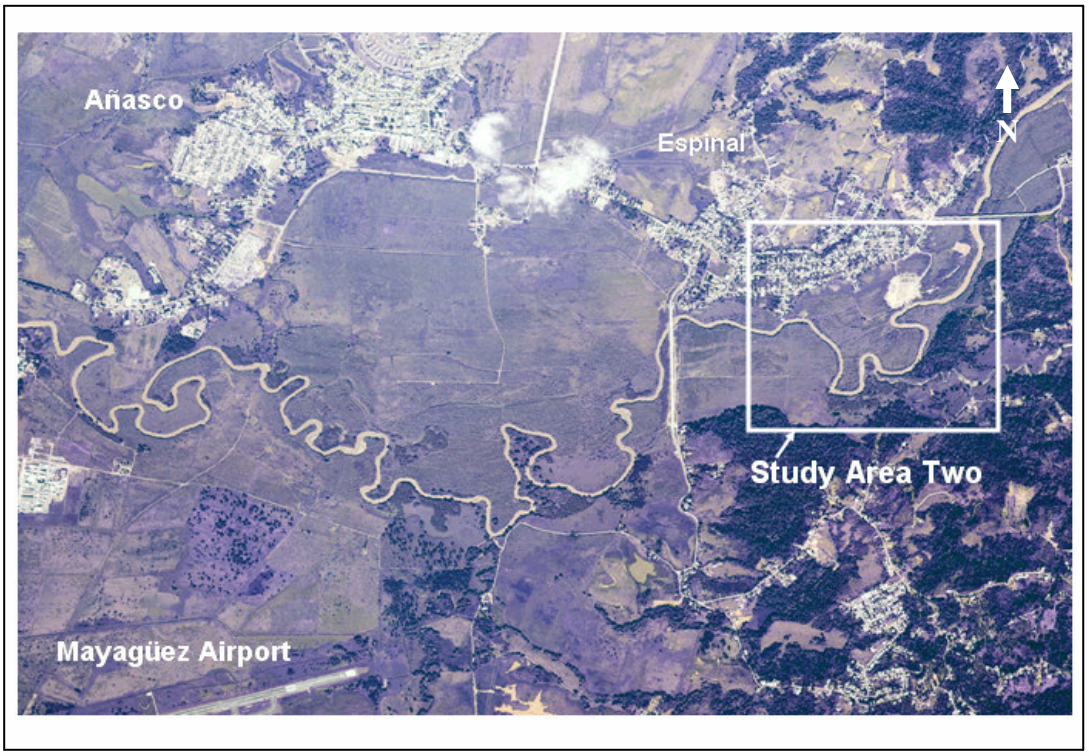

Figure 20 *Study Area Two within the Rio Grande de Añasco Valley.*

stream planform for periods one year before, two weeks, nine months, and 14 months after passage of the event.

Width Changes

Width changes for the three least sinuous reaches within the study area were selected following Costa (1974), who noted that it took longer for straight reaches in the Western Run Creek in north central Baltimore County to recover width to pre-flood dimensions following Tropical Storm Agnes in 1972. Thus, results from these reaches would be the most conservative estimates of recovery times. Reaches were divided into 40 transects (Fig. 21) to satisfy the central limit theorem (Ott and Longnecker 2001). Transects were spaced at approximately 1.5 times the width (Hooke 1977) or approximately 25 m in order to have at least 10 cross sections per reach. Reach one was divided into 10 cross sections with a total length of approximately 250 m, the second reach also with a length of 250 m and 10 cross sections, and the third reach with 20 cross sections and 500 m in length. The third reach is longer with more cross sections because it contains the longest straight segment of Study Area Two (Fig. 20). The aerial photographs chosen for this analysis were taken on August 12, 1997 (one year before), October 8, 1998 (two weeks after), June 1, 1999 (nine months after), and November 28, 1999 (14 months after the hurricane). These are shown in a low resolution jpeg format (compressed to be less memory intensive) in Appendix C.

Using ArcGis and the selected aerial photographs, the channel width of each transect was measured using the bankfull edge (Shields *et al*. 2000; Hickin and Nanson

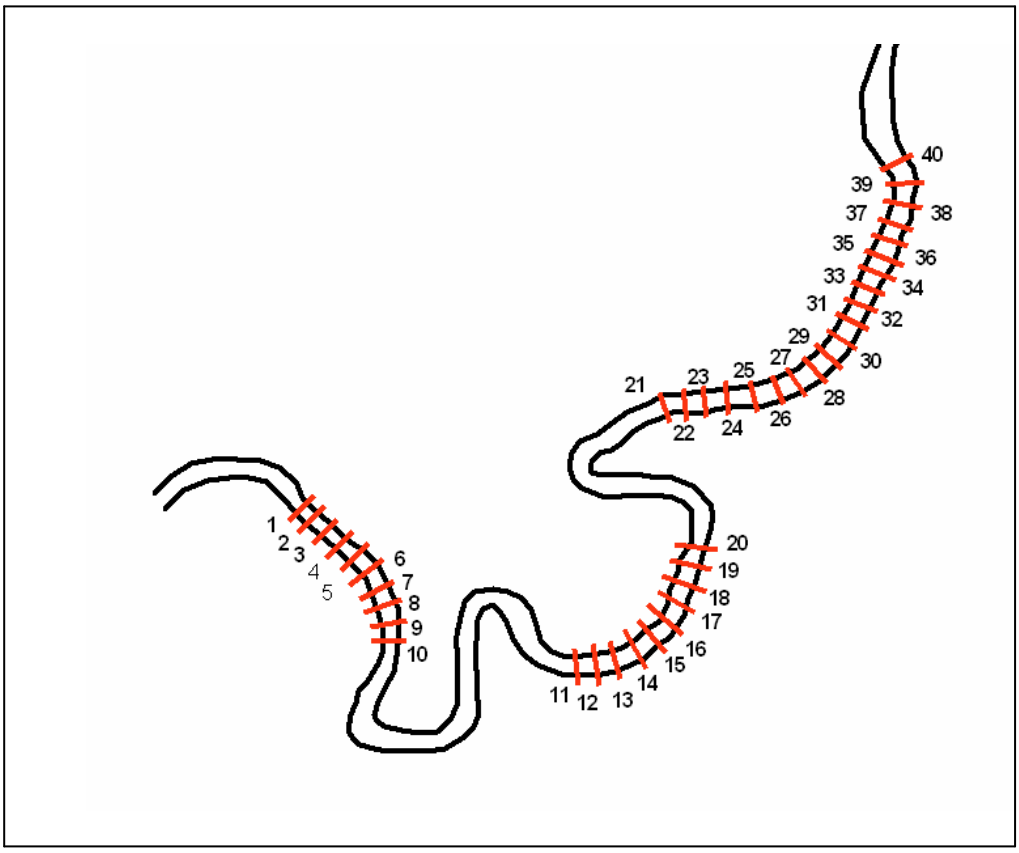

Figure 21 *Transects of Study Area Two.*

1984). Specifically, the width of each transect was determined for the periods one year before, and two weeks, eight months, and 14 months after passage of the Hurricane Georges (the elapsed time between photographs) and are presented in Table 6. One year before the hurricane, the mean width of the sampled transects was 17.7 m. Two weeks after passage of the hurricane the mean width of the sampled transects was found to be 20.7 m, an increase of 17% when compared to the year before mean width. Nine months after passage of the hurricane the mean width of the sampled transects was found to be 19.1 m, an increase of 7.5%. Fourteen months after passage of the hurricane the mean width was found to be 17.8 m, an increase of 0.5%. The measured widths after passage of the hurricane were then compared to the pre-flood mean width by a Paired Sample T Test, a Wilcoxon Rank Sum Test, and a Sign Test (Ott and Longnecker 2001).

Statistical Comparisons

Results of comparison between the widths of the 40 transects of the study area from August 12, 1997 and October 8, 1998 show an increment in mean channel width of 17% from 17.7 m to 20.7 m (Table 6). Differences between mean widths of the 40 transects of the study area for these dates were compared using statistical tests provided by SPSS 11.5 software. By conducting a Paired Sample T Test between means, a significance level of 0.00 ($p = .00$) was found indicating that there is a confidence level greater than 95% that the means of the channel widths are not equal for the two periods (Table 7).

Table 6 *Channel width measurements for the 40 transects of Study Area Two*

	Aug-12-97(a)	Oct-8-1998(b)	June-10-99(c)	Nov-28-99(d)
Transect	Width (m)	Width (m)	Width (m)	Width (m)
1	15.1	15.8	15.4	15.2
2	15.4	17.2	16.1	15.3
3	15.3	16.0	15.5	15.1
4	16.2	16.9	16.3	15.9
5	15.2	15.8	15.7	15.7
6	14.7	15.8	15.6	15.5
7	15.7	17.4	16.4	15.7
8	16.9	18.1	17.5	17.0
9	17.9	19.1	18.5	18.1
10	19.8	20.0	19.8	19.7
11	22.1	23.4	22.8	22.3
12	17.3	18.4	17.7	17.1
13	16.4	16.6	16.5	16.5
14	17.6	17.9	17.8	17.7
15	19.1	20.0	19.4	18.9
16	19.6	21.1	20.2	19.6
17	18.4	18.9	18.8	18.8
18	16.8	17.8	17.3	16.9
19	15.8	16.0	15.9	15.9
20	17.1	17.6	17.1	16.8
21	20.5	21.1	21.0	21.0
22	21.6	22.0	21.4	21.0
23	21.6	24.1	22.9	22.0
24	20.5	24.1	22.4	21.1
25	19.4	24.4	21.6	19.5
26	18.2	25.5	21.8	18.9
27	17.3	24.7	20.5	17.4
28	16.4	23.1	19.1	16.1
29	17.4	22.1	19.4	17.4
30	18.7	23.5	20.7	18.6
31	19.0	24.5	21.3	18.9
32	18.2	24.0	20.7	18.2
33	18.6	23.2	20.7	18.7
34	17.3	24.1	20.2	17.3
35	17.9	24.7	20.8	17.8
36	17.1	24.0	20.2	17.4
37	17.4	23.2	19.8	17.2
38	16.4	21.7	18.8	16.6
39	16.4	21.6	18.7	16.6
40	16.8	22.5	19.4	17.1
Average Width	17.7	20.7	19.1	17.8
Percent change		17%	7.5%	0.5%

(a) one year before hurricane; (b) two weeks after hurricane; (c) nine months after hurricane; (d) 14 months after hurricane.

Table 7 *SPSS output for Paired Sample T Test between width data for August 12, 1997 and October 8, 1998*

Paired Samples Statistics

		Mean	N	Std. Deviation	Std. Error Mean
Pair 1	A_97	17.728	40	1.8688	.2955
	A_OCT_98	20.6975	40	3.19186	.50468

Paired Samples Test

		Paired Differences					t	df	Sig. (2-tailed)
		Mean	Std. Deviation	Std. Error Mean	95% Confidence Interval of the Difference Lower	Upper			
Pair 1	A_97 - A_OCT_98	-2.9700	2.56247	.40516	-3.7895	-2.1505	-7.330	39	.000

For June 10, 1999, eight months after the event, the mean channel width was 19.1 m. This represents a difference of 7.5 % from the pre-hurricane mean width (Table 6). The difference between the mean widths of the 40 transects of the study area between the dates of August 12, 1997 and June 10, 1999 was compared using a Paired Sample T Test and results are presented in Table 8. The result of a significance level of 0.00 (*p =.00)* indicates that there is a confidence level greater than 95% that the means of the channel widths are not equal for these two periods (Table 8).

For November 28, 1999, 14 months after the event, the mean channel width was 17.8 m. This represents a difference of 0.5 % from the pre-hurricane mean width (Table 6). The difference between the mean widths of the 40 transects of the study area for the dates of August 12, 1997 and November 28, 1999 was compared using a Paired Sample T Test and results are presented in Table 9. The result of a significance level of 0.248 (*p =.248)* indicates that the hypothesis of equal means was failed to be rejected, and therefore the means of the channel widths for these two periods may be considered statistically equal at a 95% confidence level (Table 9).

In order to assess the potential impact of outliers in the measurements, non-parametric tests were also conducted to compare means (Ott and Longnecker 2001) using the Wilcoxon Signed Rank Test and the Sign Test. These tests compare rank differences in means between samples, allocating a rank to each difference in the order of their magnitude (Ott and Longnecker 2001). The results of the Wilcoxon Signed Rank Test show a significance level of 0.295 (*p =.295*), and the Sign Test a significance level

Table 8 *SPSS output for Paired Sample T test between width data for August 12, 1997 and June 10, 1999*

Paired Samples Statistics

		Mean	N	Std. Deviation	Std. Error Mean
Pair 1	A_97	17.728	40	1.8688	.2955
	A_JUN_99	19.043	40	2.2032	.3484

Paired Samples Test

		Paired Differences					t	df	Sig. (2-tailed)
		Mean	Std. Deviation	Std. Error Mean	95% Confidence Interval of the Difference Lower	Upper			
Pair 1	A_97 - A_JUN_99	-1.315	1.1342	.1793	-1.678	-.952	-7.333	39	.000

Table 9 *SPSS output for Paired Sample T Test between width data for August 12, 1997 and November 28, 1999*

Paired Samples Statistics

		Mean	N	Std. Deviation	Std. Error Mean
Pair 1	A_97	17.728	40	1.8688	.2955
	A_NOV_99	17.781	40	1.8931	.2993

Paired Samples Test

		Paired Differences					t	df	Sig. (2-tailed)
		Mean	Std. Deviation	Std. Error Mean	95% Confidence Interval of the Difference				
					Lower	Upper			
Pair 1	A_97 - A_NOV_99	-.054	.2911	.0460	-.147	.039	-1.173	39	.248

of 0.522 (p =.522). In summary, all tests indicate that the pre-hurricane channel mean width is statistically equal to the mean width on November 28, 1999. The results of the tests are shown in Table 10. Therefore, within 14 months following the passage of a 100-year extreme event, the channel of the Rio Grande de Añasco returned to its pre-hurricane width dimension.

Discussion

In their seminal 1978 paper, *Relative scales of time and effectiveness of climate in watershed geomorphology*, Wolman and Gerson described the effectiveness of climatic events, such as a 50-year flood, as the ability to affect the shape of the landscape. The resulting landform is in part related to the material removed but also to the return period of the event including the magnitude of processes that can restore the landscape during the periods between such events. They concluded that the importance of these events that change the landscape can be measured relative to the processes that restore the landform to the condition before the new landform was created. Over time, recovery may be complete and hillslopes or streams return to forms that have been maintained over longer periods of time. Effectiveness is not absolute but related to both frequency and magnitude and also to the time interval required for the landscape to reform.

Wolman and Gerson (1978) presented data to illustrate a sequence of channel width changes and recovery periods for selected rivers in different climate regions following large storm events. Using the Patuxent River in Maryland and the Baisman

Table 10 *SPSS output for Wilcoxon Signed Ranks Test and Sign Test for width data for August 12, 1997 and November 28, 1999*

Wilcoxon Signed Ranks Test

Ranks

		N	Mean Rank	Sum of Ranks
A_NOV_99 - A_97	Negative Ranks	17[a]	18.53	315.00
	Positive Ranks	22[b]	21.14	465.00
	Ties	1[c]		
	Total	40		

a. A_NOV_99 < A_97

b. A_NOV_99 > A_97

c. A_NOV_99 = A_97

Test Statistics[b]

	A_NOV_99 - A_97
Z	-1.048[a]
Asymp. Sig. (2-tailed)	.295

a. Based on negative ranks.

b. Wilcoxon Signed Ranks Test

Sign Test

Frequencies

		N
A_NOV_99 - A_97	Negative Differences[a]	17
	Positive Differences[b]	22
	Ties[c]	1
	Total	40

a. A_NOV_99 < A_97

b. A_NOV_99 > A_97

c. A_NOV_99 = A_97

Test Statistics[a]

	A_NOV_99 - A_97
Z	-.641
Asymp. Sig. (2-tailed)	.522

a. Sign Test

Run in north central Baltimore County to represent humid temperate regions (precipitation of approximately 1000 mm per year), Wolman and Gerson (1978) showed that the impacts of an extreme event resulted in a 40 percent increase in stream width with a recovery period of 15 years for the Patuxent River, and a 20 percent increase in width and a recovery period of 10 years for the Baisman Run (Fig. 22).

The semi-arid climate region, represented by the Cimarron River in southern Kansas, showed an effectiveness of over 200 percent with a recovery period of over 28 years. Further observations by Wolman and Gerson (1978) in the Sinai desert showed a widening more than 200 percent during individual storms, with a recovery period in the 100-year interval (Fig. 22).

The flood events for the Patuxent River and the Baisman Run were produced by precipitation from Tropical Storm Agnes from June 21 to 23. Gupta and Fox (1974) estimated this to be an over 100-year flood event with rainfall of 305 mm (12 inches) over a three day period. They estimate that 75% of this precipitation (229 mm; 9 inches) occurred during the first 24 hours (Gupta and Fox 1974). The drainage area of the Baisman Run is 4.0 km^2 (Costa 1974), and the drainage area of the Patuxent River is 100 km^2 (Gupta and Fox 1974). The Patuxent River experienced overbank flow for 24 hours (Gupta and Fox 1974) while the Baisman Run overbank flow time was not reported.

Hurricane Georges produced a similar 100-year event for the Rio Grande de Añasco with a rainfall of 560 mm (22 inches; Garza and Atwell 1999) during the first 24 hours, or 244% (560/229 mm) higher than the 100-year flood of the Patuxent River. The

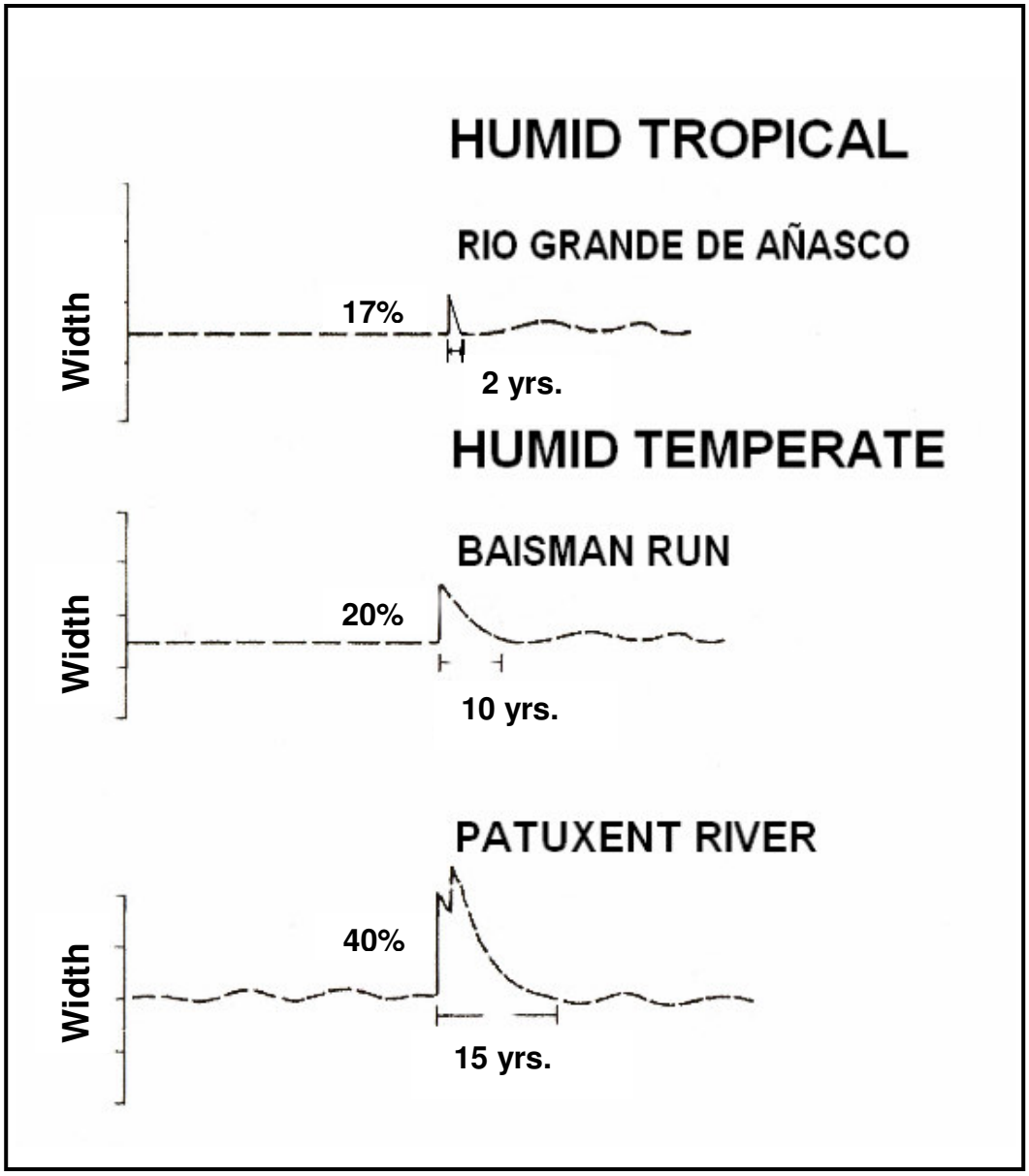

Figure 22 *Combined sequence of changes in channel width showing recovery periods following large storm events for selected rivers for humid temperate and humid tropical climate regions (adapted from Wolman and Gerson 1978).*

drainage area of the Rio Grande de Añasco is larger than the Patuxent at 515 km^2. While the Patuxent experienced overbank flow during one day, the Rio Grande de Añasco overflowed its banks for approximately four days from September 21 to September 25 (Fig. 23). It seems that the input of energy into the system was much higher in magnitude for the 100 year event of the humid tropical Rio Grande de Añasco than for the 100 year event of the representative humid temperate rivers used by Wolman and Gerson (1978). Yet, the response of the Rio Grande de Añasco to a higher magnitude event was a 17% increase in width and a less than two-year recovery period, as compared to a 40 percent increase in stream width with a recovery period of 15 years for the Patuxent River, and a 20 percent increase in width and a recovery period of 10 years for the Baisman Run.

The trend of shorter recovery times in channel width following a major perturbation has been demonstrated for humid temperate regions compared to other areas. The Rio Grande de Añasco watershed receives a mean annual precipitation of 2283 mm (89.9 inches; Slack 1993) double the 1000 mm of the humid temperate region (Wolman and Gerson 1978). The response and recovery of channel width for the Rio Grande de Añasco after a 100-year flood are graphically summarized in Figure 24. These measurements of an in increase in channel width of 17% and recovery period of approximately two years are smaller and more rapid than the representative humid temperate rivers reported by Wolman and Gerson (1978). A reconstructed representation

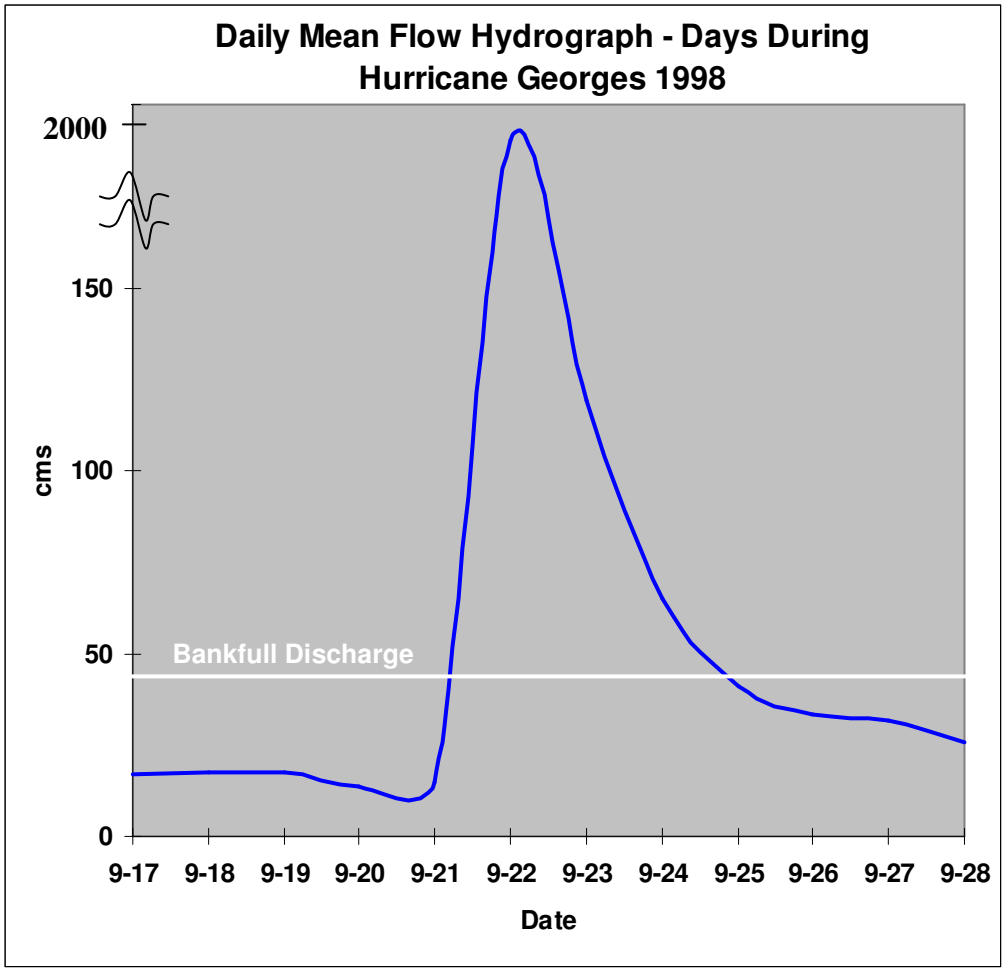

Figure 23 *Daily mean flow hydrograph for days during Hurricane Georges.*

of the response and recovery results of the representative of humid temperate rivers reported in Fig. 4 of Wolman and Gerson (1978) are combined with the representative humid tropical river results presented in Figure 24 to produce Figure 22. Wolman and Gerson (1978) used change of channel width as an index to scale the relative impact of similar magnitude flood events in watersheds of different climates. Changes in depth and cross sectional area were not reported. Some studies suggest that the rate of change of depth and consequently recuperation of channel depth after a variation of discharge is faster in finer grained cohesive banks. In studying the recovery of the humid temperate Piedmont watershed after Tropical Storm Agnes in 1972, Costa (1974) was able to document the recovery of width and depth of the main channel of Western Run. After being scoured 18 feet and widened 67 feet, in one year the bank-full width remained unchanged. However, the scoured channel recuperated nearly 50% of the pre-Agnes depth. The recovery time of channel width was estimated to be 10 years. The author also suggests that the stable channel form of this Piedmont stream seems to be related to a much lower discharge such as the bank-full stage.

Chin *et al.* (2002) studied the impact of dam closure by Somerville Dam, Texas to Yegua Creek channel geometry and observed that the rate of change of depth was more rapid than that of width after closure. The authors state "*The relatively rapid increase of depth compared to that of width is similar to that of channels with fine-grained cohesive banks (Leopold, 1994), which limit bank erosion.*" This observation also suggests that depth recuperates faster than width in finer-grained cohesive banks, such as those found in the humid temperate and humid tropical regions.

The use by Wolman and Gerson (1978) of channel width change as an index to illustrate the relative impact of similar magnitude flood events in watersheds of different climates, may not necessarily address a complete measure of effectiveness of the high magnitude event without documenting cross sectional and depth recuperation. It is suggested that future research address this issue.

Summary

The objective of this chapter was to document the response and recovery of channel planform after a 100-year flood on the humid tropical Rio Grande de Añasco. The working hypothesis was that, when disturbed by an extreme flood event, both channel width enlargement and the recovery period would be less in the study river than those in humid temperate environments. The objective of this section was accomplished by measuring channel width changes, and results of this study indicate that this hypothesis is supported. The trend of shorter recovery times in channel width following a major perturbation has been demonstrated. In the long term, a large flood such as a 100-year event apparently plays a relatively minor role as a formative event in shaping the overall planform of the humid tropical landscape. The moderate more frequent events as first exposed by Wolman and Miller (1960) apparently play a preponderant role in this climate regime.

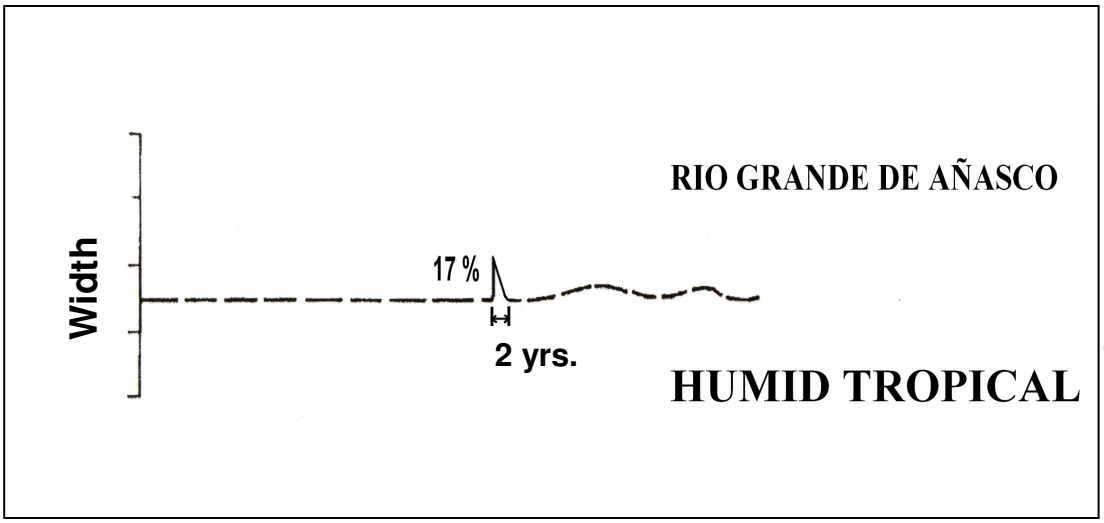

Figure 24 *Change in channel width and recovery period following a 100 year flood for the Rio Grande de Añasco.*

CHAPTER VII

MEANDER MIGRATION MODEL

Several theoretical and empirical approaches have been used to create models of meander bend migration. Theoretical approaches include mathematical models founded upon simplified physical principles and models that postulate a particular condition regarding the behavior of stable channels. Using the Ikeda and Parker model (1981), for example, Beck (1988) predicted the migration distance of three bends over five years on the Genesee River in Mount Morris, New York within ± 30 percent.

Because theoretical mathematical models can require vast quantities of data and be costly to implement, meander migration has also been investigated with empirical approaches. Hickin and Nanson (1975) derived empirical relationships to predict mean meander migration distance in meters per year (M) for the Beatton River, Canada, using the radius of curvature (r) to channel width (w) ratio, and spacing of meander scrolls (d) as independent variables. The results of their study were presented in chapter II, and the authors reported a standard error of 0.091 m per year but did not report the adjusted coefficient of determination of their empirical model. Furthermore, their model estimates long term average meander migration (Hickin and Nanson 1975).

Another empirical meander migration model was developed by Hooke (1980) to predict mean meander migration distance in meters per year (M) emphasizing watershed area (A) as a surrogate for discharge. Using data from various rivers, Hooke (1980) derived the following regression relation for an average yearly meander migration rate (M) related to drainage area of a basin (A):

$$M = 2.45\ A^{0.45}$$

The author reported a coefficient of determination (R^2) of 0.40 (Hooke 1980).

The empirical models described above were developed using data from temperate climate regions. However, relationships between process control variables may not be the same as for humid tropical climates. For example, these empirical models assume constant movement of the meander bend each year. This implies the assumption of uniform frequency of channel forming discharge, which is unlikely in the highly variable precipitation regime of a humid tropical river. Additionally, these models estimate annual long-term mean migration rates, and not actual meander migration distance, which may be more suitable for shorter-term applications. In contrast, the mathematical models described in chapter II, such as the Ikeda and Parker (1981) model, predict actual mender migration distance. Furthermore, the empirical models reviewed do not include other potentially important process control variables such as bank composition or bank strength, which may be significant in controlling meander migration in humid tropical rivers.

This study seeks to develop an empirical meander migration model applicable to humid tropical rivers that will be able to predict meander migration with a higher degree of predictability, i.e. coefficient of determination, than the ones previously discussed by Nanson and Hickin (1975) and Hooke (1980). Also, and maybe more important for shorter-term applications, the empirical model will predict meander migration distance. Therefore, the objective of this chapter is to develop an empirical model for predicting bend migration that may be more suitable for humid tropical rivers. The working

hypothesis is that meander migration in tropical rivers will be controlled by a set of independent variables that represent force, resistance, and channel geometry components in the river system. Force in this system is represented by bankfull discharge frequency and valley slope. The silt-clay content of the meander banks and bank strength will characterize resistance. The r/w ratio will further represent channel geometry. The approach to develop this empirical model will be to combine these five parameters as independent variables in a multiple regression analysis that should therefore account for a large portion of the variability in channel migration rates.

The empirical model was developed by relating maximum migration distance of a meander bend as a function of potential control variables. The independent variables are defined as: number of bankfull discharge events occurring over a specified time period (N_{bkf}), the radius of curvature to width ratio of the bend (r/w), the silt-clay content of the banks (B), the bank strength (Φ), and the valley slope (s). The following sections describe selection of independent variables and model development.

Bankfull Discharge

Background

Wolman and Miller (1960) developed a conceptual model to describe the relative importance of extreme catastrophic events versus more frequent moderate events in fluvial processes. The authors concluded that in terms of geomorphic effectiveness related to sediment load transport, the more frequent moderate events surpass the less frequent high magnitude events. Furthermore, they related the channel forming

discharge for sediment transport as the bankfull flow. It is also sometimes referred to as the dominant or effective discharge. Bankfull discharge therefore is a primary causative variable representing the driving force within a river system (Nash 1994; Pickup and Warner 1976; Williams 1978). Although the frequency of the dominant or effective discharge is highly variable and may or may not be equal to bankfull discharge which is a function of the unique circumstances of each river system, Knighton (1998) recommends that the bankfull channel discharge be used as a reference level, and is advocated for study purposes.

Leopold *et al.* (1964) and Leopold (1994) confirm that actual field observations indicate that the erosion rate and the sediment transport rate are most active when discharge is near bankfull. For the purposes of this model, the geomorphically effective channel forming discharge that induces meander migration is considered best represented by the bankfull discharge. The number of such events occurring within a specified time period will influence in a proportional manner the amount of erosion occurring at a bend. Therefore, the frequency of bankfull discharge is considered an important independent variable

Determination of Bankfull Discharge

The methods described above have been used to estimate the frequency of bankfull discharge for temperate climate regions and are useful as an approximation when no other data is available. The frequency of bankfull discharge may be higher in humid tropical climates due to higher precipitation regimes and the frequent influence of

cold fronts, tropical depressions, storms, and hurricanes. For this study, an estimate of the frequency of bankfull discharge was determined by observing this phenomenon directly at a location of the river near the entrance to the meander belt of the Rio Grande de Añasco (Study Area One, Fig. 2), and relating it with the daily mean streamflow recorded at the U.S. Geological Survey Station gauge station upstream (U.S.G.S. station 50144000). The meander belt of the valley commences approximately at the road 430 bridge (Study Area One, Fig. 2). Since June, 2003, Lcdo. Eiton Arroyo, who has lived in this town all his life, volunteered to observe the river at a specified location near the bridge where bankfull level is clearly visible and observed as the major break separating the well defined channel from the floodplain (Chin *et al*. 2002; Riley 1972). From that date to the present, Arroyo has observed bankfull level occurring for large portions of the day on three occasions: on October 31, 2003, November 17, 2003, and September 19, 2004. The daily mean discharge recorded at the gauge station for those days was 1,720 cfs (48.7 cms), 1,560 cfs (44.2 cms), and 1,760 cfs (49.8 cms), with a mean of 1,680 cfs (47.6 cms) for the three readings. With the estimate of bankfull discharge, the number of such events occurring between aerial photographs can be determined from the streamflow records spanning from 1963 to 2004. This analysis will be presented in the following section.

Frequency of Bankfull Discharge

A flood frequency curve developed from streamflow data at station 50144000 (Fig. 25) shows that the flow of 1,680 cfs (47.6 cms), the average observed bankfull

discharge, represents a 1.09 year recurrence interval. This type of curve is based on a ranking of the maximum annual streamflow data for the period of record. The frequency

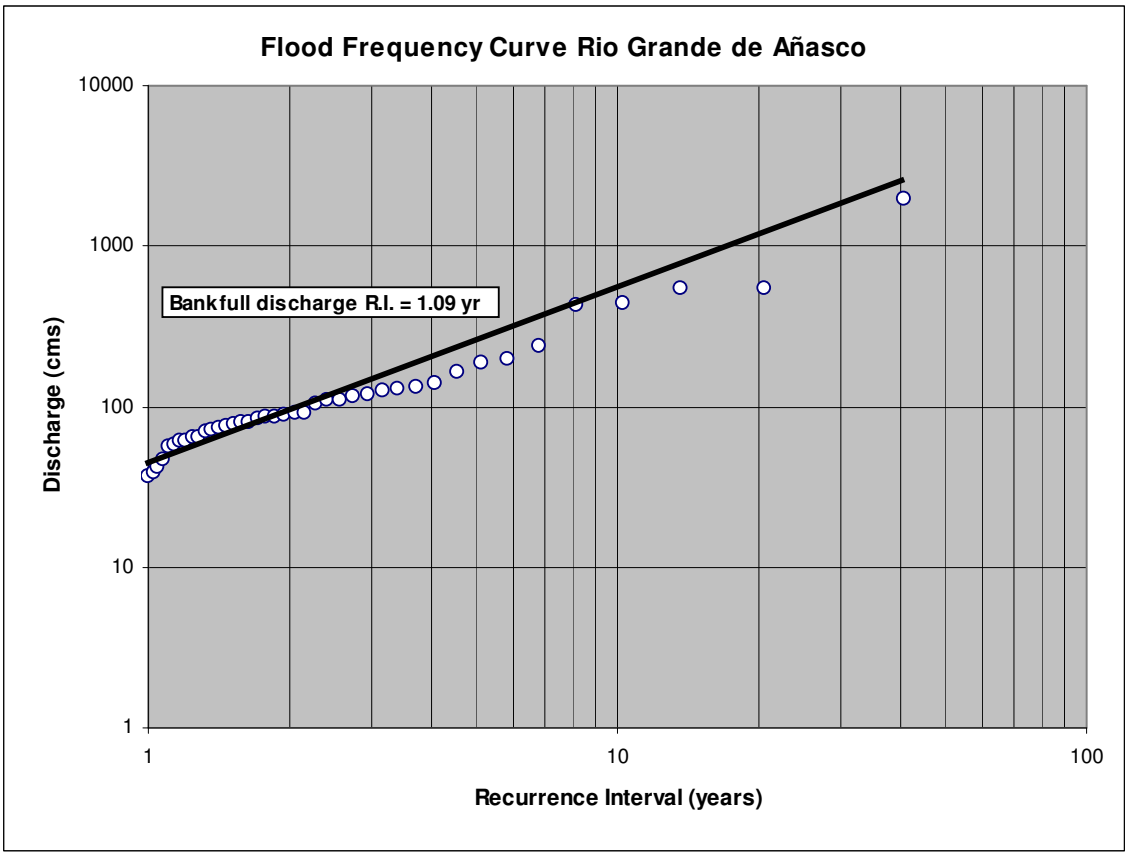

Figure 25 *Flood frequency curve of the Rio Grande de Añasco.*

of the event was then calculated as a probability or recurrence interval (R.I.), also called return period. This recurrence interval is calculated as: R.I. = $(n+1)/m$, where n is the number of years of record; m is the rank of the event (Dunne and Leopold 1978).

A flow duration curve was also computed to estimate flow exceedance (Fig. 26). This curve shows that the bankfull discharge is equaled or exceeded 1.5% of the time. This type of curve represents the amount of time a certain flow is exceeded and is derived by making a table and grouping all data values into separate flow quantity classes. The frequency, cumulative frequency (frequency divided by the total number of observations), and percentage cumulative frequency is then computed and plotted (Davie 2003).

The number of daily mean flows equal or higher than the bankfull discharge of 47.6 cms occurring between the elapsed times of the aerial photographs was determined from the streamflow data from the U.S.G.S. station for the period from 1964 to 2004 (Table 11). In this table, for example, the elapsed time between the first two aerial photographs is from July 1, 1966 and March 20, 1977. By determining the frequency of bankfull discharge events that have occurred during this time period, the number can be related to the meander bend migration distance measured for the same period (Table 11). Therefore, for the measurements of the eight study bends for the periods from 1966 to 1999, data points relating the number of bankfull discharge events to the migration distance can be plotted for each of the elapsed time periods between photographs. The frequency of bankfull discharge events by calendar year were also determined and are presented in Figure 27.

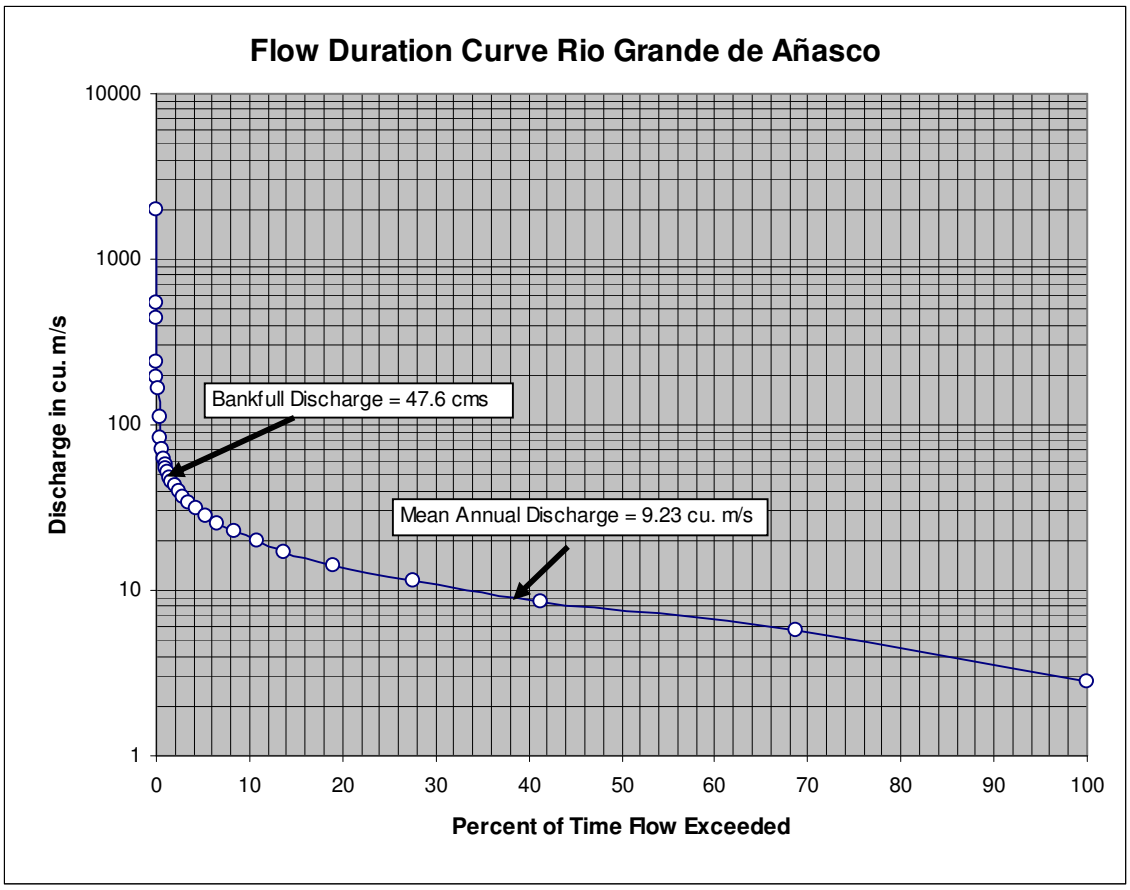

Figure 26 *Flood duration curve for the Rio Grande de Añasco.*

Table 11 *Elapsed years and number of bankfull discharge events between aerial photographs*

Date	Years	Number of bankfull events	N bkf/year
7/1/1966	-	-	
3/20/1977	10.73	32	3.0
2/7/1983	5.89	29	4.9
1/22/1990	6.96	29	4.2
10/29/1993	3.77	29	7.7
9/21/1995	1.90	2	1.1
8/12/1997	1.89	12	6.3
11/28/1999	2.30	45	19.6
8/8/2004	4.70	32	6.8

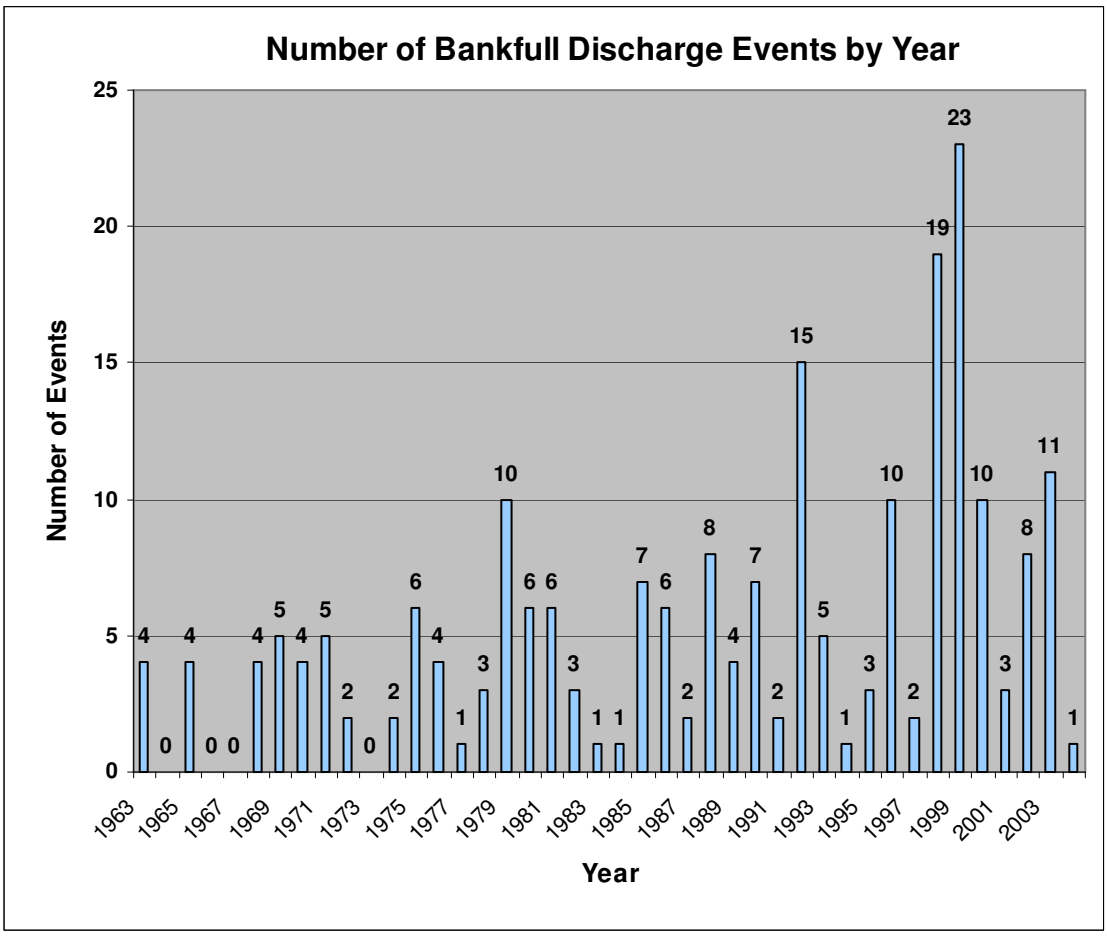

Figure 27 *Number of bankfull discharge events per calendar year.*

Bend Curvature and Bankfull Event Frequency

Using the information from the analysis of bankfull discharge and the meander migration distance measurements for all 8 bends over the 33 year period of the study, these were scaled as a ratio of meander migration distance per bankfull discharge event and are presented as M/bkf in Table 12. This scaling is necessary in order to predict meander migration distance, and not a mean annual meander migration rate. The actual meander migration distance at each bend measured divided by the number of bankfull discharge events provides the bend migration distance per bankfull discharge event. In this manner, by determining the actual bend migration per bankfull discharge event over the elapsed time for all observations, the amount of movement can then be related to the radius of curvature to width ratio (r/w), and the ratio at which maximum migration at a bend can be determined per bankfull discharge event. This ratio of meander migration distance per bankfull discharge event was computed and then plotted versus the bend curvature (r/w) and is presented in Figure 28.

The relationship between meander bend migration distance and the r/w ratio is nonlinear. It increases toward a maximum occurring at approximately r/w = 2.20, and then decreases as the r/w ratio increases. This plot is different from that presented in Figure 18, where maximum migration is scaled in meters per year and was shown to be approximately r/w = 2.42. This is due mainly to the fact that bankfull discharge is a discrete event caused by the intermittent energy inputs to the system that cause channel movement. The r/w of 2.20 is related to an actual measurement of channel

Table 12 *Meander migration distance per bankfull discharge event*

Bend	Year	radius of curv.	width	r/w	M	N bkf	M / bkf
1	1966-1977	35	20.5	1.71	12.8	32	0.40
1	1977-1983	37.5	20.5	1.83	8.1	29	0.28
1	1983-1990	30	20.5	1.46	13	29	0.45
1	1990-1993	27	20.5	1.32	3.4	29	0.12
1	1993-1995	30	20.5	1.46	1	2	0.50
1	1995-1997	27.5	20.5	1.34	3	12	0.25
1	1997-1999	30	20.5	1.46	14.4	45	0.32
2	1966-1977	41.3	15.8	2.61	22	32	0.69
2	1977-1983	40	15.8	2.53	16	29	0.55
2	1983-1990	30	15.8	1.90	10.6	29	0.37
2	1990-1993	27	15.8	1.71	4.6	29	0.16
2	1993-1995	27	15.8	1.71	1	2	0.50
2	1995-1997	29	15.8	1.84	1.9	12	0.16
2	1997-1999	32	15.8	2.03	10.2	45	0.23
3	1977-1983	65	17	3.82	12	29	0.41
3	1983-1990	49	17	2.88	20	29	0.69
3	1990-1993	29	17	1.71	9.9	29	0.34
3	1993-1997	26	17	1.53	5.7	14	0.41
3	1997-1999	26	17	1.53	10.7	45	0.24
4	1966-1977	95	19	5.00	7.1	32	0.22
4	1977-1983	85	19	4.47	10.9	29	0.38
4	1983-1990	65	19	3.42	13.6	29	0.47
4	1990-1993	46	19	2.42	26.1	29	0.90
4	1993-1997	35	19	1.84	10.4	14	0.74
4	1997-1999	31	19	1.63	6.3	45	0.14
5	1983-1990	26	14	1.86	23.2	29	0.80
5	1990-1993	27	14	1.93	10.6	29	0.37
5	1993-1995	27	14	1.93	1	2	0.50
5	1995-1999	28	14	2.00	12.8	57	0.22
6	1977-1983	65	17	3.82	14.5	29	0.50
6	1983-1990	90	17	5.29	17.6	29	0.61
6	1990-1993	60	17	3.53	11.2	29	0.39
6	1993-1995	58	17	3.41	1.8	2	0.90
6	1995-1997	56	17	3.29	4	12	0.33
6	1997-1999	52	17	3.06	12.5	45	0.28
7	1966-1977	40	15	2.67	25	29	0.86
7	1977-1983	28	15	1.87	19.4	29	0.67
7	1983-1990	33	15	2.20	31.9	29	1.10
7	1990-1993	29	15	1.93	5	29	0.17
7	1993-1995	29	15	1.93	1	2	0.50
7	1995-1997	31	15	2.07	4.7	12	0.39
7	1997-1999	42	15	2.80	6.4	45	0.14
8	1977-1983	54	14	3.86	12	29	0.41
8	1983-1990	79	14	5.64	11.7	29	0.40
8	1990-1993	82	14	5.86	9.7	29	0.33
8	1993-1995	84	14	6.00	1	2	0.50
8	1995-1997	85	14	6.07	2.5	12	0.21
8	1997-1999	95	14	6.79	9	45	0.20

M = migration distance (m); r/w = radius of curvature to width ratio; N bkf = number of bankfull discharges; M/bkf = migration per bankfull event

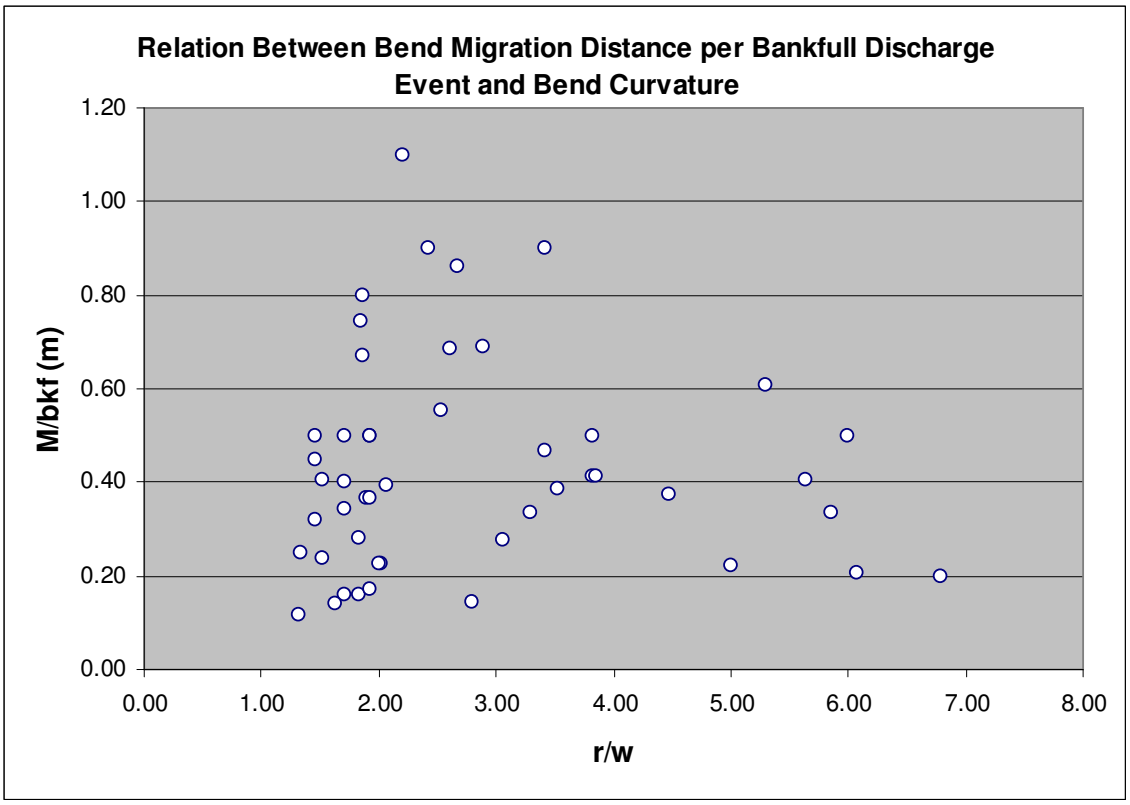

Figure 28 *Relation between bend migration per bankfull discharge event and bend curvature ratio.*

movement at the bend relative to the number of energy inputs and bend curvature over a specific time period. Therefore, for the purpose of predicting maximum migration distance at the bend it is considered an appropriate parameter to be used.

Silt-Clay Composition of Banks

Standard mechanical sediment analysis was used to determine the silt-clay content of the concave banks of the Rio Grande de Añasco and the procedure was described in Chapter IV. The sampling sites were bends B1 through B8 of Study Area One (Fig. 10). The results are summarized in Table 13.

An important controlling variable in the ability of a stream to shift laterally is the resistance of its banks (Hickin and Nanson 1984). Although bank resistance is not simply the function of one material property, it does depend on the degree of cohesion, which can be expressed by its silt-clay content (Ferguson 1973). Most river banks contain significant amounts of silt and clay, and possess some degree of cohesion and resistance to erosion through inter-particle, and electromagnetic bonding (Robert 2003). This parameter, in addition to bank strength, was chosen as a variable of resistance because in humid tropical climates the finer-grained soils of the banks of streams increase cohesiveness that is expected to increase resistance.

Bank Strength

This parameter, in addition to silt-clay composition of banks, was also chosen as a variable of resistance because in humid tropical climates the finer-grained soils of the

Table 13 *Silt-clay percent composition of outside bank of meanders*

Bend	Silt-clay percentage of banks
B1	**80 %**
B2	**64 %**
B3	**89 %**
B4	**89 %**
B5	**98 %**
B6	**72 %**
B7	**93 %**
B8	**77 %**

banks of streams increase cohesiveness that is expected to increase strength of the bank. For this study, the vane shear test was used and the methodology described in Chapter IV. The results of these measurements are reported in Table 14. The measurements are shown in kg/cm^2, the parameter of the instrument, and also as kilo Pascals (kPa) the international metric (SI) units for stress (Pascal = 1 N/m^2 ; 1 kg/cm^2 = 98 kPa; Braja 2000).

Valley Slope

Valley slope was selected as a variable because it determines the overall rate of energy loss along a river and is therefore an additional potential control variable on channel processes and meandering (Richards 1982). Valley slope was determined by using elevation values obtained from the digital elevation model (DEM) U.S.G.S. 800301270700 for the area of the Rio Grande de Añasco. The DEM is a digitized version of U.S. Geological Survey topographic map *Rincón Quadrangle N1815-W6707*. The slope is the difference between the elevations of two points divided by the distance between them. The valley altitude at the entrance of the meander belt close to the road number 430 bridge is 10.0 m. The altitude at the center of the meander belt is 7.5 m, with a valley distance of 1825 m. The slope for the first half of the meander belt is 0.00137 (2.5/1825).

Table 14 *Bank strength of outside bank of bends in kg/cm^{2}and kilo-Pascals*

Bend	kg/ sq.cm	Std Dev.	kPa	Std. Dev.
B1	0.13	0.028	12.7	2.74
B2	0.10	0.013	9.8	1.27
B3	0.15	0.041	14.7	4.02
B4	0.15	0.048	14.7	4.70
B5	0.35	0.028	34.3	2.74
B6	0.10	0.013	9.8	1.27
B7	0.25	0.041	24.5	4.02
B8	0.15	0.024	14.7	2.35

The altitude of the valley at the end of the meander belt, close to the road number 2 bridge is 5.0 m. The distance from the center of the meander belt to the bridge is 1825 m. The slope for the second half of the meander belt is 0.00137 (2.5/1825). Any change of valley slope for this portion of the flat alluvial valley is not discernable at the elevation precision offered by the DEM or the U.S. Geological Survey topographic map *Rincón Quadrangle N1815-W6707.* In conclusion, valley slope of the meander belt is relatively constant at 0.00137, and it was decided that its use as an independent variable for model development is fruitless. Because of this, it was ultimately not included in the development of the meander migration model.

The previous paragraphs examined the selection of independent variables to be used in the empirical model. The following sections describe multiple regression analysis and the development of the meander migration model.

Multiple Regression Analysis

Using the data obtained for the five independent variables, an empirical model was developed using multiple regression analysis to predict meander migration distance for the study river. The multiple regression model explains and predicts variation of a single dependent variable from a number of predictor terms (independent variables). These independent variables may or may not be correlated among themselves, and it is generally better that they are not. The general multiple regression equation takes the form:

$$Y = a + b_1 X_1 + b_2 X_2 + \ldots b_j X_j \pm e$$

Where a = intercept term; b_1 to b_j = regression coefficients; e = error term (Ott and Longnecker 2001). For this study, five independent variables were used to predict "Y" the dependent variable, which is meander bends migration distance.

Before the regression model was run, tests for homogeneity of variance (equality of variance) between treatments, normality, and collinearity were conducted. This was done with a Breush-Pagan test, Shapiro-Wilk test, and Variance Inflation Factor (VIF) test respectively (Field 2000). When the variance was not homogeneous, the variables were transformed by a logarithmic transformation to the base ten (log Y). The model was run with transformations of the dependent and independent variables and homogeneity of variance tested. After testing and achieving homogeneity of variance, the independent variables were tested for collinearity, which is the condition where the independent variables are themselves correlated. The variance inflation factor (VIF) test is used to assess how serious the collinearity problem is. If the VIF is 1, there is no collinearity at all, if it is larger closer to 10 or larger, collinearity is a serious problem. If this is the case, the responsible variable should be eliminated from the analysis because it will result in very high standard errors (Ott and Longnecker 2001).

This statistical analysis used SPSS version 11.5 software. The regression model was run and the coefficient of determination computed (R^2; the square of the correlation coefficient). A value of 1.0 indicates that the model predicts 100% of the variability of the dependent values by variability of the independent variables, and there is nothing left unexplained. This parameter will vary greatly depending on the complexity of the system being tested. If the R^2 is found to be too small, the Cook's and Leverage tests can

be conducted to determine errors and possible problems points. Once the variables have been selected, these can be further analyzed to select the best regression using the criterion of the highest adjusted R^2 (Ott and Longnecker 2001).

In SPSS, the best variables for regression can be selected using several approaches. A model can be developed by adding variables one by one until a combination that achieves the highest adjusted R^2 is attained, or by using backward elimination, stepwise regression, or forward selection. Backward elimination starts with the complete model with all independent variables entered and eliminates variables one at a time until a reasonable candidate regression model is found. Stepwise regression, on the other hand, works in the other direction adding variables one at a time. A simplified stepwise is also used called forward selection, whereby, once a variable is entered, it cannot be eliminated from the regression equation at a later stage (Ott and Longnecker 2001). The method chosen between backward, stepwise and forward was the one that produced the highest adjusted R^2. The details of model development follow.

Model Development

The model development requires data for bends B1 to B8 for migration distance (M), bankfull discharge (N_{bkf}), radius of curvature to width ratio (r/w), silt-clay percentage of bank (B), and bank strength (Φ), and are summarized and sorted by bend in Table 15. Because the data for the r/w values is nonlinear, they were divided into two approximately linear segments with the first segment consisting of points increasing in r/w value or positive slope from the lowest r/w value of 1.32 to less than the maximum

Table 15 *Data used for meander migration model development*

Bend	Year	M (m)	r/w	N bkf	Silt-clay	Bank strength (kPa)
1	1966-1977	12.8	1.71	32	0.800	12.7
1	1977-1983	8.1	1.83	29	0.800	12.7
1	1983-1990	13	1.46	29	0.800	12.7
1	1990-1993	3.4	1.32	29	0.800	12.7
1	1993-1995	1	1.46	2	0.800	12.7
1	1995-1997	3	1.34	12	0.800	12.7
1	1997-1999	14.4	1.46	45	0.800	12.7
2	1966-1977	22	2.61	32	0.639	9.8
2	1977-1983	16	2.53	29	0.639	9.8
2	1983-1990	10.6	1.90	29	0.639	9.8
2	1990-1993	4.6	1.71	29	0.639	9.8
2	1993-1995	1	1.71	2	0.639	9.8
2	1995-1997	1.9	1.84	12	0.639	9.8
2	1997-1999	10.2	2.03	45	0.639	9.8
3	1977-1983	12	3.82	29	0.890	14.7
3	1983-1990	20	2.88	29	0.890	14.7
3	1990-1993	9.9	1.71	29	0.890	14.7
3	1993-1997	5.7	1.53	14	0.890	14.7
3	1997-1999	10.7	1.53	45	0.890	14.7
4	1966-1977	7.1	5.00	32	0.887	14.7
4	1977-1983	10.9	4.47	29	0.887	14.7
4	1983-1990	13.6	3.42	29	0.887	14.7
4	1990-1993	26.1	2.42	29	0.887	14.7
4	1993-1997	10.4	1.84	14	0.887	14.7
4	1997-1999	6.3	1.63	45	0.887	14.7
5	1983-1990	23.2	1.86	29	0.980	34.3
5	1990-1993	10.6	1.93	29	0.980	34.3
5	1993-1995	1	1.93	2	0.980	34.3
5	1995-1999	12.8	2.00	57	0.980	34.3
6	1977-1983	14.5	3.82	29	0.720	9.8
6	1983-1990	17.6	5.29	29	0.720	9.8
6	1990-1993	11.2	3.53	29	0.720	9.8
6	1993-1995	1.8	3.41	2	0.720	9.8
6	1995-1997	4	3.29	12	0.720	9.8
6	1997-1999	12.5	3.06	45	0.720	9.8
7	1966-1977	25	2.67	29	0.930	24.5
7	1977-1983	19.4	1.87	29	0.930	24.5
7	1983-1990	31.9	2.20	29	0.930	24.5
7	1990-1993	5	1.93	29	0.930	24.5
7	1993-1995	1	1.93	2	0.930	24.5
7	1995-1997	4.7	2.07	12	0.930	24.5
7	1997-1999	6.4	2.80	45	0.930	24.5
8	1977-1983	12	3.86	29	0.770	14.7
8	1983-1990	11.7	5.64	29	0.770	14.7
8	1990-1993	9.7	5.86	29	0.770	14.7
8	1993-1995	1	6.00	2	0.770	14.7
8	1995-1997	2.5	6.07	12	0.770	14.7
8	1997-1999	9	6.79	45	0.770	14.7

r/w of 2.20, and presented in Table 16. These represent values of r/w lower than the value where maximum migration because the bend has tightened so much that the flow has collapsed and shear stress has been reduced on the boundary. The negative slope portion of r/w values from 2.20 to 6.79 are presented in Table 17, and represents bends that are opening (larger r/w) and where migration distance decreases. In summary, several empirical equations were determined for r/w values from 1.32 to less than 2.20 ($1.32 \leq r/w < 2.20$), and for r/w values from equal to 2.20 to 6.79 ($2.20 \leq r/w \leq 6.79$). A similar approach was taken by Hickin and Nanson (1975) in their development of their empirical models previously mentioned. All data were first tested for homogeneity of variance using the Breusch-Pagan Test (Field 2000). Where data were not homogeneous (rejected with a significance level $p = .0107$), they were transformed using a logarithmic to the base 10 transformation. The Breusch-Pagan test was conducted again with the log transformed data, and the resulting significance level was $p = .6206$. The hypothesis of homogeneous variance was failed to be rejected, and therefore homogeneous variance can be assumed after log transformation.

All data were then tested for normality using the Shapiro-Wilk Test (Ott and Longnecker 2001). This test is used when the number of measurements is less than 50, and tests the hypothesis that the data is normal. The significance level was $p = .527$, results are shown in Figure 29, and the data is assumed normal.

The variance inflation factor (VIF) test was then used to assess collinearity. If VIF = 1, there is no collinearity at all, and the closer it gets to 10 the higher the collinearity. If there is collinearity, the responsible variable should be eliminated from

Table 16 *Positive slope portion of r/w data used in model (1.32 < r/w < 2.20)*

Bend	Year	M (m)	r/w	N bkf	Silt-clay	Bank strength (kPa)
1	1990-1993	3.4	1.32	29	0.800	12.7
1	1995-1997	3	1.34	12	0.800	12.7
1	1983-1990	13	1.46	29	0.800	12.7
1	1993-1995	1	1.46	2	0.800	12.7
1	1997-1999	14.4	1.46	45	0.800	12.7
3	1993-1997	5.7	1.53	14	0.890	14.7
3	1997-1999	10.7	1.53	45	0.890	14.7
4	1997-1999	6.3	1.63	45	0.887	14.7
3	1990-1993	9.9	1.71	29	0.890	14.7
1	1966-1977	12.8	1.71	32	0.800	12.7
2	1990-1993	4.6	1.71	29	0.639	9.8
2	1993-1995	1	1.71	2	0.639	9.8
1	1977-1983	8.1	1.83	29	0.800	12.7
2	1995-1997	1.9	1.84	12	0.639	9.8
4	1993-1997	10.4	1.84	14	0.887	14.7
5	1983-1990	23.2	1.86	29	0.980	34.3
7	1977-1983	19.4	1.87	29	0.930	24.5
2	1983-1990	10.6	1.90	29	0.639	9.8
5	1990-1993	10.6	1.93	29	0.980	34.3
5	1993-1995	1	1.93	2	0.980	34.3
7	1990-1993	5	1.93	29	0.930	24.5
7	1993-1995	1	1.93	2	0.930	24.5
5	1995-1999	12.8	2.00	57	0.980	34.3
2	1997-1999	10.2	2.03	45	0.639	9.8
7	1995-1997	4.7	2.07	12	0.930	24.5

Table 17 *Negative slope portion of r/w data used in model* ($2.20 \leq r/w \leq 6.79$)

Bend	Year	M (m)	r/w	N bkf	Silt-clay	Bank strength (kPa)
7	1983-1990	31.9	2.20	29	0.930	24.5
4	1990-1993	26.1	2.42	29	0.887	14.7
2	1977-1983	16	2.53	29	0.639	9.8
2	1966-1977	22	2.61	32	0.639	9.8
7	1966-1977	25	2.67	29	0.930	24.5
7	1997-1999	6.4	2.80	45	0.930	24.5
3	1983-1990	20	2.88	29	0.890	14.7
6	1997-1999	12.5	3.06	45	0.720	9.8
6	1995-1997	4	3.29	12	0.720	9.8
6	1993-1995	1.8	3.41	2	0.720	9.8
4	1983-1990	13.6	3.42	29	0.887	14.7
6	1990-1993	11.2	3.53	29	0.720	9.8
3	1977-1983	12	3.82	29	0.890	14.7
6	1977-1983	14.5	3.82	29	0.720	9.8
8	1977-1983	12	3.86	29	0.770	14.7
4	1977-1983	10.9	4.47	29	0.887	14.7
4	1966-1977	7.1	5.00	32	0.887	14.7
6	1983-1990	17.6	5.29	29	0.720	9.8
8	1983-1990	11.7	5.64	29	0.770	14.7
8	1990-1993	9.7	5.86	29	0.770	14.7
8	1993-1995	1	6.00	2	0.770	14.7
8	1995-1997	2.5	6.07	12	0.770	14.7
8	1997-1999	9	6.79	45	0.770	14.7

Case Processing Summary

	Cases					
	Valid		Missing		Total	
	N	Percent	N	Percent	N	Percent
Standardized Residual	48	100.0%	0	.0%	48	100.0%

Tests of Normality

	Kolmogorov-Smirnov[a]			Shapiro-Wilk		
	Statistic	df	Sig.	Statistic	df	Sig.
Standardized Residual	.088	48	.200*	.979	48	.527

*. This is a lower bound of the true significance.

a. Lilliefors Significance Correction

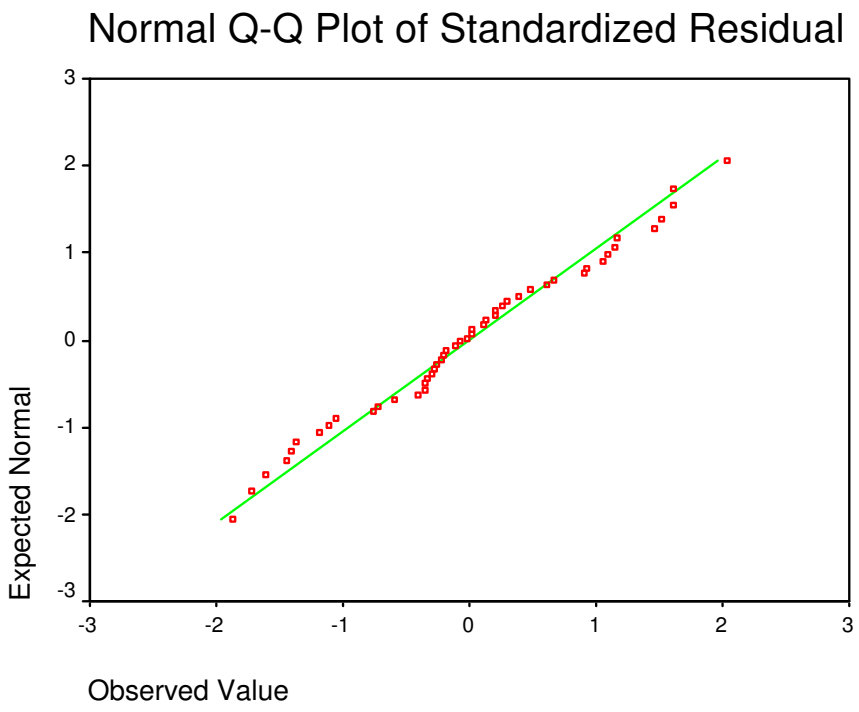

Figure 29 *Test for normality of all transformed data.*

the analysis because it may produce very high standard errors (Ott and Longnecker 2001). The VIF Test was run and an index of 8.04 was obtained for the bank strength variable (Φ). Since this implies high collinearity, this variable was eliminated from the model and the VIF Test conducted again. Without the bank strength variable, the VIF index was 1.038, indicating low collinearity between variables when N_{bkf}, r/w, and B are used as independent variables. In summary, the preliminary analysis of data has eliminated the independent variables slope (s) and bank strength Φ from the model.

Using the independent variables of bankfull discharge frequency (N_{bkf}), radius of curvature to width ratio (r/w), and silt-clay percentage of banks (B), multiple regression analysis was run using the options provided by SPSS in order to obtain the highest adjusted R^2 combination. First, the regression was run for the range of radius of curvature to width values from $1.32 \leq r/w < 2.20$ and then for the range from $2.20 \leq r/w \leq 6.79$. For each of these segments, the regression was run four ways: all variables, stepwise, backward, and forward.

For the first regression from $1.32 \leq r/w < 2.20$, the output is summarized in Table 18. The results for the backward method show two similar best results possibilities of combinations of independent variables for adjusted R^2. When the three variables of bankfull discharge frequency (N_{bkf}), radius of curvature to width ratio (r/w), silt-clay percentage of banks (B) are included in the model, an adjusted $R^2 = 0.768$ is obtained. When the variables N_{bkf} and B alone are included, an adjusted $R^2 = 0.770$ is obtained. Prediction is slightly improved by including the bankfull discharge frequency (N_{bkf}),

Table 18 *Regression analysis results for 1.32 ≤ r/w < 2.20*

1. All variables entered:

Model Summary

Model	R	R Square	Adjusted R Square	Std. Error of the Estimate
1	.893[a]	.797	.768	.20339

a. Predictors: (Constant), LOG_S_C, LOG_N_BK, LOG_R_W

2. Stepwise:

Model Summary

Model	R	R Square	Adjusted R Square	Std. Error of the Estimate
1	.870[a]	.757	.747	.21268

a. Predictors: (Constant), LOG_N_BK

3. Backward:

Model Summary

Model	R	R Square	Adjusted R Square	Std. Error of the Estimate
1	.893[a]	.797	.768	.20339
2	.888[b]	.789	.770	.20280

a. Predictors: (Constant), LOG_S_C, LOG_N_BK, LOG_R_W

b. Predictors: (Constant), LOG_S_C, LOG_N_BK

4. Forward:

Model Summary

Model	R	R Square	Adjusted R Square	Std. Error of the Estimate
1	.870[a]	.757	.747	.21268

a. Predictors: (Constant), LOG_N_BK

representing force, and the silt-clay composition of the banks (*B*), representing resistance. The influence of *r/w*, representing geometry, decreases at *r/w* values lower than the maximum of 2.20. Results indicate that *r/w* has no *additional* predictive value. This point will be further assessed after determining the best model for the receding limb.

The second segment was also run four ways: all variables, stepwise, backward, and forward. The output is summarized in Table 19. In this range of values, the results that produce the best model are bankfull discharge frequency (N_{bkf}) and *r/w*. In three of the methods, stepwise, backward, and forward, these two variables give the highest adjusted $R^2 = 0.749$. For this range, the silt-clay composition of the banks (*B*) is not a predominant controlling variable, and the radius of curvature to width ratio (r/w), representing geometry, becomes more influential in controlling meander erosion at the bend. Results indicate that silt-clay composition has no *additional* predictive value over and above that contributed by the other variables.

To further assess the decreasing impact of the radius of curvature to width ratio (r/w) after reaching the maximum value of 2.20 as the bend gets tighter (lower than r/w = 2.20), two regressions where performed using only the r/w value as the independent variable for both ranges, $1.32 \leq r/w < 2.20$ and $2.20 \leq r/w \leq 6.79$, to determine its correlation with meander migration distance. The results are summarized in Figures 30 and 31. The low R^2 of 0.02 for r/w as a predictor for the $1.32 \leq r/w < 2.20$ range indicates that the radius of curvature to bend ratio has less influence as a control variable of bend migration.

Table 19 *Regression analysis results for 2.20 ≤ r/w < 6.79*

1. All variables entered:

Model Summary

Model	R	R Square	Adjusted R Square	Std. Error of the Estimate
1	.878[a]	.772	.736	.19323

a. Predictors: (Constant), LOG_S_C, LOG_R_W, LOG_N_BK

2. Stepwise:

Model Summary

Model	R	R Square	Adjusted R Square	Std. Error of the Estimate
1	.803[a]	.644	.627	.22942
2	.878[b]	.772	.749	.18835

a. Predictors: (Constant), LOG_N_BK

b. Predictors: (Constant), LOG_N_BK, LOG_R_W

3. Backward:

Model Summary

Model	R	R Square	Adjusted R Square	Std. Error of the Estimate
1	.878[a]	.772	.736	.19323
2	.878[b]	.772	.749	.18835

a. Predictors: (Constant), LOG_S_C, LOG_R_W, LOG_N_BK

b. Predictors: (Constant), LOG_R_W, LOG_N_BK

4. Forward:

Model Summary

Model	R	R Square	Adjusted R Square	Std. Error of the Estimate
1	.803[a]	.644	.627	.22942
2	.878[b]	.772	.749	.18835

a. Predictors: (Constant), LOG_N_BK

b. Predictors: (Constant), LOG_N_BK, LOG_R_W

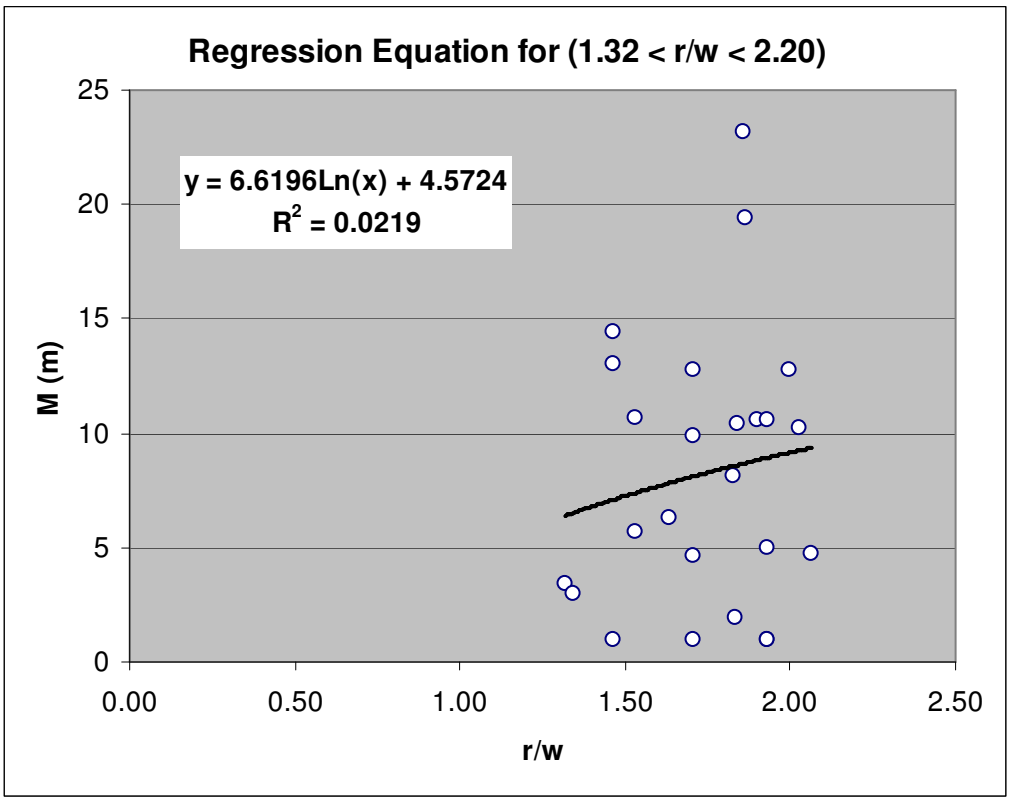

Figure 30 *Regression equation for meander migration as a function of r/w for the range (1.32 ≤ r/w < 2.20).*

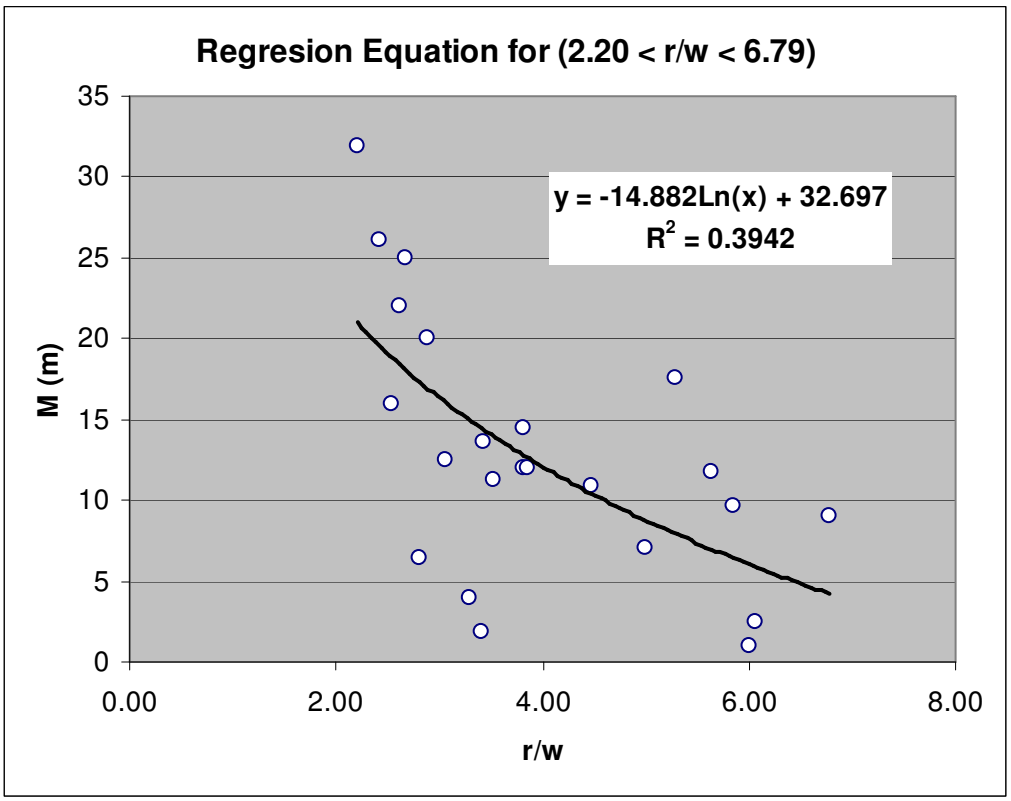

Figure 31 *Regression equation for meander migration as a function of r/w for the range (2.20 ≤ r/w ≤6.79).*

When running the multiple regression analysis the SPSS software tests the hypothesis of no predictive value for each of the independent variables. For the range $1.32 \leq r/w < 2.20$ the significance level for each variable is shown in Table 20. For both models, the bankfull discharge frequency (N_{bkf}) shows a p=.000 indicating that the hypothesis of no predictive value is strongly rejected. The radius of curvature to width ratio (r/w) shows a $p = 0.36$ indicating that the hypothesis of no prediction was failed to be rejected. The silt-clay percentage (B) shows a $p = .08$ indicating that the hypothesis was rejected but at a 92% level. For the range $2.20 \leq r/w \leq 6.79$ the significance level for silt-clay (B) in model one and shown in Table 21, $p = .96$, indicating that the hypothesis of no predictive value for this variable was failed to be rejected with a high level of certainty.

In summary, the results suggest that the radius of curvature to width ratio (r/w), representing geometry, is an important independent variable affecting meander migration in open bends ($2.20 \leq r/w \leq 6.79$). In tighter bends ($1.32 \leq r/w < 2.20$), the silt-clay content of the banks, representing resistance, becomes more significant as a predictor of bend migration.

Equations

The general multiple regression equation takes the form:

$$Y = a + b_1 X_1 + b_2 X_2 + \ldots b_j X_j \pm e$$

Where a = intercept term; b_1 to b_j = regression coefficients; e = error term (Ott and Longnecker 2001). In this application, the dependent and independent variables have

been transformed logarithmically (base 10) with the resulting regression equation taking the form of a power function. The transformed equation takes the form:

$$Log\ y = log\ a + b_1\ log\ (X_1) + b_2\ log\ (X_2) + \ldots b_j\ log\ (X_j) \pm log\ (e)$$

That can also be expressed as:

$$Y = k\ X_1^{\,b1}\ X_2^{\,b2} \ldots Xj^{\,bj}$$

Where Y is the dependent variable, k is a constant = log a, and X_1, X_2, X_j, are the independent variables with b_1, b_2, and b_j as the exponents.

The result of the multiple regression analysis produces several expressions for predicting meander migration distance at the bend apex and are summarized below and shown in the SPSS output in Tables 20, 21, and 22:

(1) $M = 0.740\ N_{bkf}^{0.791}\ B^{1.158}$ $(1.32 \le r/w < 2.20)$ adjusted $R^2 = 0.770$

(2) $M = \dfrac{3.18\left(N_{bkf}\right)^{0.761}}{\left(r/w\right)^{0.933}}$ $(2.20 \le r/w \le 6.79)$ adjusted $R^2 = 0.749$

(3) $M = 0.617\ N_{bkf}^{0.834}$ (for all r/w values) adjusted $R^2 = 0.694$

where M is the meander migration distance in meters at the bend apex, N_{bkf} is the number of bankfull discharge events, r/w is the radius of curvature to width ratio, and B is the silt-clay composition of the banks in decimals.

Equation (1) shows the highest correlation for predicting maximum meander migration when the radius of curvature to width ratio (r/w) is below the maximum of 2.20 ($1.32 \le r/w < 2.20$). Equation (2) shows the highest correlation for predicting

Table 20 *Regression analysis, SPSS output for 1.32 ≤ r/w < 2.20*

Model Summary

Model	R	R Square	Adjusted R Square	Std. Error of the Estimate
1	.893[a]	.797	.768	.20339
2	.888[b]	.789	.770	.20280

a. Predictors: (Constant), LOG_S_C, LOG_N_BK, LOG_R_W

b. Predictors: (Constant), LOG_S_C, LOG_N_BK

Coefficients[a]

Model		Unstandardized Coefficients		Standardized Coefficients		
		B	Std. Error	Beta	t	Sig.
1	(Constant)	-.303	.226		-1.339	.195
	LOG_R_W	.685	.734	.093	.934	.361
	LOG_N_BK	.792	.090	.867	8.823	.000
	LOG_S_C	1.070	.646	.164	1.654	.113
2	(Constant)	-.131	.131		-.999	.329
	LOG_N_BK	.791	.090	.866	8.833	.000
	LOG_S_C	1.158	.638	.178	1.815	.083

a. Dependent Variable: LOG_M

Table 21 *Regression analysis, SPSS output for 2.20 ≤ r/w ≤ 6.79*

Model Summary

Model	R	R Square	Adjusted R Square	Std. Error of the Estimate
1	.878[a]	.772	.749	.18835

a. Predictors: (Constant), LOG_N_BK, LOG_R_W

Coefficients[a]

Model		Unstandardized Coefficients		Standardized Coefficients		
		B	Std. Error	Beta	t	Sig.
1	(Constant)	.498	.272		1.830	.083
	LOG_R_W	-.934	.288	-.365	-3.246	.004
	LOG_N_BK	.762	.119	.729	6.400	.000
	LOG_S_C	-.042	.824	-.006	-.051	.960
2	(Constant)	.503	.248		2.031	.056
	LOG_R_W	-.933	.279	-.365	-3.340	.003
	LOG_N_BK	.761	.114	.728	6.671	.000

a. Dependent Variable: LOG_M

Table 22 *Regression analysis, SPSS output for bankfull discharge events for all data values*

Model Summary

Model	R	R Square	Adjusted R Square	Std. Error of the Estimate
1	.837[a]	.701	.694	.22919

a. Predictors: (Constant), LOG_N_BK

Coefficients[a]

Model		Unstandardized Coefficients		Standardized Coefficients		
		B	Std. Error	Beta	t	Sig.
1	(Constant)	-.210	.110		-1.918	.061
	LOG_N_BK	.834	.080	.837	10.374	.000

a. Dependent Variable: LOG_M

maximum meander migration when the radius of curvature to width ratio (*r/w*) is higher than the maximum of 2.20 ($2.20 \leq$ r/w ≤ 6.79). The most important predictor variable is bankfull discharge frequency (N_{bkf}), and equation (3) shows a high correlation that can be used when no other independent variables are known.

For tighter bends, the silt-clay content of the banks, representing resistance, becomes more significant as a predictor variable ($1.32 \leq$ r/w < 2.20). As the stream changes from tighter bends ($1.32 \leq$ r/w < 2.20) to more open bends ($2.20 \leq$ r/w ≤ 6.79), this condition changes. The radius of curvature to width ratio (*r/w)*, a geometric planform relationship that influences flow characteristics at the bend, becomes the second predictor variable in importance after bankfull discharge frequency. This suggests that a shift occurs at a threshold of radius of curvature to width ratio (*r/w*) from tighter to more open bends, from a resistance control variable represented by the silt-clay contents of the banks to a geometric relationship (*r/w*) that influences channel flow as the dominating predictor variable after bankfull discharge frequency.

Summary

The objective of this chapter was to develop an empirical model for predicting bend migration in a representative humid tropical river. The working hypothesis was that meander migration in tropical rivers would be controlled by variables representing force (bankfull discharge frequency and valley slope), channel geometry (r/w ratio), and resistance (the silt-clay content of the banks and bank strength), and that a high coefficient of determination could be achieved by combining these variables.

Preliminary analysis of the independent variables eliminated two of these from model development: valley slope, for being relatively constant, and bank strength, for showing a high VIF index of collinearity. The remaining variables are banhfull discharge frequency to represent force, silt-clay content to represent resistance, and r/w ratio to characterize channel geometry.

The resulting empirical relationships show that meander migration has a high degree of correlation with the number of bankfull discharge events under all scenarios (adjusted $R^2 = 0.694$). Thus, this may be the most single most important parameter capable of predicting migration distance. Model correlation was further enhanced when the silt-clay composition of the banks was included as an independent variable for tighter bends, or specifically for radius of curvature to width ratios that are below the maximum index of 2.20 ($1.32 \leq r/w < 2.20$; adjusted $R^2 = 0.770$). After reaching the maximum threshold value, the silt-clay content of the banks becomes the second controlling variable in importance at r/w values less than maximum r/w value ($1.32 \leq r/w < 2.20$).

The empirical relationships that provide the highest coefficients of determination (R^2) are:

$$M = 0.740\, N_{bkf}^{0.791}\, B^{1.158} \qquad (1.32 \leq r/w < 2.20) \qquad \text{adjusted } R^2 = 0.770$$

$$M = \frac{3.18\left(N_{bkf}\right)^{0.761}}{\left(r/w\right)^{0.933}} \qquad (2.20 \leq r/w \leq 6.79) \qquad \text{adjusted } R^2 = 0.749$$

As the meander bend opens or expands, i.e. as the r/w value increases beyond the maximum of 2.20, the secondary controlling variable in importance after bankfull

discharge frequency becomes the geometric relationship of radius of curvature to width ratio. This suggests that there is a shift in secondary influence from a sedimentological control, i.e. silt-clay composition of the concave bank, to a geometric one, i.e. radius of curvature to width ratio, at a threshold of maximum r/w value for the representative humid tropical river studied. As the bend planform tightens (lower r/w values) it seems that the resistance of the banks increases in importance in controlling meander migration.

Migration rate varies according to tightness of bend because this planform relationship influences flow characteristics. Bagnold (1960) found that total resistance reaches a local minimum, and therefore more erosion, when the r/w is at a maximum that he theorized as approximately two in his studies of flow in pipes. At values below the maximum (tighter bends), the flow along the inner boundary becomes unstable and breaks away from the boundary. Energy dissipation occurs and the flow loses force. Empirical evidence to support this theory was provided by Hickin and Nanson (1984) who showed that migration rates for the Beatton River, British Columbia were greatest when the bend curvature was between 2.0 and 3.0, and erosion fell rapidly beyond this critical range of values. The results of this empirical model for the Rio Grande de Añasco, also supports Bagnold's theory (1960), as the maximum r/w was found to be in the 2.20 to 2.42 range, depending on the scaling factor. As discussed in Chapter V, these values are also within the range of 2.0 to 3.0 reported in the literature for humid temperate rivers. Therefore, during the period of study the results for the Rio Grande de

Añasco support the stipulated hypothesis that the r/w ratio for maximum migration would be similar to those of humid temperate regions.

The objective of this chapter was to develop an empirical meander migration model applicable to the Rio Grande de Añasco that would be able to predict meander migration distance with a higher degree of predictability, i.e. coefficient of determination, than the ones previously discussed by Nanson and Hickin (1983) and Hooke (1980). Also, the model is aimed to predict meander migration distance, not an average long term yearly rate, a parameter more appropriate to shorter-term practical applications.

The Hooke (1980) empirical model reported a coefficient of determination of 0.40, while the Nanson and Hickin (1975) model did not report this value, but did report a standard error of 0.091 m per year. The empirical model developed in this study resulted in empirical relationships that provide higher coefficients of determination than these:

$$M = 0.740\, N_{bkf}^{0.791}\, B^{1.158} \qquad (1.32 \le \text{r/w} < 2.20) \qquad \text{adjusted } R^2 = 0.770$$

$$M = \frac{3.18\left(N_{bkf}\right)^{0.761}}{\left(r/w\right)^{0.933}} \qquad (2.20 \le \text{r/w} \le 6.79) \qquad \text{adjusted } R^2 = 0.749$$

Therefore, the objectives of this chapter were accomplished.

CHAPTER VIII

MODEL TESTING

To test the empirical meander migration model developed in the previous chapter, the meander migration distance at the apex for two selected meander bends was predicted for the year 2004 using the prediction equations developed. These projections are compared with the actual distance of migration as determined from aerial photography measurements for these two bends for the year 2004. Accuracy of the model was established as a percentage of predicted versus actual distances for the two meanders.

The model equations tested are the ones with the highest adjusted R^2:

(1) $M = 0.740\, N_{bkf}^{0.791}\, B^{1.158}$ $\quad (1.32 \le r/w < 2.20)$ $\quad$ adjusted $R^2 = 0.770$

(2) $M = \dfrac{3.18\left(N_{bkf}\right)^{0.761}}{\left(r/w\right)^{0.933}}$ $\quad (2.20 \le r/w \le 6.79)$ $\quad$ adjusted $R^2 = 0.749$

Equation (1) can be applied to river bends with a radius of curvature to width ratio lower than 2.20 (tight bends), and equation (2) can be used to predict maximum migration distance for bends with radius of curvature to width ratios equal to or greater than 2.20 up to 6.79 (wider bends). In order to test these equations, a test meander was chosen for each of these two ranges of values of radius of curvature to width ratio (r/w).

Study Bends Chosen

The first meander bend chosen for the verification of the model is B2, which is located in the western portion of the meander belt (Fig.10), and the second is B9 which

was not previously analyzed and located in the eastern portion of the belt (Fig. 10). Both of these bends are within the two ranges of r/w values ($1.32 \leq r/w < 2.20$ and $2.20 \leq r/w \leq 6.79$). This equation predicts migration distance using the silt-clay composition of the banks, and number of bankfull discharge events for the period.

Predicted vs. Actual: First Case

The period from 1997 to 2004 was chosen in order to make a prediction of seven years which is longer than the prediction made by Beck (1988) using the Ikeda and Parker (1981) mathematical model that predicted the migration of three bends over five years on the Genesee River in Mount Morris, New York within ± 30 percent. Furthermore, this period includes the passage of Hurricane Georges in 1998 and a 100-year flood event. In addition, the aerial photographs for 1997 and 2004 are both of the same scale (1: 5000) and are high resolution providing pixels of 0.5 m.

Bend B2 had an r/w value of 1.84 in 1997 (Table 5), within the range of $1.32 \leq r/w < 2.20$ where the first equation is applicable. This bend is shown on August 12, 1997 in Figure 32 with lines drawn tracing the banks and the centerline. The same bend is shown on August 8, 2004 in Figure 33 with lines also drawn tracing the banks and the centerline. The centerlines were overlayed from 1997 and 2004 and are shown in Figure 34 with transects drawn showing the migration from one period to the next using the TCTM method previously explained. The distances for each transect are reported in Table 23. From this table, the actual maximum meander migration distance for B2 from August 12, 1997 to August 8, 2004 is 12.027 m.

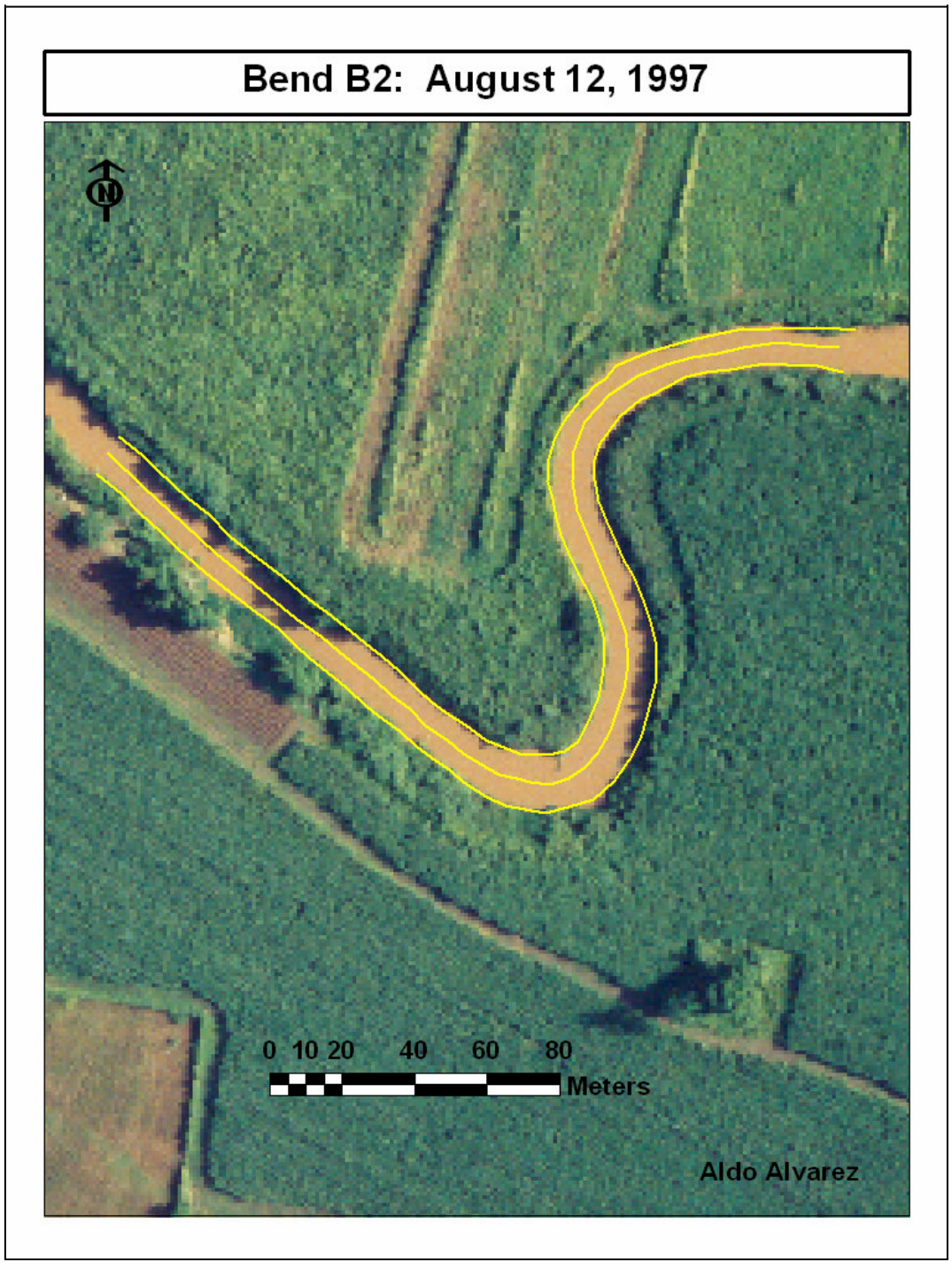

Figure 32 *Bend B2 on August 12, 1997 with centerline and banklines drawn.*

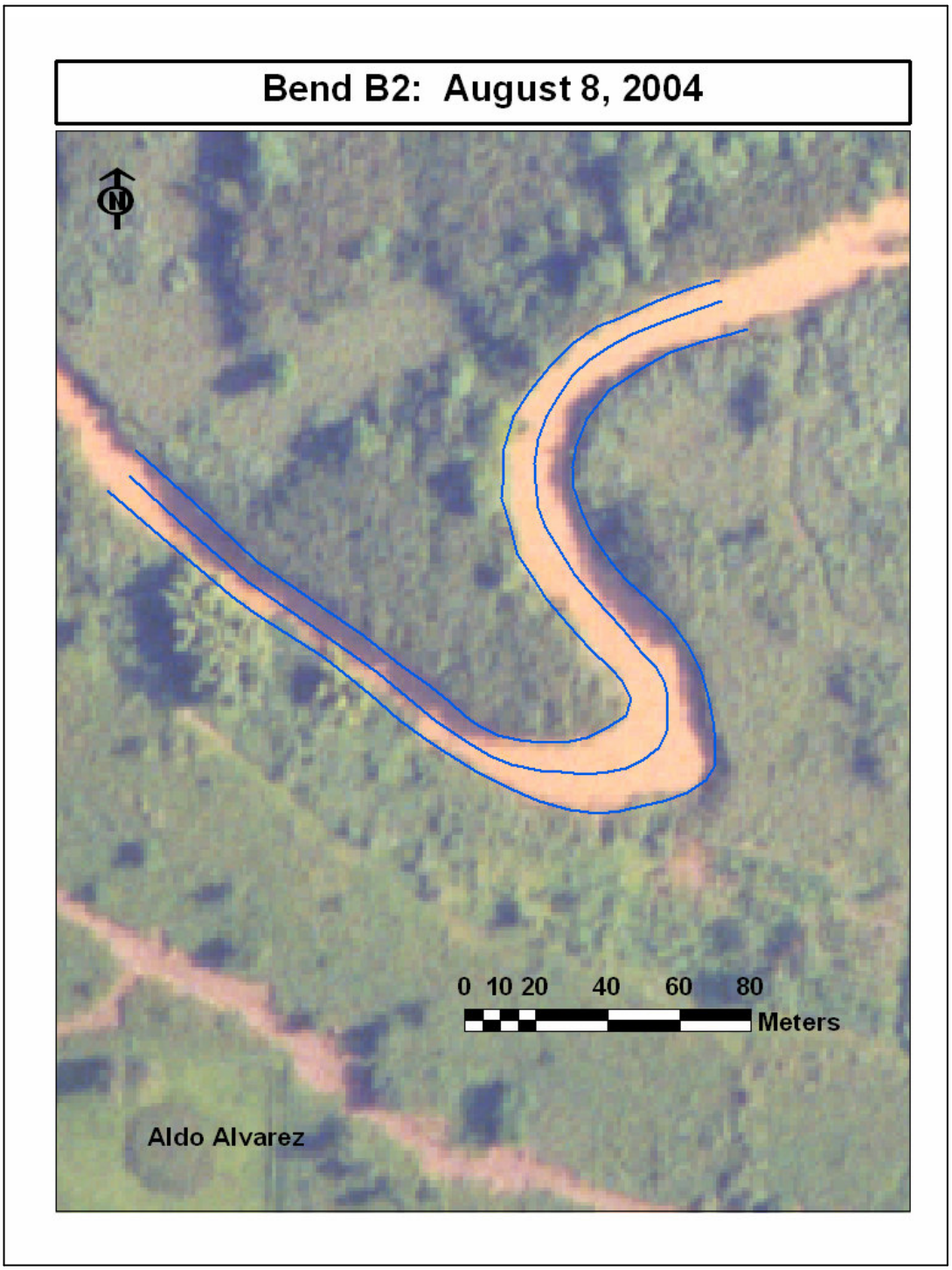

Figure 33 *Bend B2 on August 8, 2004 with centerline and banklines drawn.*

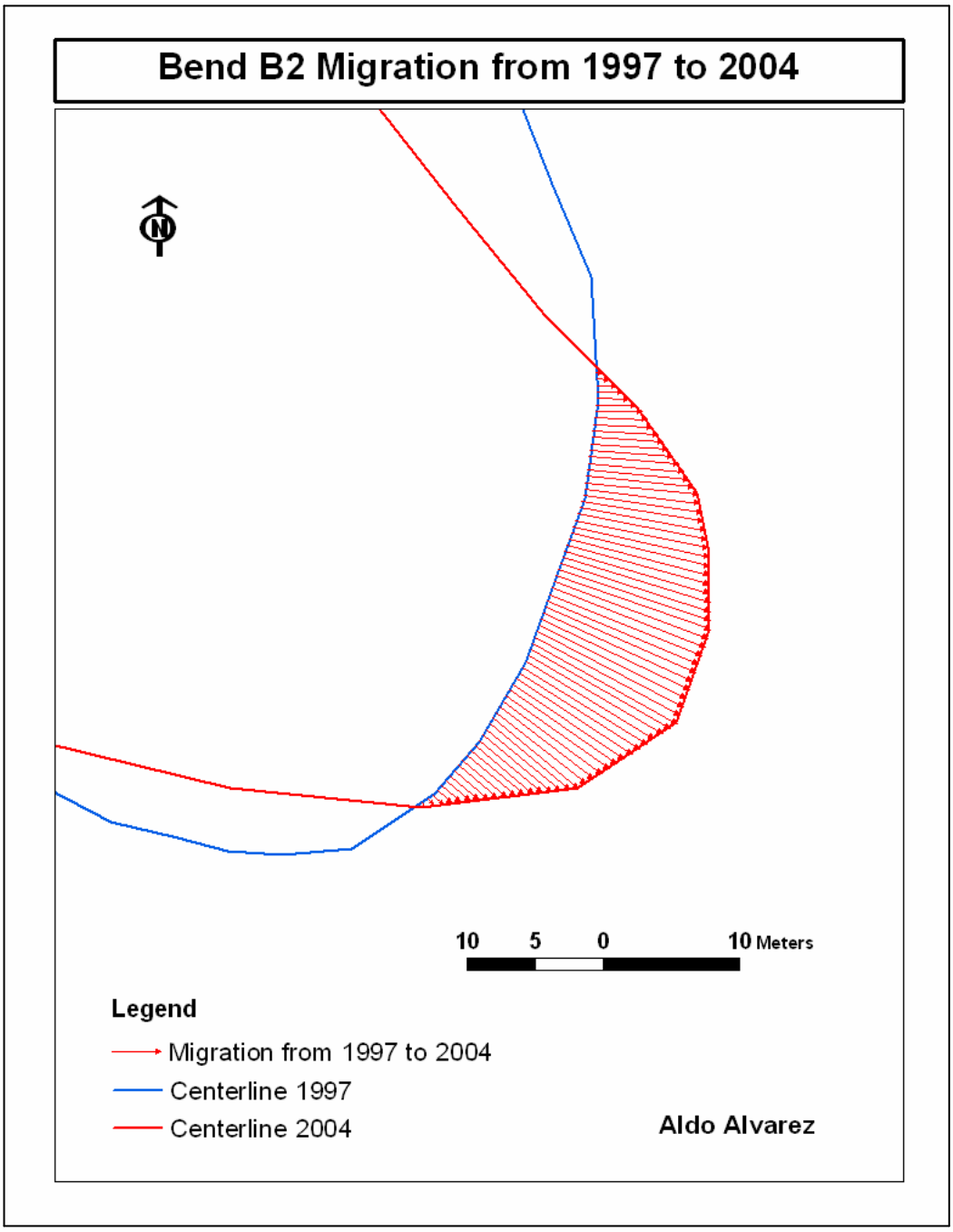

Figure 34 *Bend B2 migration of centerlines from 1997 to 2004.*

Table 23 *Migration distance TCTM output from 1997 to 2004 for bend B2*

Transect	Azimuth	Distance (m)
1	94.788	6.538
2	95.087	6.990
3	95.350	7.441
4	95.583	7.893
5	95.979	8.294
6	97.055	8.505
7	98.077	8.719
8	99.087	9.009
9	100.039	9.318
10	100.930	9.629
11	101.765	9.942
12	102.657	10.199
13	103.605	10.406
14	104.515	10.616
15	105.389	10.829
16	106.230	11.044
17	107.039	11.262
18	107.816	11.481
19	108.565	11.703
20	109.285	11.926
21	110.122	11.987
22	111.019	11.978
23	111.917	11.971
24	112.816	11.968
25	113.715	11.968
26	114.614	11.970
27	115.513	11.976
28	116.410	11.984
29	117.306	11.995
30	118.200	12.010
31	119.091	12.027
32	119.723	11.697
33	120.345	11.303
34	121.009	10.914
35	121.660	10.626
36	122.347	10.339
37	123.073	10.054
38	123.841	9.770
39	124.655	9.488
40	125.519	9.208
41	126.437	8.931
42	127.413	8.656
43	128.453	8.383
44	129.561	8.113
45	129.607	7.582
46	129.659	7.050
47	129.720	6.518
48	129.790	5.988
49	129.819	5.526
50	129.853	5.064

The silt-clay composition of B2 = 0.64 (from Table 13), and the number of bankfull discharge events are 77 (from Table 11). The maximum migration distance predicted by using the empirical equation (1) is:

(1) $M = 0.740\ N_{bkf}^{0.791}\ B^{1.158}$; $M = 0.740\ (77)^{0.791}\ (0.64)^{1.158} = 13.71$ m.

Comparing the actual distance with the predicted distance by equation (1) = 12.027/13.71 = 0.877, the predicted is 14% higher than the actual distance. The same exercise was then conducted for bend B9.

Predicted vs. Actual: Second Case

Bend B9 is shown on August 12, 1997 in Figure 35 with lines drawn tracing the banks and the centerline. The same bend is shown on August 8, 2004 in Figure 36 with lines also drawn tracing the banks and the centerline. The centerlines were again overlayed from 1997 and 2004 and are shown in Figure 37 with transects drawn showing the migration from one period to the next using the TCTM method previously explained. The distances for each transect are reported in Table 24. From this table, the actual maximum meander migration distance is seen to be 35.2 m. The radius of curvature was measured to be 43.5 m, and the width of the channel 15 m. This gives an r/w ratio of 2.9 in 1997, within the values from $2.20 \leq r/w \leq 6.79$.

Equation (2) uses the number of bankfull discharge events (77 from Table 11) and the r/w value (2.9). The maximum migration distance predicted by using the empirical equation (2) is:

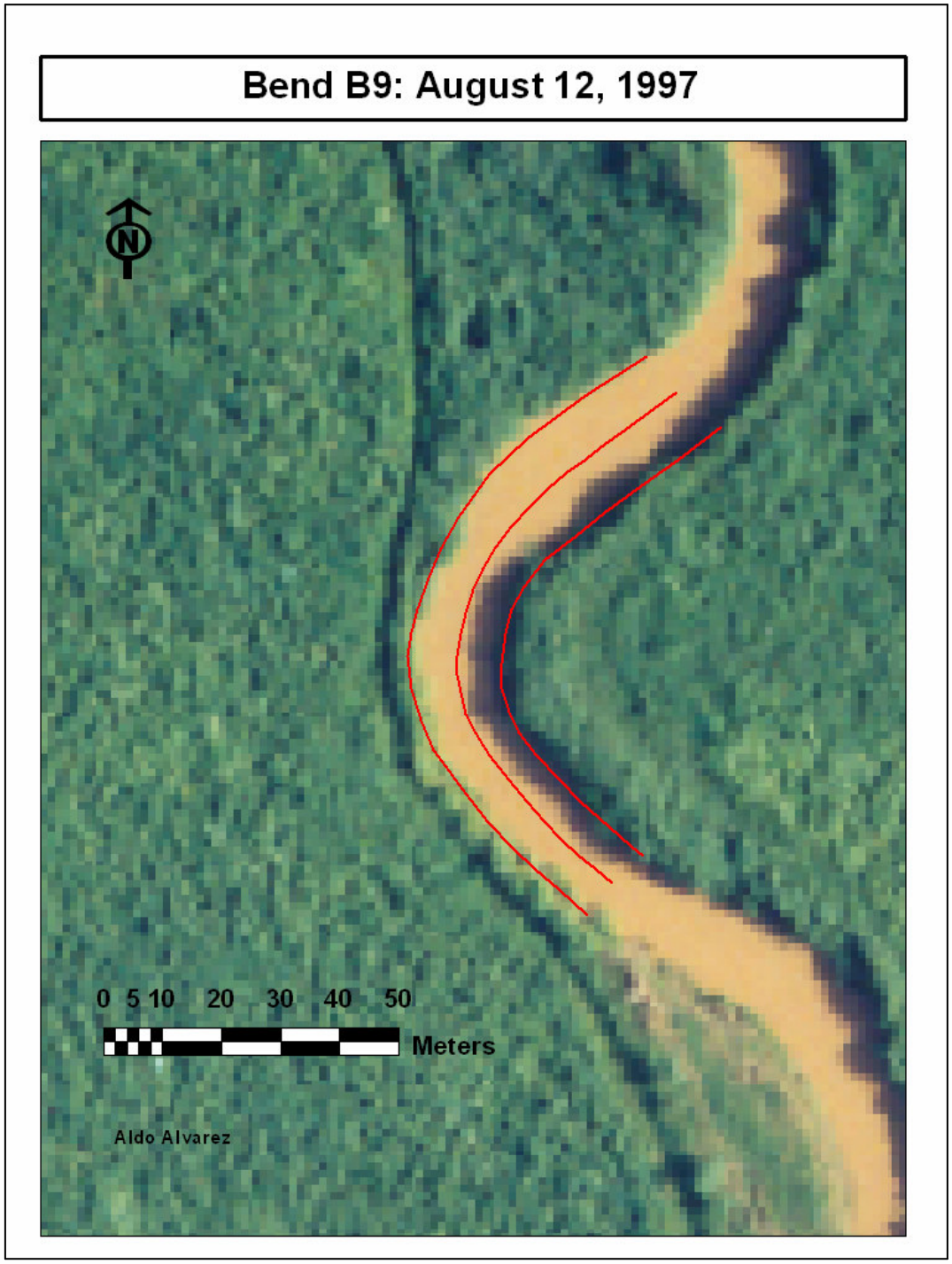

Figure 35 *Bend B9 on August 12, 1997 with centerline and banklines drawn.*

Figure 36 *Bend B9 on August 8, 2004 with centerline and banklines drawn.*

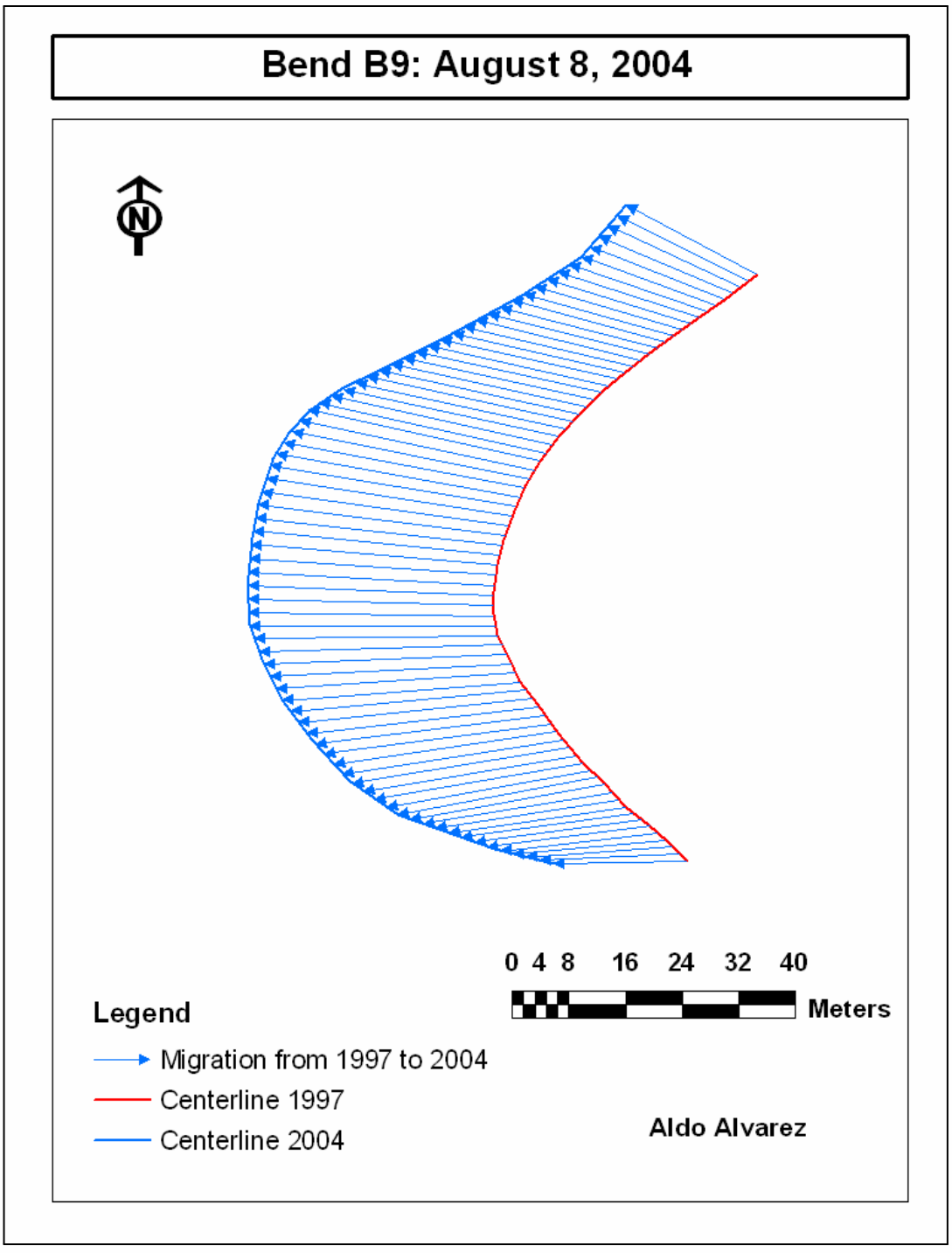

Figure 37 *Bend B9 migration of centerlines from 1997 to 2004.*

Table 24 *Migration distance TCTM output from 1997 to 2004 for bend B9*

Transect	Azimuth	Distance (m)
1	283.999	23.39
2	283.571	23.90
3	283.160	24.40
4	282.766	24.90
5	282.579	25.51
6	282.470	26.14
7	282.382	26.78
8	282.405	27.50
9	282.428	28.21
10	282.453	28.93
11	282.442	29.66
12	282.402	30.37
13	282.381	31.09
14	282.464	31.93
15	282.542	32.77
16	282.624	33.61
17	282.022	33.97
18	281.370	34.28
19	280.746	34.63
20	280.184	35.08
21	279.478	35.20
22	278.671	35.15
23	277.890	35.16
24	277.107	35.17
25	276.305	35.08
26	275.523	35.08
27	274.731	34.98
28	273.942	34.88
29	273.149	34.79
30	272.357	34.67
31	271.571	34.65
32	270.772	34.71
33	270.007	34.76
34	269.327	34.46
35	268.498	34.43
36	267.721	34.32
37	267.017	34.10
38	266.306	33.87
39	265.564	33.68
40	264.848	33.45
41	264.126	33.23
42	263.402	33.00
43	262.807	32.65
44	262.294	32.22
45	261.767	31.78
46	261.145	31.43
47	260.656	31.00
48	260.444	30.38
49	260.195	29.78
50	259.776	29.30

(2) $$M = \frac{3.18\left(N_{bkf}\right)^{0.761}}{\left(r/w\right)^{0.933}}$$; $M = 3.18\ (77)^{0.761} / (2.9)^{0.933} = 32.1$ m.

Comparing the actual distance with the predicted distance by equation (2) = 32.1 / 35.22 = 0.91, the predicted distance is 9% lower than the actual migration distance. The empirical model has been tested for two bends for both ranges of r/w values ($1.32 \leq r/w < 2.20$ and $2.20 \leq r/w \leq 6.79$) and the results of these tests of are summarized in Table 25. It is considered that the empirical model produces satisfactory prediction results. The model prediction compares favorably with those reviewed in the literature that have documented their tests.

Summary

Using the Ikeda and Parker (1981) model, Beck (1988) predicted the migration of three bends over five years on the Genesee River in Mount Morris, New York within ± 30 percent. Hickin and Nanson (1975) derived empirical relationships to predict migration rate per year for the Beatton River, Canada, using the radius of curvature to channel width ratio, and the spacing of meander scrolls as independent variables. Their regression analysis generated the following equations:

$$M = 0.05\ (r/w)^{2.05} + 0.00035d^{2.63} \quad (1.3 < r/w < 2.9)$$

$$M = 2.75\ (r/w)^{-1.73} + 0.00035d^{2.63} \quad (2.9 < r/w < 7.0)$$

Table 25 *Comparison of actual versus predicted meander migration distances using model equations*

Equation	Predicted (m)	Actual (m)	Error
$M = 0.740\ N_{bkf}^{0.791}\ B^{1.158}$ $(1.32 \leq r/w < 2.20)$ adjusted $R^2 = 0.770$	14.6	12.0	+18%
$M = \frac{3.18\left(N_{bkf}\right)^{0.761}}{\left(r/w\right)^{0.933}}$ $(2.20 \leq r/w \leq 6.79)$ adjusted $R^2 = 0.749$	32.1	35.2	-9%

The authors also report a standard error of 0.091 m per year. Using data from various temperate rivers, Hooke (1980) derived the following regression relation for meander migration rate (M):

$$M = 2.45\ A^{0.45}$$

For this equation the coefficient of correlation (R) was 0.63, which indicates a coefficient of determination (R^2) of 0.40 (Hooke 1980). This model therefore explained 40 percent of the variability in meander migration rates for the study streams.

A test was conducted of Hooke's (1980) empirical model that relates maximum meander migration distance in meters per year and the area of a watershed in km^2. Applying this equation to the Rio Grande de Añasco basin yields: M (m/yr) = 2.45 $(515)^{0.45}$ = 40.7 meters per year. The actual measured mean maximum migration rate was found to be 2.39 m/yr. The predicted value is much larger than the actual. It is the opinion that the equation published in the literature either has a typographical error or is a poor predictor for this watershed. The Hooke (1980) equation may have been properly expressed as:

$$M = 0.245\ A^{0.45}$$

With this equation, predicted migration rate would be M (m/yr) = 0.245 $(515)^{0.45}$ = 4.07 meters per year, much closer to the actual and at least the same order of magnitude.

The derived equations from this research estimate meander migration distance as a function of bankfull discharge events, r/w values, and the silt-clay composition of the banks. These empirical meander migration equations show adjusted R^2 values higher than those previously reported in the literature. Furthermore, the model has been tested

for the study area versus actual future measurements for a seven year period, a longer period than the five years on the Genesee River reported by Beck (1988) using the Ikeda and Parker (1981) model with better results.

CHAPTER IX

SUMMARY AND CONCLUSIONS

Major Findings

Channel Planform

The overall objective of this research was to gain an increased understanding of meandering planform dynamics in humid tropical rivers. This was accomplished by pursuing three specific objectives. The first objective was to examine the pattern and channel planform dynamics of a representative alluvial humid tropical river in order to characterize planform change. The working hypotheses were that change in channel pattern of a representative humid tropical river would be highly dynamic, that the primary mechanism for planform change would be through cutoffs and avulsions, rather than braiding, and that the mean meander migration rate and the ratio of meander-bend curvature to channel width (r/w) for maximum migration in the humid tropical river, would be similar to those experienced in humid temperate rivers.

Of the hypotheses stipulated for the first objective, the results for the first showed that overall, the rate of change in sinuosity of the Rio Grande de Añasco increased 13% for the 33 year study period. This rate is comparable to the rate of change found for several temperate rivers. In this regard, the representative humid tropical river can be considered similar in rate of change in sinuosity to those documented for temperate climate rivers. In addition, the mean sinuosity was found to be 2.40 over the period of study, and comparable not only to temperate rivers but to the semi-arid White River in Crawford, Nebraska that had a sinuosity of 2.40 in 1963, with a mean silt-clay

composition of its banks of 79%, a basin area of 801 km^2 (Schumm 1963), and a mean annual precipitation of 406mm (16 in.; Ferrick *et al.* 1995). These parameters are very similar to the Rio Grande de Añasco, although they are in different precipitation regimes. The results indicate that the humid tropical river is similar in rate of change and sinuosity value with temperate rivers reported in the literature. In summary, the results for the representative humid tropical river indicate that it is not more dynamic than its temperate counterparts, even though the climatic regime is different with mean annual precipitation more than double.

The second working hypothesis was that the primary mechanism for planform change in the representative humid tropical river would be through cutoffs and avulsions, rather than braiding. Results of this study indicate that three cutoffs and no avulsions or braiding were observed during the study period. For the study river, the principal mechanism of planform change was through cutoffs during the 33 year period of study. This partially supports the stated hypothesis that cutoffs and avulsions are the primary mechanism. Although cutoffs, avulsions, and braiding have been documented as a mechanism for planform change in temperate rivers, this study cannot conclude from its observations if the humid tropical river studied is any different than temperate rivers in this aspect.

The third working hypothesis was that the mean meander migration rate of the study river would be similar to rates experienced in humid temperate rivers. Due to the high range of migration rates that have been documented in temperate rivers, the mean rate of 2.39 meters per year for the Rio Grande de Añasco was found to be within the

range of values found in temperate rivers. Therefore, the hypothesis is supported, in that there is no apparent difference in mean meander migration rate between the representative humid tropical river and temperate rivers documented in the literature.

The fourth working hypothesis was that the r/w ratio for maximum migration would be similar to those of humid temperate regions. The results of this study show that the maximum yearly mean meander migration rate occurs at approximately a radius of curvature to width ratio of 2.42. This value is within the range of 2.0 to 3.0 reported in the literature for humid temperate rivers. Therefore, the results of this study support the stipulated hypothesis for the period of study for the Rio Grande de Añasco that the r/w ratio for maximum migration would be similar to those of humid temperate regions.

Response and Recovery of Planform to an Extreme Flood Event

Another goal of this study was to document the response and recovery of a humid tropical river to an extreme flood event. The working hypothesis was that, when disturbed by an extreme flood event, both channel width enlargement and the recovery period would be significantly less in a representative humid tropical river than in humid temperate ones.

The objective of this section was accomplished by measuring the effectiveness of the flood in terms of channel width changes, and results of this study indicate that the stipulated hypothesis is supported. The response of the Rio Grande de Añasco to a 100 year flood was a 17% increase in width and a less than two year recovery period, as compared to a 40 percent increase in stream width with a recovery period of 15 years for the Patuxent River, and a 20 percent increase in width and a recovery period of 10 years

for the Baisman Run. These measurements of an in increase in channel width of 17% and recovery period of approximately two years are smaller and more rapid than those reported by Wolman and Gerson (1978) for humid temperate rivers. A reconstructed graphical representation of the response and recovery results for representative arid, semi-arid, and humid temperate rivers reported in Fig. 4 of Wolman and Gerson (1978) were combined with the representative humid tropical river results to produce Figure 22. The trend of shorter recovery times for channel width following a major perturbation for a humid tropical river when compared to humid temperate rivers was demonstrated. The moderate more frequent events as first exposed by Wolman and Miller (1960) apparently play a preponderant role in controlling channel planform dynamics in this climate regime.

Meander Migration Model

The third objective was to develop an empirical model for predicting bend migration rates in the representative humid tropical river. The working hypothesis was that meander migration in humid tropical rivers would be controlled by a set of independent variables that represent force and resistance components in the river system including bankfull discharge frequency, the r/w ratio, the silt-clay content of the meander banks, bank strength, and valley slope.

The resulting empirical relationships show that meander migration has a high degree of correlation with the number of bankfull discharge events under all scenarios (adjusted R^2 = 0.694). Model correlation was further enhanced when the silt-clay

composition of the banks was included as an independent variable for tighter bends, or specifically for radius of curvature to width ratios below the maximum index of 2.20 ($1.32 \leq r/w < 2.20$; adjusted $R^2 = 0.770$). At tighter bends, the silt-clay content of the banks becomes the second variable in prediction value after bankfull discharge frequency. The empirical relationships resulting from this study that provide the highest coefficients of determination for predicting maximum meander migration are:

(1) $M = 0.740\, N_{bkf}^{0.791}\, B^{1.158}$ $(1.32 \leq r/w < 2.20)$ adjusted $R^2 = 0.770$

(2) $M = \dfrac{3.18\left(N_{bkf}\right)^{0.761}}{\left(r/w\right)^{0.933}}$ $(2.20 \leq r/w \leq 6.79)$ adjusted $R^2 = 0.749$

The results of this empirical model for the Rio Grande de Añasco also supports Bagnold's theory (1960) that maximum r/w would occur at approximately 2.0. The maximum r/w value for the Rio Grande de Añasco was found to be in the 2.20 to 2.42 range, depending on the scaling factor. As discussed in Chapter V, these values are also within the range of 2.0 to 3.0 reported in the literature for humid temperate rivers. Therefore, the model results also support the stipulated hypothesis that the r/w ratio for maximum migration would be similar to those of humid temperate regions.

Model Testing

To test the empirical meander migration model developed in this study, the meander migration distance at the apex for two meander bends was predicted for the year 2004. The projections from the model were compared with the actual distance of

migration as determined from aerial photography measurements for two bends for the year 2004. Accuracy of the model was established as a percentage of predicted versus actual distances for the two meanders.

The empirical model was tested for two bends for both ranges of r/w values, the rising (1) and receding limb (2) equations. Equation (1) was used to predict maximum meander migration distance for bend B2, with a predicted distance 14% higher than the actual distance. The same exercise was then conducted for bend B9 but using equation (2). The predicted distance was 9% lower than the actual migration distance. It is considered that the empirical model developed produced satisfactory results when compared with the Hickin and Nanson (1975) and Hooke (1980) empirical models.

The central hypothesis of this research was that due to a climate regime that produces approximately double the amount of precipitation than the humid temperate one, tropical rivers might develop different morphological characteristics than those of temperate regions. The higher precipitation, sediment loads, and frequencies of bankfull discharge combined with greater vegetation resilience and faster chemical weathering rates of the humid tropical climate might produce different force-resistance relationships resulting in channel morphologies distinct from those in temperate regions. In this regard, the planform of the representative humid tropical river can be considered similar in value and rate of change of sinuosity to those documented for temperate climate rivers. Schumm (1960) observed in his studies of alluvial rivers in the Great Plains that discharge itself did not affect sinuosity. Changes in sinuosity are principally controlled

by silt-clay composition of the channel boundary, the type of riparian vegetation and the characteristics of the sediment load, and not by a particular precipitation regime.

In summary, the processes that govern planform operating in humid tropical rivers are similar to those operating in temperate rivers. Changes in sinuosity are principally controlled by silt-clay composition of the channel boundary, the type of riparian vegetation and the characteristics of the sediment load, and not by a particular precipitation regime. Furthermore, results of this study indicate that for the period of study meander migration rate for the representative humid tropical river was similar to those found in temperate rivers. This indicates that although there may be a higher precipitation rate in the humid tropical regime, the high silt-clay content in the channel banks coupled with a resilient vegetation also provide higher resistance to deformation, leading to similar overall migration rates.

The Rio Grande de Añasco also shows r/w values of maximum meander migration similar to those generally found for rivers located in temperate climate regimes. What this suggests is that the resulting balance between form and control variables that dictate channel planform is adjusted not only by the prevailing levels of the control variables such as precipitation and discharge but also presents the question of whether a general physical principle is governing channel form adjustment. The search for the answer to that question is still an ongoing concern.

The results of this study indicate that humid tropical rivers may recuperate more quickly their channel width than temperate rivers channels after a high magnitude flood event. Mainly due to rapid vegetation growth, higher precipitation rates, and abundant

sediment flow, the trend of shorter recovery times in channel width following a major perturbation was demonstrated. The moderate more frequent events as first exposed by Wolman and Miller (1960) apparently play a preponderant role in this climate regime as they relate to channel planform dynamics.

Evaluation of Methodology

There are several limitations in the methods used in this study. First, the use of aerial photographs has its limitations. The digitizing of aerial photographs produces images with cell sizes from 0.5 to 1.0 m. When the images are registered or georeferenced, the RMSE error is approximately 1m. This indicates that measurements below one meter should not be used, and for the purposes of this study all measurements less than one meter were eliminated.

Second, the use of the Topologically Constrained Transect Method (TCTM; Arias-Moran 2003) greatly reduces the work of measuring meander migration. Yet, the method must be carefully applied and length of shapefiles carefully chosen in order for transects to be perpendicular to the stream banks. On many occasions, this careful calibration can take much time, limiting the time-saving usefulness of the method.

Suggestions for Future Work

The next logical area to explore would be to determine what additional control variables could be added to the empirical model in order to increase its explanatory power. One such potential variable could be the effect of the radius of curvature to width

ratio of the preceding bend whose flow is entering the meander being studied. It seems that there is some influence of the preceding bend on flow characteristics.

Another area for future study is the potential prediction of future bankfull discharge events based on climatological data. The frequency of these events in the Rio Grande de Añasco basin seems to be correlated with the frequency and magnitude of EL Niño and La Niña episodes in the Pacific Ocean. The use of the Oceanic El Niño Index (ONI), for example, may provide a control variable for model development.

A third area for study would be to develop a similar empirical meander migration model but using different discharge magnitudes such as, the one year flood, two percent exceedance flow or others, instead of bankfull discharge events. If the resulting coefficient of determination is satisfactory, this would eliminate the need to observe bankfull discharge for model development for a particular river. Lastly, test this model in other rivers of Puerto Rico, and then tropical rivers elsewhere. This would enable broader generalizations to be developed.

Other Considerations

Few models consider all of the processes known to be involved in meander migration and those that do are impractical for routine use due to their complexity and need for very accurate field data. While the past behavior of a meandering reach is not necessarily indicative of its future behavior, the historical record at least integrates the effects of all the relevant variables as they operate in that location. If changes in flow regime, sediment availability, bank materials, land use, or human activities are known to

have occurred during the period of record, the response of the river in the past can indicate how the river may respond to continued changes in the future. In short, although various approaches to modeling exist, the conclusion to be drawn is that there is no one best method and the only complete model of a river is the river itself.

In comparing the channel planform dynamics of humid tropical rivers with that of temperate rivers, it is important to consider the limits of inference from similarity of parameters. Schumm (1991) has discussed the limits of inferring similar results when combining different processes and causes. He called this situation convergence, when it is difficult to infer processes and the causative agents simply from the effects. Chorley (1962) referred to this situation as equifinality.

The Rio Grande de Añasco, a humid tropical river, shows similar planform indices than those of temperate rivers. Sinuosity, rate of change of sinuosity, mean meander migration rate, and radius of curvature to width ratio where maximum meander migration occurs, are similar to those found in temperate rivers. Although this may be the case, it is still to be proved that similar or different processes combined with similar or different causes are producing these similar effects. On the other hand, there may be similar processes operating with similar causes in both climate regimes, but with different combinations of magnitudes and relative scales whose overall combination produce similar results. In conclusion, predictions based upon data from one location may not be valid elsewhere, and extrapolation to others locations must be considered with great caution.

Conclusions

In conclusion, the research presented in this document represents an attempt to gain an increased understanding of meandering planform dynamics in humid tropical rivers. The answers to the research questions summarized above represent a contribution toward theoretical understanding of humid tropical rivers. The statements and results provide explanation for planform behavior, as well as describing spatial and temporal variations. In addition to increasing basic understanding of meander processes in tropical areas and for developing fluvial geomorphological theory, the knowledge gained has potentially important benefits to society. Results of this study could be useful to planners, engineers, and other professionals in estimating meander movement and other hazards.

LITERATURE CITED

Ackers, P., and F.G. Charlton. 1970. Meander geometry arising from varying flows. *Journal of Hydrology* 11:230 - 252.

Ahmad, R., F.N. Scatena, and A. Gupta. 1993. Morphology and sedimentation in Caribbean montane streams: examples from Jamaica and Puerto Rico. *Sedimentary Geology* 85:157 - 169.

Arias-Moran, C. A. 2003. *Spatio-temporal Analysis of Texas Shoreline Changes Using GIS Technique.* M.S. Thesis. Texas A&M University. College Station.

Ayala-Silva, T., and Y.A. Twumasi. 2004. Hurricane Georges and vegetation change in Puerto Rico using AVHRR satellite data. *International Journal of Remote Sensing* 25(9):1629 - 1640.

Bagnold, R. A. 1960. Some aspects of the shape of river meanders. *U.S. Geological Survey Professional Paper 282-E.* Reston, VA: U.S. Geological Survey.

Baker, V. R. 1977. Stream channel response to floods with examples from central Texas. *Geological Society of America Bulletin* 88:1057 - 1070.

Baker, V. R. 1988. Flood erosion. In *Flood Geomorphology,* ed. V. R. Baker, R.C. Kochel, and P.C. Patton, 81 - 96. New York: John Wiley and Sons.

Begin, Z. B. 1986. Curvature ratio and rate of river bend migration-update. *Journal of Hydraulic Engineering* 112:904 - 908.

Biedenharn, D. S., P.G. Combs, G.J. Hill, C.F. Pinkard, and C.B. Pinkston. 1989. Relationship between channel migration and radius of curvature on the Red River. In *Sediment Transport Modeling: Proceedings of the International Symposium,* 536 - 541. New York: American Society of Civil Engineers.

Blake, D. H., and C.D. Ollier. 1971. Alluvial plains of the Fly River, Papua. *Zeitschrift fur Geomorphologie* 12:1-17.

Braja, M. D. 2000. *Fundamentals of Geotechnical Engineering*. Pacific Grove, CA: Brooks/Cole.

Brice, J. C. 1984. Planform properties of meandering streams. In *River Meandering,* ed. C. M. Elliot, 1 - 15. New York: American Society of Civil Engineers.

Bridge, J. S. 2003. *Rivers and Floodplains: Forms, Processes, and Sedimentary Record.* Oxford: Blackwell Publishing.

Brook, G. A., and E. Luft. 1987. Channel pattern changes along the lower Oconee River, Georgia, 1805-1949. *Physical Geography* 8(3):191-209.

Bryant, R. G., and D.J. Gilvear. 1999. Quantifying geomorphic and riparian land cover changes either side of a large flood event using airborne remote sensing: River Tay, Scotland. *Geomorphology* 29:307 - 321.

Cangialosis, J., and S.S. Chen. 2002. A numerical study of the topographic effects on structure and rainfall in Hurricane Georges (1998). In *Proceedings 25th Conference on Hurricanes and Tropical Meteorology*, 231-240. Miami: American Meteorological Society.

Chang, H. H. 1988. *Fluvial Processes in River Engineering*. Malabar, Fl: Krieger Publishing.

Chang, K. T. 2002. *Introduction to Geographic Information Systems*. New York: McGraw-Hill.

Chin, A., D.L. Harris, T.H. Trice, and J.L. Given. 2002. Adjustment of stream channel capacity following dam closure, Yegua Creek, Texas. *JAWRA* 38(6):1521 - 1530.

Chitale, S. 1970. River channel patterns. *Journal of the Hydraulics Division of ASCE.* 1:201 - 221.

Chorley, R. J. 1962. Geomorphology and general systems theory. *U.S. Geological Survey Professional Paper 500-B.* Reston, VA: U.S. Geological Survey.

Christopherson, R. W. 2003. *Geosystems: An Introduction to Physical Geography*. Upper Saddle River, NJ: Prentice Hall.

Clark, J. J., and P.R. Wilcock. 2000. Effects of land-use change on channel morphology in northeastern Puerto Rico. *Geological Society of America Bulletin* 112(12):1763 - 1777.

Costa, J. E. 1974. Response and recovery of a Piedmont watershed from tropical storm Agnes, June 1972. *Water Resources Research* 10(1):106 - 112.

Costa, J. E., and J.E. Conner. 1995. Geomorphically effective floods. In *Natural and Anthropogenic Influences in Fluvial Geomorphology,* ed. J. E. Costa, A.J. Miller, K.W. Potter, and P.R. Wilcock, 45 - 56. Washington, DC: American Geophysical Union.

Daniel, J. F. 1971. Channel movement of meandering Indiana streams. *U.S. Geological Survey Professional Paper 732-A* . Reston, VA: U.S. Geological Survey.

Diaz, J. R., and D.J. Jordan. 1987. Water resources of the Rio Grande de Añasco-lower valley Puerto Rico. *U.S. Geological Survey Water Resources Investigations Report 85-4237.* Reston, VA: U.S. Geological Survey.

Dunne, T., and L.B. Leopold. 1978. *Water in Environmental Planning*. New York: W.H. Freeman and Company.

Dury, D. H. 1977. Underfit streams: retrospect, perspect, and prospect. In *River Channel Changes.* ed. K. J. Gregory, 281 - 293. Belfast, Ireland: John Wiley and Sons.

Ferrick, M. G., N.D. Mulherin, and D.J. Calkins. 1995. Analysis of the winter low-flow balance of the semiarid White River, Nebraska and South Dakota. *Water Resources Research* 31(8):1999-2009.

Ferguson, R. I. 1987. Hydraulic and sedimentary controls of channel pattern. In *River Channels: Environment and Process.* ed. K. S. Richards, 129-158. New York: Blackwell.

Garza, R., and J. Atwell. 1999. Georges over Puerto Rico. In *Hurricane Georges Report,* 1-11. Southeast River Forecast Center. Peachtree City, GA: National Oceanographic and Atmospheric Administration.

Gillespie, B. M., and J.R. Giardino. 1996. Determining the migratory activity index for a river: An example from the Brazos River, Texas. *Zeitschrift fur Geomorphologie* 40:417 - 428.

Goudie, A. 1990. *Geomorphological Techniques*. London: Routledge.

Gupta, A., and H. Fox. 1974. Effects of high magnitude floods on channel form: a case study in Maryland Piedmont. *Water Resources Research* 10(3):499 - 509.

Gupta, A., and A. Dutt. 1989. The Auranga: description of a tropical monsoon river. *Zeitschrift fur Geomorphologie* 33(1):73-92.

Gupta, A. 1995. Magnitude, frequency, and special factors affecting channel form and processes in the seasonal tropics. In *Natural and Anthropogenic Influences in Fluvial Geomorphology,* ed. J. E. Costa, A.J. Miller, K.W. Potter, and P.R. Wilcock, 125 - 136. Washington, DC: American Geophysical Union.

Hickin, E. J. 1974. The development of meanders in natural river-channels. *American Journal of Science* 274:414 - 442.

Hickin, E. J., and G.C. Nanson. 1975. The character of channel migration on the Beatton River, northeast British Columbia, Canada. *Geological Society of America Bulletin* 86:487 - 494.

Hickin, E. J. 1977. The analysis of river planform responses to changes in discharge. In *River Channel Changes,* ed. K. J. Gregory, 249 - 263. Belfast, Ireland: John Wiley and Sons.

Hickin, E. J., and G.C. Nanson. 1984. Lateral migration rates of river bends. *Journal of Hydraulics Engineering* 110:1557 - 67.

Hickin, E. J., and H.M. Sichingabula. 1988. The geomorphic impact of the catastrophic October 1984 flood on the planform of Squamish River, southwestern British Columbia. *Canadian Journal of Earth Science* 25:1078 - 1087.

Hooke, J. M. 1977. The distribution and nature of changes in river channel patterns: the example of Devon. In *River Channel Changes,* ed. K. J. Gregory, 265 - 280. Belfast, Ireland: John Wiley and Sons.

Hooke, J. M. 1980. Magnitude and distribution of rates of bank erosion. *Earth Surface Processes and Landforms* 5:143 - 157.

Hooke, J. M. 1987. Changes in meander morphology. In *International Geomorphology 1986, Part I,* ed. V. Gardiner, 591 - 609. Belfast, Ireland: John Wiley & Sons.

Hooke, J. M., and C.E. Redmond. 1989. Use of cartographic sources for analysing river channel changes with examples from Britain. In *Historical Change of Large Alluvial Rivers: Western Europe,* ed. G. E. Petts, 79 - 99. New York: John Wiley and Sons.

Hooke, J. M. 1997. Styles of channel change. In *Applied Fluvial Geomorphology for River Engineering and Management,* ed. C. R. Thorne, R.D. Hey, and M.D. Ewson, 237 - 268. New York: John Wiley & Sons.

Hudson, P. F., and R. Kesel. 2000. Channel migration and meander-bend curvature in the lower Mississippi River prior to major human modification. *Geology* 28(6):531 - 534.

Hutchinson, S. 2004. *Inside ArcView GIS 8.3*. Clifton Park, NY: Delmar Publishing.

Jensen, J. R. 2005. *Introductory Digital Image Processing*. Upper Saddle River, NJ: Prentice Hall.

Khan, N. I., and A. Islam. 2003. Quantification of erosion patterns in the Brahmaputra-Jamuna River using geographical information system and remote sensing techniques. *Hydrological Processes* 17(959 - 966).

Kilpatrick, F. A., and H.H. Barnes. 1964. Channel geometry of Piedmont streams as related to frequency of floods. *U.S. Geological Survey Professional Paper 422 - E.* Reston, VA: U.S. Geological Survey.

Knighton, D. 1998. *Fluvial Forms and Processes*. New York: Oxford University Press.

Kochel, R. G. 1988. Geomorphic impact of large floods: review and new perspectives on magnitude and frequency. In *Flood Geomorphology,* ed. V. R. Baker, R.C. Kochel, and P.C. Patton, 169 - 187. New York: John Wiley and Sons.

Komar, P. D. 1988. Sediment transfer by floods. In *Flood Geomorphology,* ed. V. R. Baker, R.C. Kochel, and P.C. Patton, 97 - 111. New York: John Wiley and Sons.

Larsen, M. C. 2000. Analysis of 20th century rainfall and streamflow to characterize drought and water resources in Puerto Rico. *Physical Geography* 21(6):494 - 521.

Leopold, L., and M.G. Wolman. 1957. River channel patterns - braided, meandering, and straight. *U.S. Geological Survey Professional Paper 422-H*. Reston, VA: U.S. Geological Survey.

Leopold, L., M.G. Wolman, and J.P. Miller. 1964. *Fluvial Processes in Geomorphology*. San Francisco: W.H. Freeman Co.

Leopold, L. B. 1994. *A View of the River*. Cambridge, MA: Harvard University Press.

Lewin, J. 1977. Channel pattern changes. In *River Channel Changes,* ed. K. J. Gregory, 168 - 183. Belfast, Ireland: John Wiley and Sons.

Li, M. H., and K.E. Eddleman. 2002. Biotechnical engineering as an alternative to traditional engineering methods, a biotechnical streambank stabilization design approach. *Landscape and Urban Planning* 60:225-242.

Longley, P. A., M.F. Goodchild, D.J. Maguire, and D.W. Rhind. 2001. *Geographic Information Systems and Science*. New York: John Wiley & Sons.

Magilligan, F. J., J.D. Phillips, L.A. James, and B. Gomez. 1998. Geomorphic and sedimentological controls on the effectiveness of an extreme flood. *Journal of Geology* 106:87 - 95.

Mark, B. G. 2002. Hot ice: glaciers in the tropics are making the press. *Hydrological Processes* 16:3297-3302.

Mattson, P. H. 1960. Geology of the Mayaguez area. *Geological Society of America Bulletin* 71:319-362.

Mertes, L. A. K., D.L. Danial, J.M. Melack, B. Nelson, L.A. Martinelli, and B.R. Forsberg. 1995. Spatial patterns of hydrology, geomorphology, and vegetation on the floodplain of the Amazon River in Brazil from a remote sensing perspective. *Geomorphology* 13:215 - 232.

Milton, E. J., D.J. Gilvear, and I.D. Hooper. 1995. Investigating change in fluvial systems using remotely sensed data. In *Changing River Channels,* ed. A. Gurnell, and G. Petts, 277 - 302. New York: John Wiley and Sons.

Morisawa, M. 1985. *Rivers Form and Process*. London: Longman.

Nanson, G. C., and E.J. Hickin. 1983. Channel migration and incision on the Beatton River. *Journal of Hydraulic Engineering* 109(3):327 -337.

Nash, D. B. 1994. Effective sediment transporting discharge from magnitude-frequency analysis. *Journal of Geology* 102:79 - 95.

Ott, R. L., and M. Longnecker. 2001. *Statistical Methods and Data Analysis*. Pacific Grove, CA: Duxbury.

Pickup, G., and R.F. Warner. 1976. Effects of hydrologic regime on magnitude and frequency of dominant discharge. *Journal of Hydrology* 29:51 - 76.

Pickup, G., and R.F. Warner. 1984. Geomorphology of tropical rivers II. Channel adjustment to sediment load and discharge in the Fly and Lower Purari, Papua New Guinea. *Catena* 5:18 - 41.

Ramos-Ginés, O. 1999. Estimation of magnitude and frequency of floods for streams in Puerto Rico: new empirical models. *U.S. Geological Survey Water Resources Investigations Report 99-4142.* Reston, VA: U.S. Geological Survey

Richards, K. S. 1982. *Rivers: Form and Process in Alluvial Channels*. London: Methuen.

Ritter, D. F., R.C. Kochel, and J.R. Miller. 2002. *Process Geomorphology*. New York: McGraw Hill.

Robert, A. 2003. *River Processes: An Introduction to Fluvial Dynamics*. New York: Oxford University Press.

Rosgen, D. 1996. *Applied River Morphology*. Pagosa Springs, CO: Wildland Hydrology.

Salo, J., R. Kalliola, I. Hakkinen, Y. Makinen, P. Niemela, M. Puhakka, and P.D. Coley. 1986. River dynamics and the diversity of Amazon lowland forest. *Nature* 322:254-258.

Savat, J. L. 1975. Some morphological and hydraulic characteristics of river patterns in the Zaire basin. *Catena* 2:161-180.

Schumm, S. A. 1960. The shape of alluvial channels in relation to sediment type. *U.S. Geological Survey Professional Paper 352 - B.* Reston, VA: U.S. Geological Survey.

Schumm, S. A. 1963. Sinuosity of alluvial rivers on the Great Plains. *Geological Society of America Bulletin* 74:1089-1100.

Schumm, S. A. 1967. Meander wavelengths of alluvial rivers. *Science* 157(3796):1549 - 1550.

Schumm, S. A. 1977. *The Fluvial System*. New York: John Wiley & Sons.

Schumm, S. A. 1991. *To Interpret the Earth, Ten Ways to Be Wrong*. Cambridge: Cambridge University Press.

Seul, M., L. O'Gorman, and M.J. Sammon. 2000. *Practical Algorithms for Image Analysis*. New York: Cambridge University Press.

Shields, F. D., A. Simon, and L.J. Steffen. 2000. Reservoir effects on downstream river channel migration. *Environmental Conservation* 27(1):54 - 66.

Simon, A., and P. Downs. 1995. An interdisciplinary approach to evaluation of potential instability in alluvial channels. *Geomorphology* 12:215-232.

Simon, A., W. Dickerson, and A. Heins. 2004. Suspended-sediment transport rates at the 1.5 year recurrence interval for ecoregions of the United States: transport conditions at the bankfull and effective discharge? *Geomorphology* 58:243 - 262.

Slack, J. R., A.M. Lumb, and J.M. Landwehr. 1993. Streamflow data set: 1874 - 1988. *U.S. Geological Survey Water Resources Investigations Report 93 - 4076*. Reston, VA: U.S. Geological Survey.

Soderstrom, T. R., and C.E. Calderon. 1979. A commentary on the bamboos (*Poaceae: Bambusoideae*). *Biotropica* 11(3):161 - 172.

Speight, J. G. 1965. Meander spectra of the Angabunga River. *Journal of Hydrology* 3:1- 15.

Sun, T., P. Meakin, and T. Jossang. 1996. A simulation model for meandering rivers. *Water Resources Research* 32:2937 - 2954.

Swanson, D. C. 1993. The importance of fluvial processes and related reservoir deposits. *Journal of Petroleum Technology* 45:368-377.

Thorne, C. R. 1992. Bend scour and bank erosion on the meandering Red River, Louisiana. In *Lowland Floodplain Rivers,* ed. P. A. Carling, and G.E. Petts, 95 - 116. New York: John Wiley & Sons.

Tiegs, S. D., and Pohl, M. Article in Press. Planform channel dynamics of the lower Colorado River: 1976-2000. *Geomorphology*.

U.S. Department of Commerce. 2000. *Census Summary File 1 (SF 1).* Washington, DC: U.S. Bureau of the Census.

U.S. Federal Emergency Management Agency. 1999. *Building Performance Assessment Report 399*. Washington, DC: Federal Emergency Management Agency

U.S. Geological Survey. 1999. *Hurricane Georges Fact sheet 040-99.* Reston, VA: U.S. Geological Survey.

U.S. Geological Survey. 2004. *Rio Grande de Añasco Gauge Station 50144000*. http://nwis.waterdata.usgs.gov/nwis/nwisman/?site_no=50144000_cd=USGS (accessed October 14, 2004).

Veve, T., and B. Taggart. 1994. Atlas of ground water resources in Puerto Rico and the U.S. Virgin Islands, *U.S. Geological Survey Water Resources Report 94-4198.* Reston, VA: U.S. Geological Survey.

.

Werrity, A. 1997. Short-term changes in channel stability. In *Applied Fluvial Geomorphology for River Engineering and Management,* ed. C. R. Thorne, R.D. Hey, and M.D. Ewson, 47 - 66. New York: John Wiley & Sons.

Westrup, H. 1998. Furious Georges. *Current Science* 84(6):1 -2.

Williams, G. P. 1978. Bankfull discharge of rivers. *Water Resources Research* 14(6):1141 - 1154.

Williams, G. P. 1986. River meanders and channel size. *Journal of Hydrology* 88:147-64.

Wolman, M. G., and J.P. Miller. 1960. Magnitude and frequency of forces in geomorphic processes. *Journal of Geology* 68:54-74.

Wolman, M. G., and R. Gerson. 1978. Relative scales of time and effectiveness of climate in watershed geomorphology. *Earth Surface Processes and Landforms* 3:189 - 208.

APPENDIX A

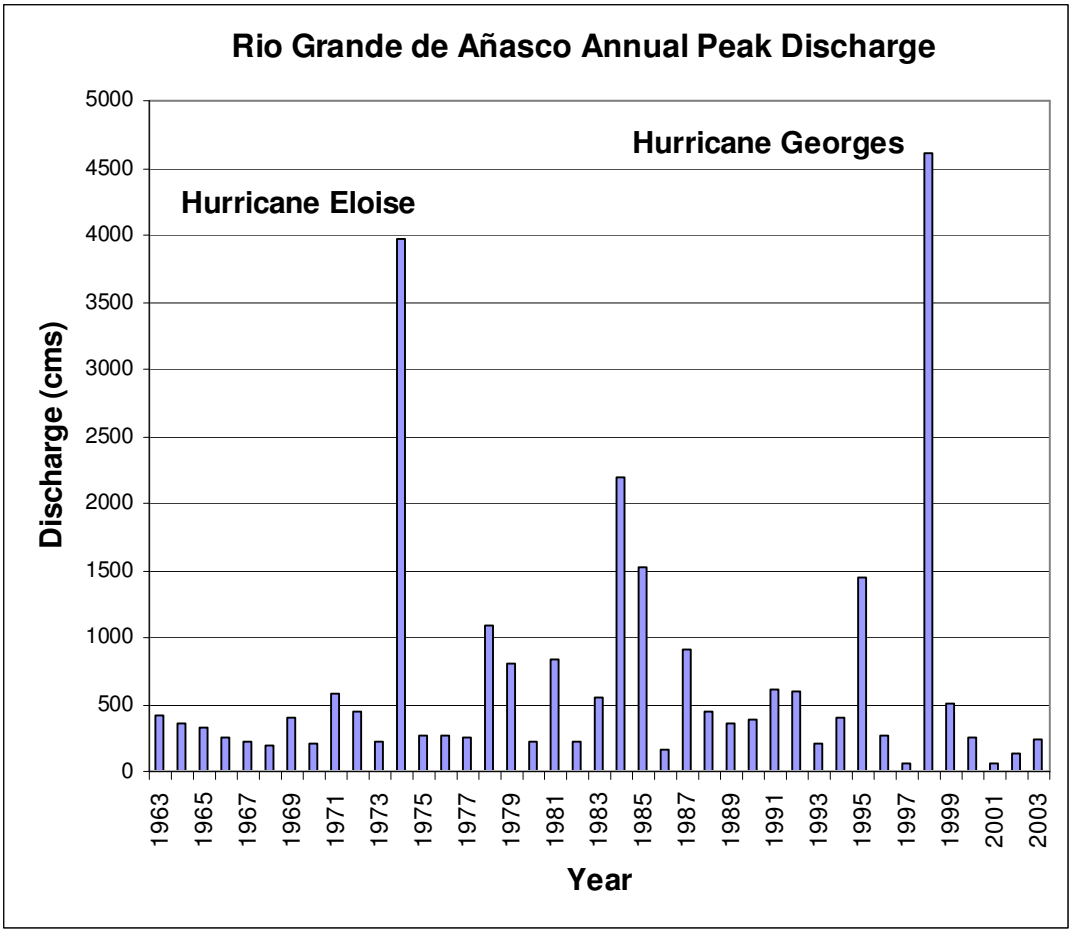

Figure A-1 *Rio Grande de Añasco Annual Peak Discharge.*

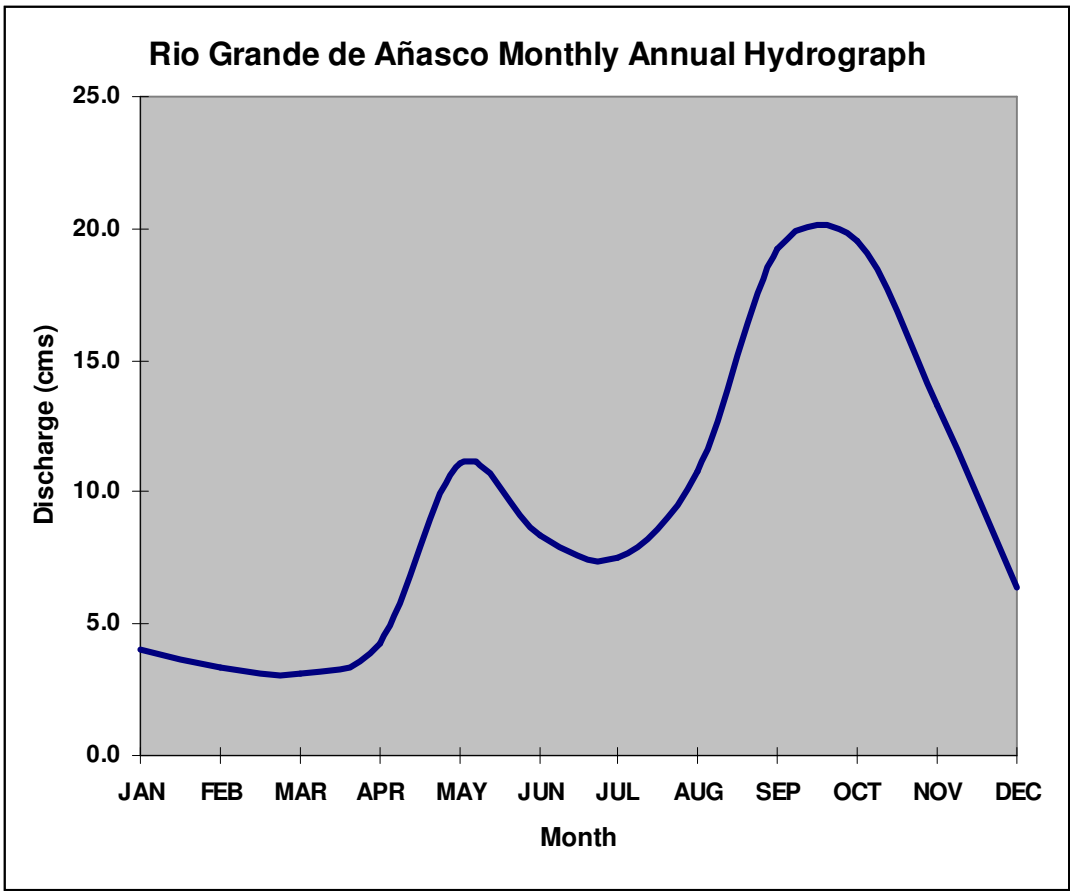

Figure A-2 *Rio Grande de Añasco Monthly Annual Hydrograph.*

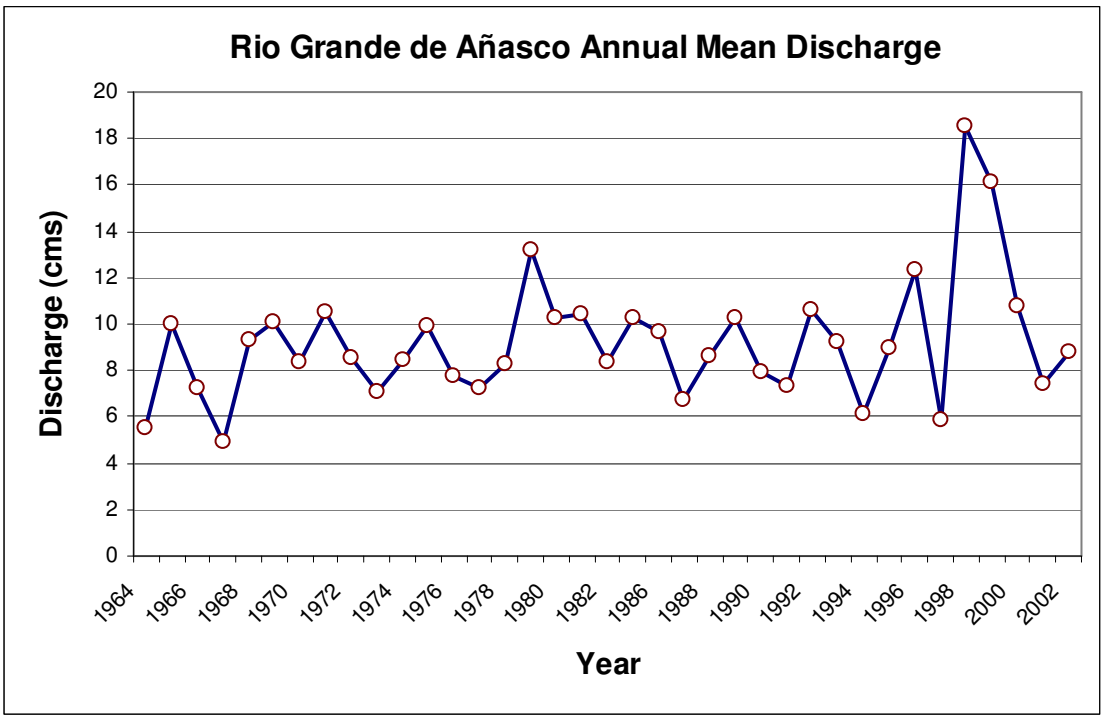

Figure A-3 *Rio Grande de Añasco Annual Mean Discharge*.

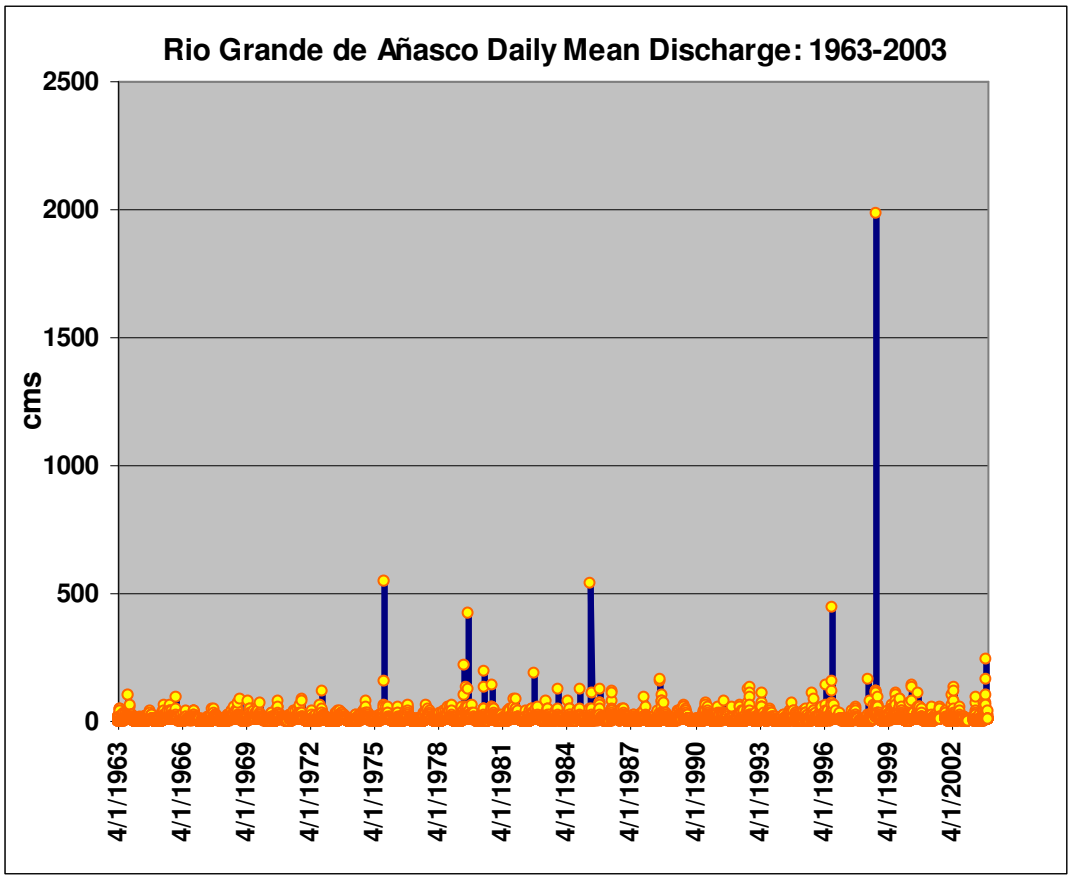

Figure A-4 *Rio Grande de Añasco Daily Mean Discharge.*

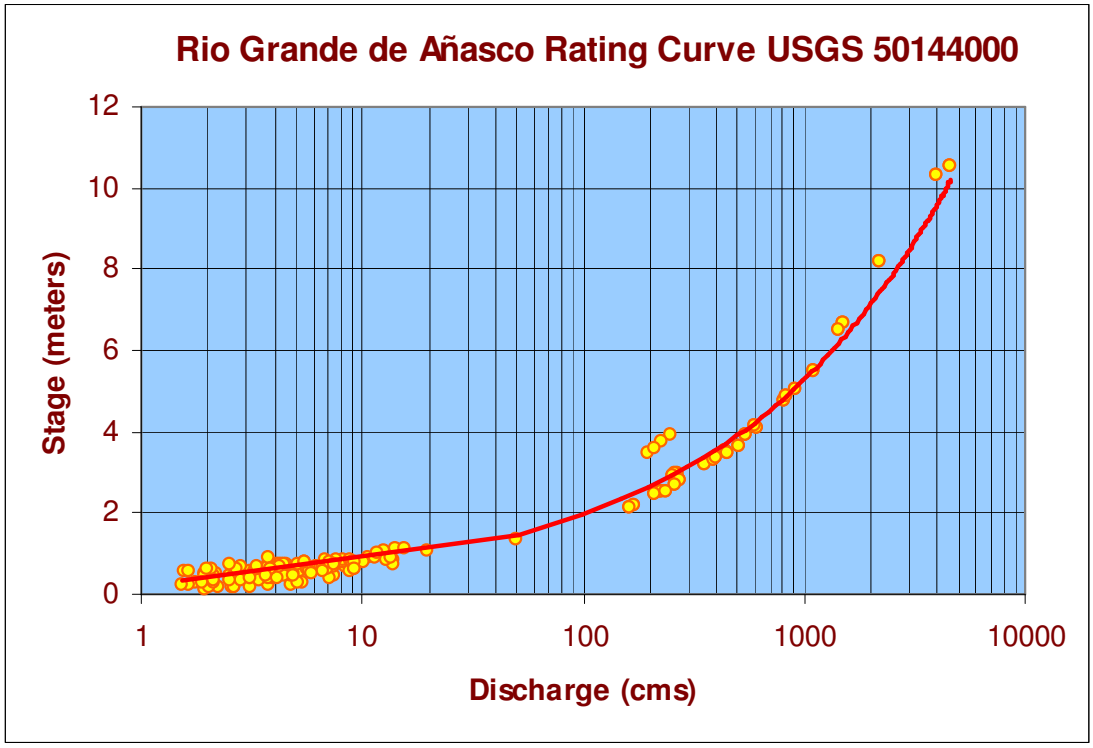

Figure A-5 *Rio Grande de Añasco Rating Curve USGS 50144000.*

APPENDIX B

Table B-1 *Aerial photographs with source data*

Number	Type	Date	ID	Source	Scale
1	DRG	1-Jul-66	DRG0800301270700_007_1	*USGS	1:24,000
2	Air Photo	20-Mar-77	ARH7701000400238	*USGS	1:24,000
3	Air Photo	7-Feb-83	ABL82058004	*USGS	1:24,000
4	Air Photo	22-Jan-90	AR5900039931782	*USGS	1:24,000
5	DOQQ	29-Oct-93	DOQDI00000001087950	*USGS	1:20,000
6	Air Photo	21-Sep-95	AR5950050040033	*USGS	1:24,000
7	Air Photo	12-Aug-97	**series	Aerofoto Internacional	1: 5,000
8	Air Photo	8-Oct-98	**series	Aerofoto Internacional	1: 5,000
9	Air Photo	1-Jun-99	**series	Aerofoto Internacional	1: 5,000
10	Air Photo	28-Nov-99	5565	NOAA	1:24,000
11	Air Photo	8-Aug-04	**series	West Wings	1: 5,000

* USGS is the United States Geological Survey

** Series denotes a series of photographs representing several high-resolution images taken on the same date of different reaches of the river.

Table B-2 *Aerial photographs with pixel size and RMSE measurements*

Number	Type	Date	Pixel size (meters)	Total RMSE (meters)
1	DRG	1-Jul-66	1.0	0.770
2	Air Photo	20-Mar-77	1.0	0.797
3	Air Photo	7-Feb-83	0.9	0.740
4	Air Photo	22-Jan-90	1.0	0.853
5	DOQQ	29-Oct-93	1.0	orthorectified
6	Air Photo	21-Sep-95	0.7	0.243
7	Air Photo	12-Aug-97	0.6	0.618
8	Air Photo	8-Oct-98	0.6	0.468
9	Air Photo	1-Jun-99	0.5	0.535
10	Air Photo	28-Nov-99	1.0	0.842
11	Air Photo	8-Aug-04	0.5	0.563

APPENDIX C

Figure C-1 *Low resolution renditions of* aerial *photographs taken on August 12, 1997 (a) one year before, October 8, 1998 (b) two weeks after, June 1, 1999 (c) nine months after, and November 28, 1999 (d) 14 months after passage of Hurricane Georges on September 22, 1998.*

VITA

Aldo Alvarez

Date of Birth: May 13, 1952

Address: P.O. Box 385
Cabo Rojo, Puerto Rico 00623

Education:

1975	B.S., Civil Engineering, University of Puerto Rico
1977	M.S., Civil Engineering, Massachusetts Institute of Technology
2005	Ph.D. Geography, Texas A&M University